AN AGENT-BASED MODEL TO SIMULATE VIRUS-BASED BIOCONTROL FOR THE SOYBEAN CYST NEMATODE, *HETERODERA GLYCINES*

BY

SAFYRE ANDERSON

THESIS

Submitted in partial fulfillment of the requirements
for the degree of Master of Science in Agricultural and Biological Engineering
in the Graduate College of the
University of Illinois at Urbana-Champaign, 2014

Urbana, Illinois

Master's Committee:

Associate Professor Kaustubh Bhalerao, Chair
Associate Professor Kris Lambert
Assistant Professor Leslie Domier

Abstract

Plant parasitic nematodes are responsible for food losses worth $78 billion worldwide. The damage caused by *Heterodera glycines*, or soybean cyst nematode (SCN), to the US soybean crop is estimated up to $2 billion annually making it the most destructive soybean pathogen. SCN is a microscopic obligate endoparasite with an entirely belowground life history that includes a robust dormant phase. These aspects of SCN biology make it nearly impossible to eradicate and expensive to manage. The most widely deployed strategy to manage SCN is an integrated management plan (IPM) that combines non-host crop rotations (frequently with corn) and planting SCN-resistant cultivars. SCN cyst diapause–which allows SCN to persist in the soil for several years–limits the effectiveness of alterate-year crop rotations. Furthermore, evidence that the most widely used resistant lines are losing their effectiveness is mounting. Additionally, nematicides are increasingly unavailable due to environmental regulations and also have the disadvantages of being prohibitively expensive, and performing inconsistently.

Biological control (biocontrol) has recently been seen as a promising addition to IPM. Viruses are relatively more stable and therefore more persistent in soil, they do not need to form complicated infection structures, they can be cultured on a commercial scale, and they have simpler genomes which are amenable to genetic engineering. Furthermore, viruses exhibit higher host and tissue-specificity, decreasing the risk for non-target effects seen in other non-virus-based biocontrol cases. Though these properties of viruses have been demonstrated in insect pests with favorable results, viruses have not been investigated for nematode biocontrol. This is because infectious virus in nematodes had gone unnoticed until a couple of recent discoveries. At the University of Illinois, five SCN ssRNA viruses were discovered in 2011 giving us ample opportunity–paving the way to explore their potential as biocontrol agents. While empirical data on the pathologies of these viruses emerges, we opted to use a computational approach to investigate pathotypic factors needed for desirable nematode suppression, the epizootiology of within-nematode evolution, and the long-term population-level behavior.

This study used an agent-based model, SCNSim, to simulate a virus-nematode-soybean system to investigate within-host virulence evolution. The nematode-agent recapitulates the nematode life cycle and uses purely stochastic events to advance each transition in the model. SCNSim was used to test a range of mutation rates, initial virulences, and release strategies. This investigation uses weather data and soybean planting and harvesting

patterns in Champaign, IL. Where empirical data is lacking dimensionless parameters and probabilities were used.

Results of the simulation showed viruses inoculated at 80% prevalence caused significantly more mortalities than those inoculated at 20% prevalence. Further investigation revealed the low mortality under lower prevalence was likely due to high horizontal and vertical transmission leading to rapid thinning of the overall viral burden as the disease spread to nearly 100% of the population. Mortality rate was found to be dependent on virulence and fidelity. Pathotypes with high starting virulence resulted in premature peaked mortalities which suggested shorter lifetime transmission. Furthermore, virulence and fidelity were inversely related in pathotypes with the highest mortalities. Further, these pathotypes had population-level fitnesses near the error threshold between persistence or extinction. Qualitative stability analysis revealed medial pathotypes exhibited stable long-term behavior reminiscent of a spiral sink in the mortality and transmissibility phase space.

That intermediately virulent and transmissible viruses lead to the most damaging epizootics is in agreement with the generally accepted trade-off theory in virulence evolution. However, the evolution of the transmissibility and prevalence curves through time reveal some inconsistencies in the mechanisms of disease spread with respect to theory that require further testing. Testing combinations of varying levels of transmission rates, and virus loads for instance can provide insight on how different transmission modes impact virulence evolution and the efficacy of nematode suppression. There are still many areas where SCNSim can be improved–particularly when the transmission rates and dominant transmission modes of the SCN RNA viruses becomes known. In its present state, SCNSim has predicted the attenuation of nematode mortalities within the first four crop seasons due to either a dilution of virus particles thoughout the population or the insulation of the infected population resulting from mortality rates exceeding transmission rates. The goal for the near future is to apply SCNSim alongside genetic engineering and experimental testing of the SCN viruses, in a decision-making framework for virus-agent deployment strategies and improving virus-agent efficacy within an evolutionary timescale for nematode biocontrol.

"Others have had graver sorrows,
And deeper hurts than mine;
And yet I hate those dread tomorrows
That stretch in endless line.

Others have sinned for lesser things
And darker sins than mine,
And yet they drift on blackened wings
With airs quite sanguine.

So why continue to rebel
Against this fate of mine?
I'll drink the cup that suits me well,
Though it be poisoned wine!"

–Grandma Jean

To the friends we lost along the way, and the ones who are still fighting:
Cheers.

Acknowledgments

"Your little boat goes west and you congratulate yourself, 'What a navigator I am!'
And then the wind blows you east. –Abdul's father, Karam Husain"

–Katherine Boo, **Behind the Beautiful Forevers**

Throughout my three years here as a graduate student I have often found myself with ambivalent feelings towards this far-off land known as Urbana-Champaign. Like so many of my peers, when I began I had felt honored to be accepted to a renowned program–that the surmounting, persistence, and dedication I had found myself capable of during my undergraduate studies had been acknowledged and rewarded. There were numerous opportunities to engage with enthusiastic and smart people, to take part in challenging and impactful projects, to embrace all new experiences, and absorb *everything*; I was ready to take off sprinting. Alas, one mild (relatively speaking) Midwestern winter was all it took to deflate all those happy expectations!

Graduate school is hard–that was a realization that had surprisingly more weight. I expected graduate school to be hard; I expected the long hours, the mental marathons, the complicated and self-driven schedule, the financial hardship. Still, feelings of isolation, homesickness, and the overall "Is this worth it?" were threatening to pull me out of this soybean-filled crucible back home to sunny, traffic-ey San Jose, CA. Back to the lively South Bay with the best Southeast Asian cuisine, ample sushi, close friends, family, and my husband. And this is why, from the bottom of my heart, there are people here who need copious thanking. Because without my friends, my mentors, and my big and growing family, there was not enough personal strength in me to make it out alone.

I would like to thank my advisor Dr. Kaustubh Bhalerao for his patience and supportive guidance. It is not often you get to press the restart button on your thesis, but with hindsight I am thoroughly glad I did even with the one and a half year setback. Switching to the biological engineering group was a risky and difficult choice that has ended with great rewards only because of Dr. Bhalerao's diligent coaching and *infectious* enthusiasm. Letting me present my Pokémon slides during my final defense was infinitely awesome and probably, no, *definitely* the highlight of this thesis process. I wish you well with a figurative salute five years in advance when you have eight kids. I would also like to thank my other committee members, Drs. Kris Lambert and Leslie Domier for their advice and contributions to this project. Never would I have ever guessed three years

ago that I would be working with nematodes, viruses, or modeling. This journey took me swerving around bioenergy with a stop at wastewater treatment, then tossed me into biocontrol before falling into and bouncing between epidemiology and virulence evolution. I had so much to learn in such a compact timeframe. It was only possible with the expertise and guidance of my thesis committee.

I would also like to thank Dr. Sadia Bekal, of Bekal *et al.* fame, for her invaluable feedback on this project coupled with her endearing and motherly mentoring approach. Her kind words were a great source of comfort and positivity during stressful times. I'd also like to thank Dr. Chinmay Soman for his contributions and his guidance during my introduction to the group. I'd also like to acknowledge the support of my group members: Rekha Balachandran, Vaisak Parekatt, Pratik Lahiri, Xiaowen Lin, Xiaolun Chen, Allante Whitmore, Abhishek Dhoble, and Nico Hawley-Weld. Whether it was sharing your research progress with me (or lack thereof), lending an ear, or even just being a pleasant and encouraging presence in the lab really enriched my experiences here. There is nothing like going to work in twilight with a reluctant and mindless sense of responsibility and then be greeted with an empathetic smile.

During my time at the department, I'd also had the good fortune of making wonderful friends through the Graduate Student Association, Tau Beta Pi, and GradSWE. I'd like to especially thank Aaron Oaks for teaching me LaTeX, being a sympathetic Californian, and just being a gosh-darn good friend. I'd like to thank my UIUC family for always making me feel welcome and helping me in times of need, whether it be painting my apartment or watching my cat while I'm gone. I'd like to especially mention Chih Ting Kuo, Grace Chen, Peng Zhang, Donald Darga, Ferisca Putri, Taylor Leahy, and Stephanie Herbstritt–there is no shortage of kind-hearted people here. I can only hope that I was able to reciprocate at least a fraction of what you all have shown me.

I would like to thank my friends and family from back home. Thank you all for sticking with me for so long and believing in me. Thank you to my mom and dad for raising me to appreciate how important education is as well as being well-rounded. Thank you to my mentors from UC Davis for instilling high standards in research and ethics that became my compass. Thank you to my brother and sisters for being a source of motivation and support system. Finally, thank you to my wonderful husband, Macky, for his dedication and sacrifices, which he demonstrated when he quit his job in the Silicon Valley to take care of my pitiful self. Macky, you are a singularity of all humankind possessing a limitless capacity for smiles, love, and compassion. Without you, I would be an utterly lost, emotionally-stunted, and unfulfilled child-woman. Thank you.

Table of Contents

List of Abbreviations

ASA	American Soybean Association
BLASTX	Translated Basic Local Alignment Search Tool
BLS	Bureau of Labor Statistics, US Department of Labor
BNF	Biological Nitrogen Fixation
BU	Bushels
CFR	Case Fatality Rate
CLE	CLAVATA3/ESR gene family *(see ESR below)*
CM	Chorismate mutase
CWDE	Cell Wall Degrading Enzyme
DBMS	Database Management System
ESR	Endosperm Surrounding Region
EU	European Union
FAS	Foreign Agricultural Service, USDA
FDA	Food and Drug Administration
FI	Female Index
GMO	Genetically Modified Organisms
HG	Heterodera Glycines type
IPM	Integrated Pest Management
ISC	Initial Syncytial Cell
MT	Metric Tons
NASS	National Agricultural Statistics Service, USDA FAS
NCBI	National Center for Biotechnology Information
ORF	Open Reading Frame
PI	Plant Introduced

PSD	Production, Supply and Distribution, USDA
PVP	Plant Variety Protection
RER	Rough Endoplasmic Reticulum
SCN	Soybean Cyst Nematode
ScV5	SCN virus no. 5
ScNV	SCN nyavirus
ScRV	SCN rhabdovirus
ScPV	SCN phlebovirus
ScTV	SCN tenuivirus
SIR	Susceptible-Infected-Recovered
SNP	Single Nucleotide Polymorphism
SPE	Serial Passage Experiment
USB	United Soybean Board
US	United States of America
USDA	United States Department of Agriculture

List of Symbols

R_0	Basic reproduction ratio, i.e., the number of cases of an infection one case generates over the course of its infectious period
R_v	Replication ratio. An adaptation of R_0 to suit the SCNSim viruses to describe the fitness of the virus population
N	Total host population
S	Number of susceptible hosts
I	Number of infected hosts
R	Number of recovering hosts
β^*	Rate of infectivity
d	Mortality rate from disease
b	Baseline or natural mortality rate
ρ	Recovery rate
$\tilde{\rho}_{95}$	Median fraction of infected hosts with avirulent infection
β_0, β	Horizontal transmission rate from males to females
μ	Mutation rate defined as the probability of stochastically varying pathotypic factors
i_0, i	Disease prevalence
L	Virus load defined as a scaling factor to nematode health decrement
V_0, v	Virulence defined as a scaling factor to nematode health decrement

Chapter 1

Introduction

The soybean cyst nematode, *Heterodera glycines* (SCN), is the most detrimental parasite of soybean (*Glycine max*) crops in the United States (US). SCN is estimated to cost US soybean growers between $1-$2 billion each year [1, 2]. Currently, growers impacted by SCN often employ an integrated pest management (IPM) program that consists of crop rotation, planting resistant cultivars, and nematicide treatments. These methods have been successfully adopted because they reduce SCN damage whilst being economically viable–although the latter method is considered more risky and is recommended to be used as a last resort [3]. However, long-term studies reveal SCN are becoming resistant to the more widely used lineages of resistant cultivars, most notably PI 88788 [4]. Thus biological control, or biocontrol, using natural nematode pathogens is rapidly becoming an attractive method to incorporate into IPM.

Plant-parasitic nematodes are known to vector plant viruses [5], but until recently had not been observed while infected by viruses themselves. Nematode-infecting viruses have not been previously studied because they have only recently been discovered [6, 7]. In 2011, the first documented observation of viruses in SCN were published by Bekal *et al.* [7, 8]. Five viral genomes were detected via high throughput sequencing of SCN eggs and second-stage juveniles (J2) genomes after years-old laboratory population lines inexplicably crashed [Kris Lambert, personal communication]. Of these five genomes, it was determined four were negative-sense ssRNA and one a positive-sense ssRNA. The successive protein comparison from the National Center for Biotechnology Information (NCBI) databases using the Translated Basic Local Alignment Search Tool (BLASTX) revealed the five viruses to be distantly related to flaviviruses, nyaviruses, rhabdoviruses, bornaviruses, bunyaviruses and tenuiviruses [7, 8].

Recently discovered soybean cyst nematode viruses provide possibility for a new environmentally friendly biological control method for SCN pest management [7]. SCN is a particularly difficult pathogen to diagnose due to the pest's underground life cycle and similarity of aboveground symptoms to other plant pathologies. A biocontrol method of SCN management that can be readily established would be highly beneficial for farmers whose crops suffer from chronic and/or aggressive SCN infestation. However, the intra-plant parasitic SCN life-cycle, its ability to remain dormant for up to a decade, and

variable environmental conditions encountered during field testing over multiple crop cycles for long-term performance evaluation create practical challenges for experimental testing. Furthermore, the SCN viruses described by Bekal *et al.* have not yet been evaluated for their transmission modes, virulence or nematode pathophysiology. Further evaluation is also needed to shed light on the dynamics of disease spread in the tritrophic system under various conditions before assessing the potential of the viruses as biocontrol agents.

In this study, we used numerical techniques to explore the interaction between SCN and a range of hypothetical viruses using an agent-based Monte Carlo code (SCNSim). SCNSim recapitulates the SCN life cycle as well as computes host-pathogen dynamics of a virus epizootic within an SCN metapopulation. This code uses published data to outline the SCN life cycle as well as soybean planting and growth timelines [1, 9]. The model environment uses temperature data from the Champaign County, IL area recorded by the Illinois State Water Survey [10]. Due to the scant empirical data on the viruses, the simulation used dimensionless and general definitions of virus properties to allow for qualitative analysis of epizootics and population trends. The transitions throughout the SCN life cycle and disease states are simulated as stochastic events. These probabilities of successful transition are controlled by the initial nature of the viruses, the subsequent fluctuations in their pathogenicity as the virus evolves with its host, and the current health of the nematode. Like all models, SCNSim is a simplification of the actual system. However, we are able to quickly generate large amounts of data gathered in short time intervals, over several years, and from a wide range of conditions.

Our objective was to investigate what virus characteristics resulted in the highest suppression of the nematode population and the nature of the threshold behavior expected from an ecological model. We also aimed to explore long-term population dynamics and the underlying virulence and transmissibility relationships. We expected the epizootiology to follow the adaptive virulence trade-off hypothesis: virulence is an unavoidable consequence of transmissibility which may cause successful pathogens to evolve towards an intermediate optimum that balances the two characteristics [11].

Chapter 2

Background Information

2.1 US Soybean Production & Agronomy

2.1.1 Agricultural Significance

Soybean (*Glycine max*), is one of the world's most important crops and is the second most widely grown crop in the United States (US) following corn with production in 2011 at 3.1 billion bushels (BU) [12, 13]. Phenomenally versatile, and a cheap and rich source of protein, soybeans are a valuable raw ingredient for numerous commodities. The amino acid profile of soybeans is closely aligned with human dietary requirements. Thus, soybeans play a major dietary role in many regions around the world, particularly China, Japan, and Indonesia [14, 15]. Soybeans are often processed by either mechanical crushing or solvent extraction to yield meal and oil. Soybean meal, which is approximately 50% protein by dry weight, is a popular meat substitute, but is mainly used as a protein source in animal feed [15, 16]. Soybean oil can be used for human consumption as cooking oil, used in the industrial manufacture of plastics, inks, or converted to biodiesel. Modern research continues to expand the utility of the soybean and its value-added products.

As legumes, soybeans also play an important role reducing rates of soil-nitrogen loss in crop rotations through biological nitrogen fixation (BNF) of atmospheric N_2. Soil-nitrogen contributed by soybeans allow farmers to reduce application of industrial nitrogen fertilizers thereby reducing unnecessary input costs and harmful ecological impacts of nitrates pollution. BNF is part of the soybean's symbiotic associations with *Rhizobium* bacteria–belonging to the *Bradyrhizobium* and *Sinorhizobium* generas–which reside in the soybean's root nodules. Studies have shown soybeans can sequester between 36-80 kg N $ha^{-1}yr^{-1}$ [17, 18, 19] depending on soil geochemistry and climate conditions. This property of soybeans (and legumes in general) plays a beneficial role in agriculture; even after being harvested, soybeans help maintain soil fertility improving the yield of subsequent non-legume crops [17, 20].

2.1.2 Uses and Products Derived from Soybeans

As rich and renewable sources of protein and oil, soybeans offer ample opportunities for the development of soy-based alternatives to existing products and feedstocks ranging from soyfoods, feed, biodiesel, and a variety of industrial applications [15, 16, 21, 22]. Traditional staple foods derived from whole soybeans include soy sauce, tofu, soy milk, tempeh as well as many others. Soy concentrates and isolates are prevalent in edible and non-edible products for human consumption, such as: dietary supplements, baking products, pharmaceuticals, pastas, meat protein-substitutes, baby food, and many others (**Fig. 2.1**).

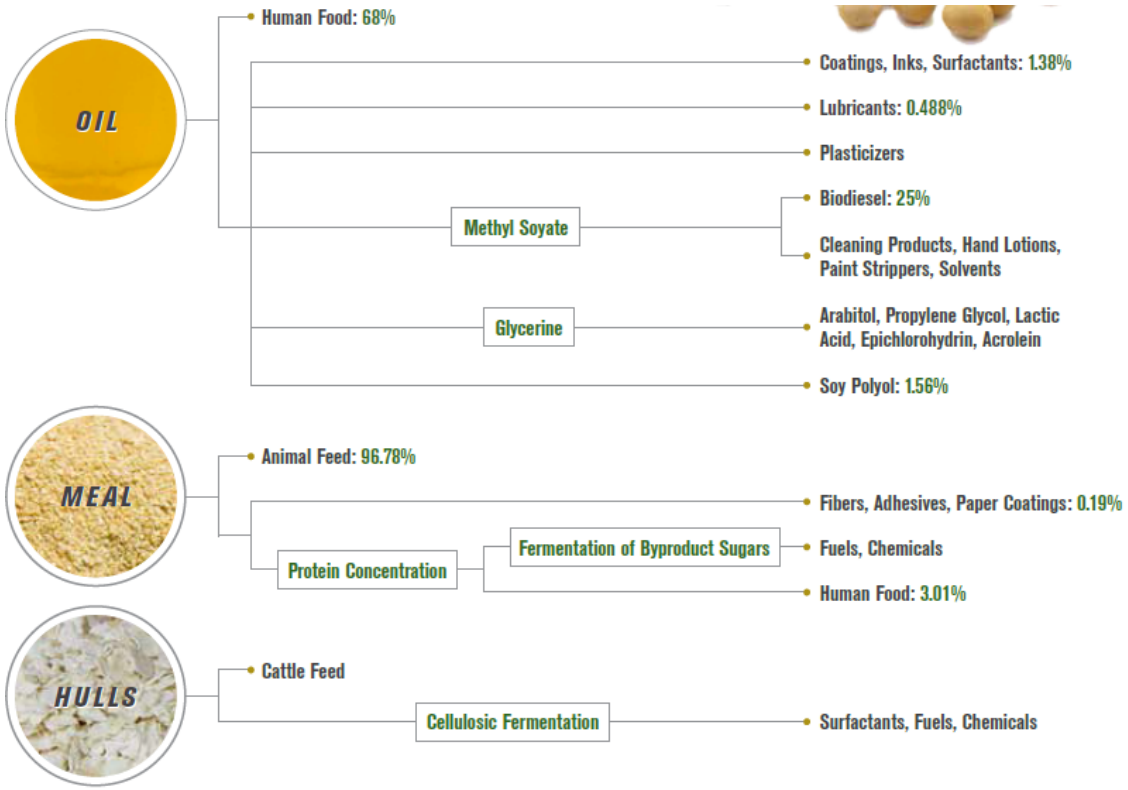

Figure 2.1: Breakdown of types of Soybean Products by Seed Component Origin [22].

Crushed soybeans yield between 63% - 79% meal and 17%- 18.5% oil [15, 16, 23]. Oil is extracted primarily by hexane extraction although mechanical pressing yields higher quality protein in the residual meal. Soybean oil is also a major ingredient in margarine, salad dressings, etc, and is used directly as cooking oil (**Fig. 2.2b**) [23]. The largest market for soybean meal is animal feed for aquaculture and animal feed mills, particularly the poultry and swine industries (**Fig. 2.2b**). Soybean meal is often mixed with corn meal, feed wheat and other ingredients to produce a feed that is high in protein and carbohydrates, and low in fiber [15].

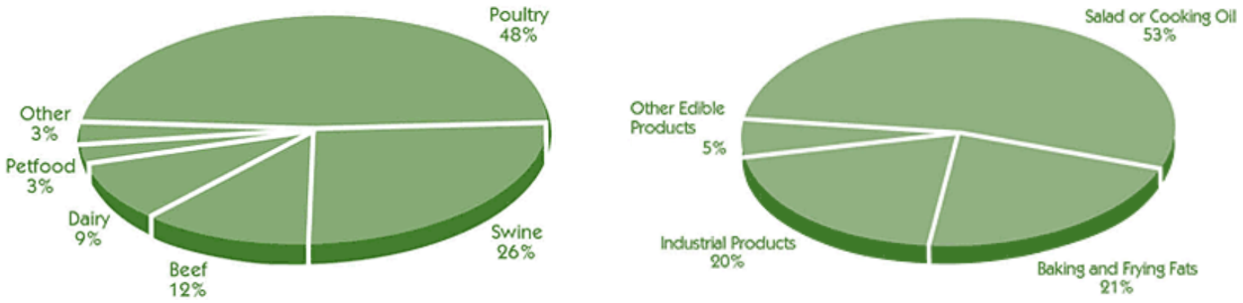

(a) Soybean Meal Consumption

(b) Soybean Oil Consumption

Figure 2.2: US Soybean Consumption in 2011. In 2011, the US consumed a total of 24.77 million MTs and 8.03 million MTs of soybean meal and soybean oil, respectively. Courtesy American Soybean Association; Reproduced from SoyStats 2012 [23].

In addition to being consumed by humans and animals, soybeans–and their valuable components–are a renewable resource for alternative components in many industrial products. With growing concerns for anthropogenic climate change, consumers and government entities are pressuring businesses to reduce their reliance on petroleum-based products and adopt alternatives from renewable and sustainable sources. The United Soybean Board (USB) releases a study regularly highlighting the advantages in life cycle impact of soy-based oils, resins, and lubricants compared to their fossil-fuel counterparts [24]. Furthermore, the complexity of soybean protein and oil compositions allow industries to create high-value secondary co-products for nutraceuticals, printing inks, adhesives, plastics, and many other specialty products [22].

2.1.3 Trends in Global and US Soybean Markets

Since the 1970's , the soybean has emerged as the dominant oilseed in the world market. In 2012, soybeans constituted 56% of global oilseed production at 268,270 million MT followed distantly by rapeseed (canola) at 13% [21, 23, 25]. Global soybean production has seen a steady growth averaging between 5-6% following the recent rapid expansions of the economies of Asian and South American countries, most notably of China, Argentina, and Brazil. Factors contributing to increased demand for soybean meal and oil in these countries include the subsequent rise of per capita income leading to increased demand for animal protein and cooking oil, improved infrastructure reducing transport related losses, and improved yields [15].

In recent years, the US remains a top producer of soybeans followed by Brazil and Argentina at 34%, 28%, and 19%, respectively (**Fig. 2.3**) [15]. However, Brazil is projected to surpass the US as a top producer within the next 1-3 years and has already surpassed

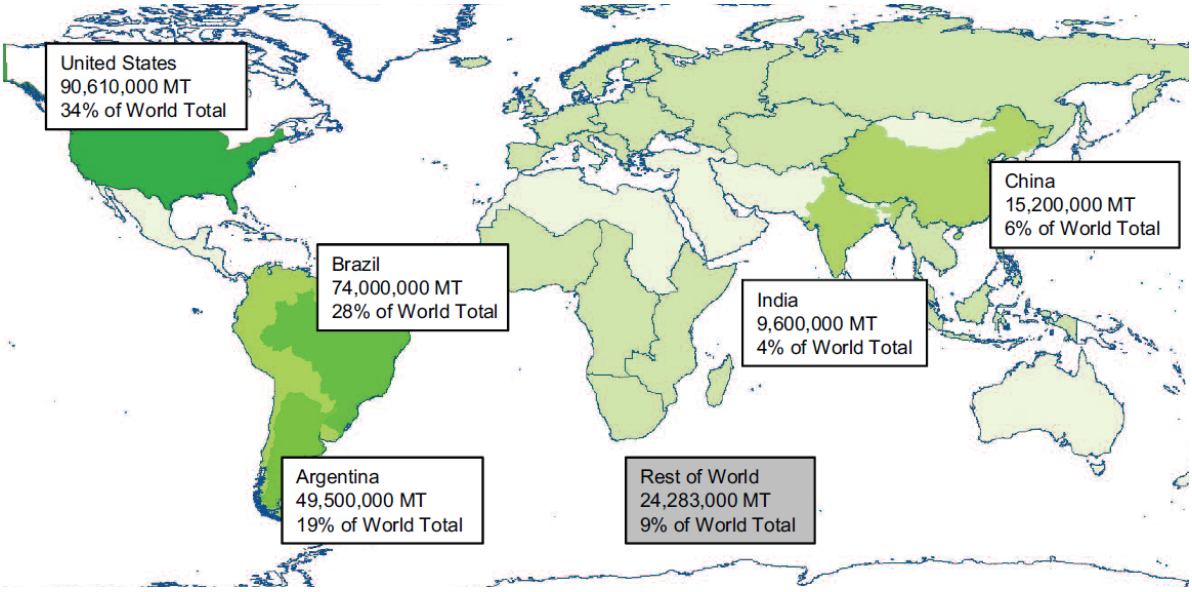

Figure 2.3: Global Production of Soybeans in 2010 - 2011 [15].

the US in exports; Brazil leads the US with 41% (37.8 million MT) of the market compared to 37% (34.7 million MT) [23]. Argentina is the leading exporter of soybean meal and soybean oil at about 46% and 49% of the market respectively due to the countries differential export tax that favors exporting soybean products over raw beans [15]. In general, international customers favor Brazilian and Argentinian soybean products because of their lower production costs, longer growing seasons, and opposition to genetically modified organisms (GMO).

Among the top importers of soybeans are the European Union (EU) followed by China whom combined import about two-thirds of global soybean exports [21]. The top 10 importers of soybeans accounted for approximately 90% of the market in 2010. In addition to China and the EU, the remaining 8 markets are Japan, Taiwan, South Korea, Mexico, Turkey, Indonesia, Thailand, and Egypt [15]. Though there is some shift in the demographics in the dominant importers for soybean meal and soybean oil, the EU, China, and a few other Asian countries have persistently high demand for soybean and soybean products. The global market for soybeans and soybean products is expected to continue growing as new economic powers emerge and drive their demand.

Soybean production has more than doubled in the US since the 1980's and has made the US the largest producer of soybeans in the world in terms of acreage and crop yield, producing 34% of the world's soybeans in the 2010–2011 crop year [15, 20]. Soybean is the second most produced field crop after corn and is primarily grown in the Corn Belt region which is responsible for 81% of the countries soybeans. In 2011, US soybean

farmers harvested 83.18 million MT valued over $35.78 billion and exported 34.7 million MT valued over $21.5 billion [12, 23, 25]. The top five producing states in the 2009–2010 crop year in order of decreasing productivity were Iowa, Illinois, Minnesota, Indiana, and Nebraska [23] (**Fig. 2.4**).

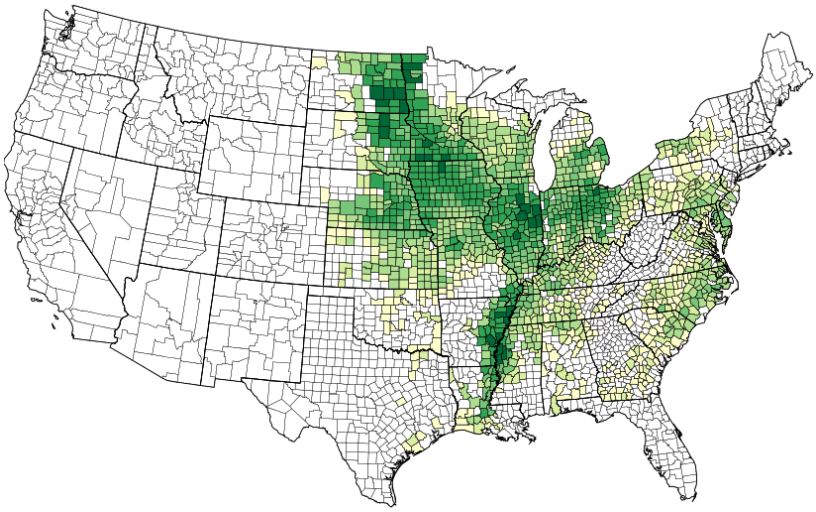

Figure 2.4: Soybean Production in US by County, 2012. The color gradient represents the amount of production in each country with the darkest and lightest greens symbolizing counties that produced over 8 million BU and less than 250 thousand BU, respectively. Image from the USDA-National Agricultural Statistics Service (NASS).

The soybean market in the US provides commercial opportunities for secondary industries. Soybeans are an important market for agrochemicals, making up over 63% of the market by value or $1.9 billion [26]. Most of the soybean market consumes herbicides over insecticides and fungicides. However, with increasing prevalence of certain diseases and pests as well as reduced efficacy of existing pesticides due to pathogens acquiring pesticide resistance, it is expected these areas of the agrochemical market will grow and expand [1, 26]. The soybean market is also important for seed technology companies. From 1970 to 2008, 2242 soybean cultivars were registered under either the US Plant Variety Protection Act (PVP), US utility patents, or academic journals (**Fig. 2.5**). Most soybean cultivars are engineered for increased nutritional value, yield, and herbicide tolerance. A smaller portion of soybean cultivars are engineered with specific disease resistances [27].

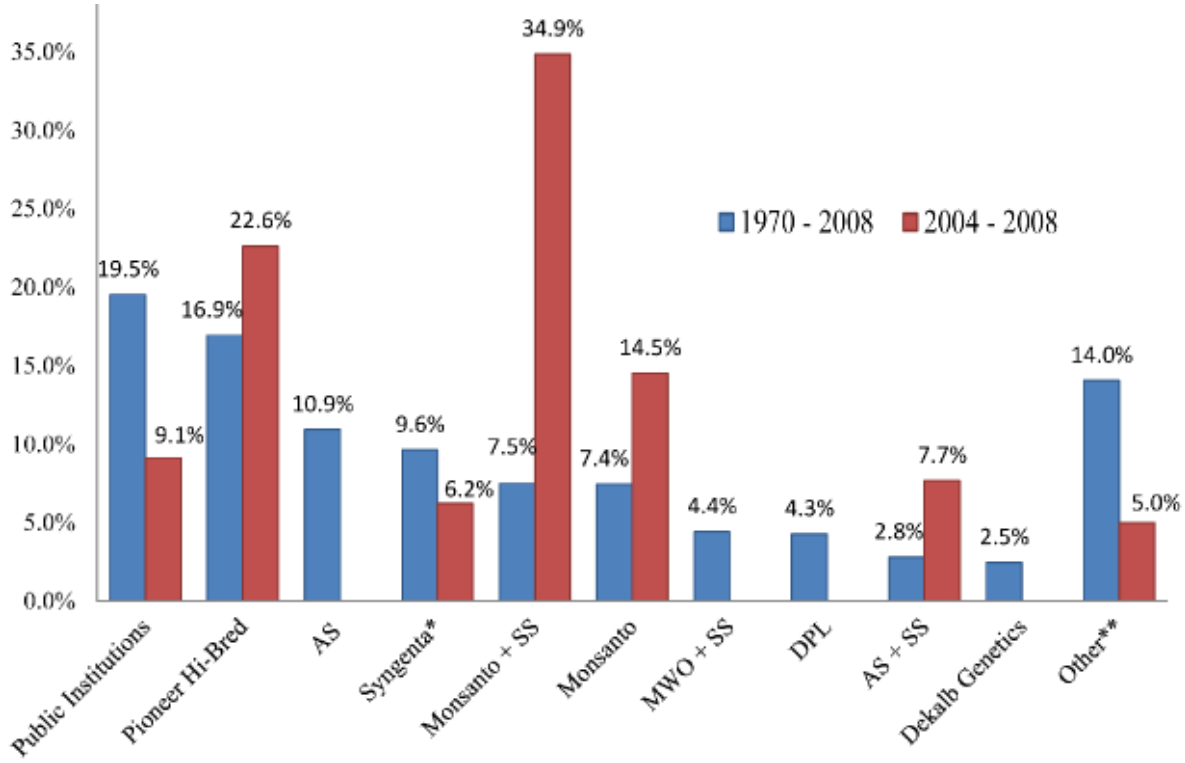

Figure 2.5: Sources of registered soybean cultivars: 2242 nonredundant cultivar registrations occurred in 1970-2008. 482 of these occurred in 2004-2008 from fewer sources: Monsanto acquired Asgrow (AS) in 1997, Dekalb Genetics in 1998, and Delta Pine & Land (DPL) in 2006 [28]. Not mentioned: Stine Seed (SS), and Midwest Oilseed (MWO). *1970-2008: Syngenta includes cultivars from Novartis Seeds, Northrup King, and Funk Seeds. **_Other_ represents numerous originators each with few registrations. Figure generated from data published in Mikel *et al.* [27].

2.2 Soybean Cyst Nematode Biology and Etiology

2.2.1 Prevalence and Scope of SCN Damage on US Soybeans

Soybean cyst nematodes (SCN) are by far the most economically detrimental pathogen to the US soybean crop (**Fig. 2.6**). It is estimated that production losses caused by SCN cost US farmers from the $100 millions to upwards of $2 billion annually; the minimum and maximum losses within the years 2001 to 2010 were $0.431 billion (2005) and $1.72 billion (2008) (**Fig. 2.7b**) [1, 2, 12, 29]. Not surprisingly, the states suffering most in terms of overall production losses from SCN infestation are the most productive soybean growers–Iowa and Illinois [30, 31].

Although soybeans are still a profitable cash crop, the above figures illustrate a significant loss of income for US soybean farmers as well as value lost in downstream industries

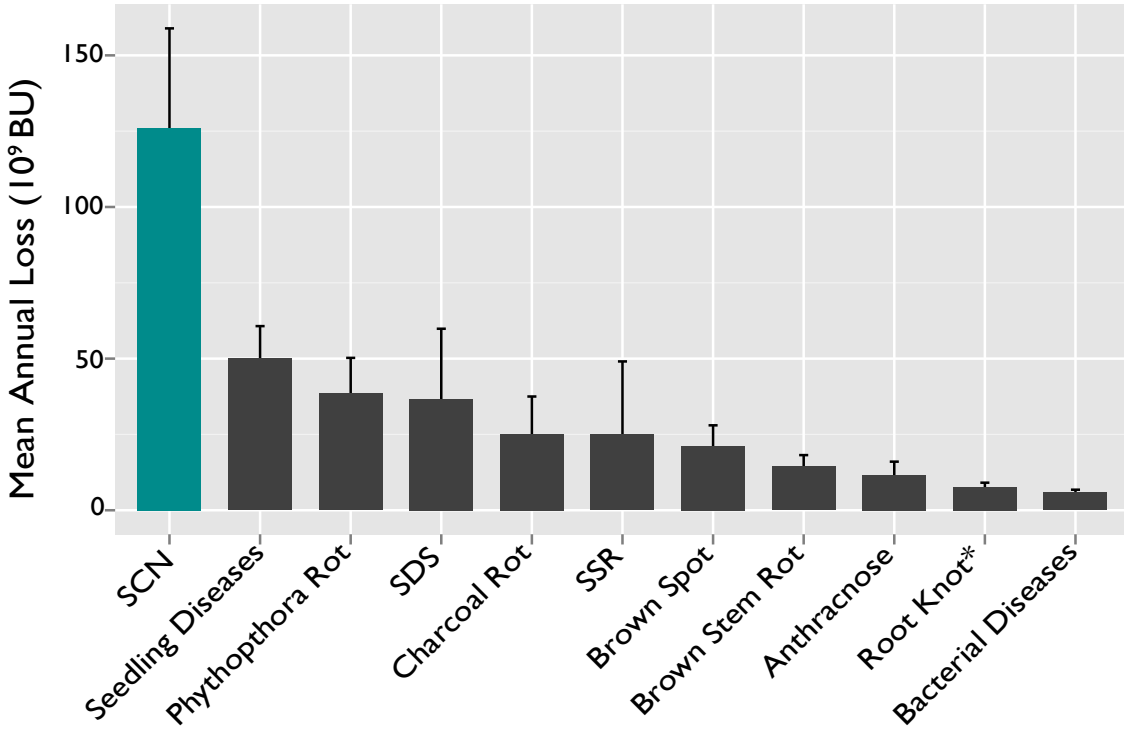

Figure 2.6: US Annual Soybean Production Loss by Disease: Mean losses with standard error bars measured in 1000s BU by common soybean diseases through 2006-2009. Data represent 28 soybean-growing states. SDS = sudden death syndrome, SSR = Scleratinia Stem Rot. *Root knot and other nematodes. (Figure generated using data from Kroenning *et al.* [2])

and international trade. Furthermore, these cost estimates do not include indirect costs associated with managing and monitoring the nematode, which are expected to increase the economic loss by up to double [1]. Addressing the economic impact of SCN in the context of global soybean trade will be key for the US in maintaining a leading position as a soybean producer and exporter over top competing countries.

Due to a number of cooperative extension programs by academic (e.g. by the University of Minnesota, University of Missouri, Iowa State University, University of Illinois, etc.) and private entities (e.g. by the United Soybean Board, American Soybean Association, etc.), producer awareness of SCN has been spreading. Percent yield losses attributed to SCN infection have generally been declining since 1996 due to widespread adoption of resistant cultivars, crop rotations, and detection methods (**Fig. 2.7a**) [1]. In recent years, however, the rising demand for soybeans and subsequent rise in market value keep economic losses increasing. From 2007 to 2010, SCN caused US soybean producers to lose over $1 billion annually (**Fig. 2.7b**) [12, 29].

SCN was first detected in North Carolina soybean fields in 1954, soon after which SCN

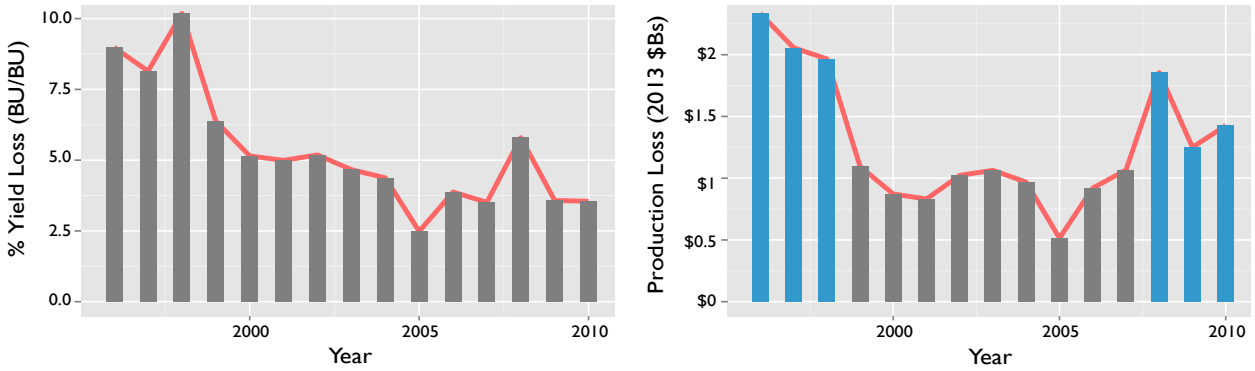

(a) Annual % production

(b) Annual monetary loss

Figure 2.7: Annual soybean losses due to SCN damage, 1996-2010: **(a)** Rapid adoption of SCN management practices decreased soybean loss. **(b)** Recent rises in market prices resulted in higher nominal monetary losses (2013 base year). Blue bars indicate losses over $1.25 billion. Figures were generated from data published by Wrather *et* Koenning, the NASS, and the Bureau of Labor Statistics (BLS) [12, 29, 32, 33].

was found in Tennessee, Missouri, Kentucky, Mississippi, and Arkansas (**Fig. 2.8a**) [34]. By the early 2000's, all soybean-growing states had fields infected with SCN; in 2003 it was estimated 93.5% of all soybean growing areas were infected (**Fig. 2.8b**) [1]. Although no investigation was conducted, it was speculated by those who first identified SCN in the US that the nematodes were most likely introduced with seed imports from China [34]. During the decades following World War 2, soybean acreage increased at a dramatic rate in the US as production expanded from the Southern US into the Corn Belt region. Uninfected fields were likely contaminated through contact with soil from infected fields carried by transport or farm vehicles moving between fields. Presently, nearly all soybean fields in the U.S. have some level of SCN infestation (**Fig. 2.8b**) [1, 35].

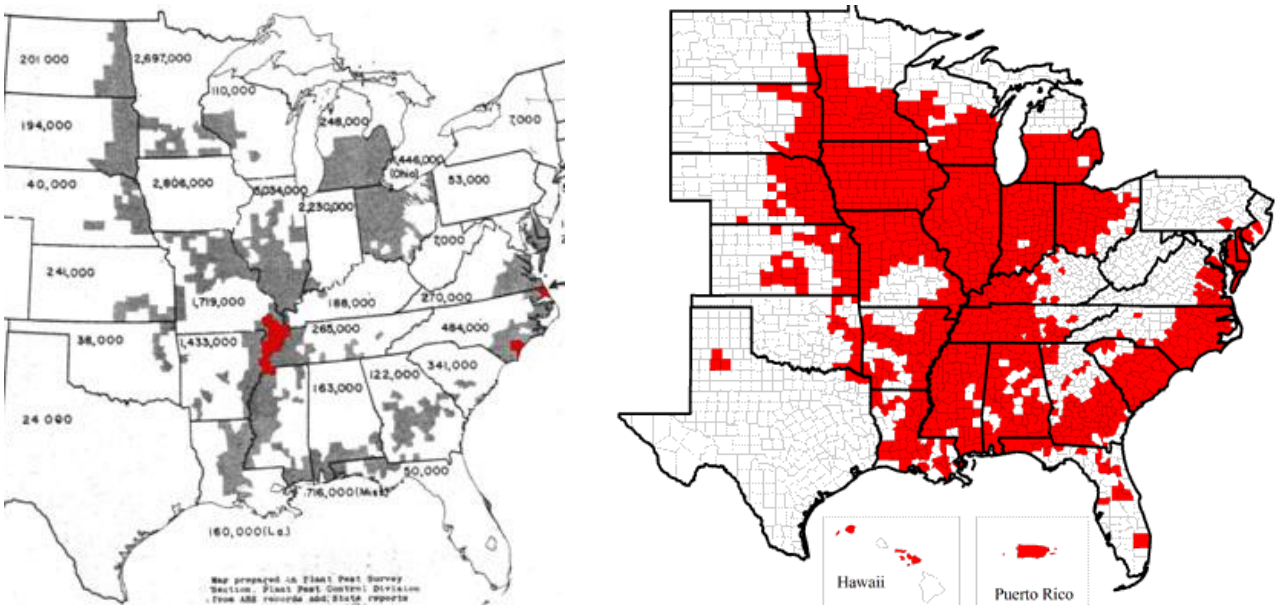

(a) **(b)**

Figure 2.8: Spread of SCN in the US in 1957 **(a)**, and 2008 **(b)**. Gray counties had no detectable SCN. Red counties had at least one SCN-positive field. **(a)** Reproduced from RD Riggs, University of Arkansas. **(b)** Reproduced from Niblack *et al.* [31].

2.2.2 Life Cycle and Parasitism of SCN

SCN, *Heterodera glycines* from phylum Nematoda, is an obligate sedentary plant endoparasite that feeds on the roots of soybeans. The SCN life cycle is typical of most plant-parasitic nematodes: six developmental stages from the egg to four juvenile stages and an adult stage. Mature females continuously produce eggs that are fertilized by males. Next, embryogenesis encompasses the first two juvenile stages (denoted J1 and J2). J2s hatch, begin parasitizing the soybean root and subsequently develop into two more juvenile stages (J3 and J4). Each juvenile stage is punctuated by molts before reaching adulthood [1]. Throughout its life, SCN remain belowground in either immediate proximity to or within soybean roots with a generation time as little as 22 days–given ideal ecological conditions (**Fig. 2.9**) [9].

As they mature, female SCN swell into large, pale, lemon-shaped cysts that eventually darken to brown as the outer wall of the cyst senesces (**Fig. 2.10c**). These cysts give the pathogen their name. Between 0.5 mm and 0.9 mm in length, cysts protrude from the soybean root surface, and are the only life stage visible to the naked eye (**Fig. 2.10b**). Fertilized females can produce between 40 and 600 eggs, up to 200 of which they deposit in gelatinous matrix for immediate hatching (**Fig. 2.10a**) while the rest remain within the female body for delayed hatching or diapause [36, 37]. Dead female cysts eventually

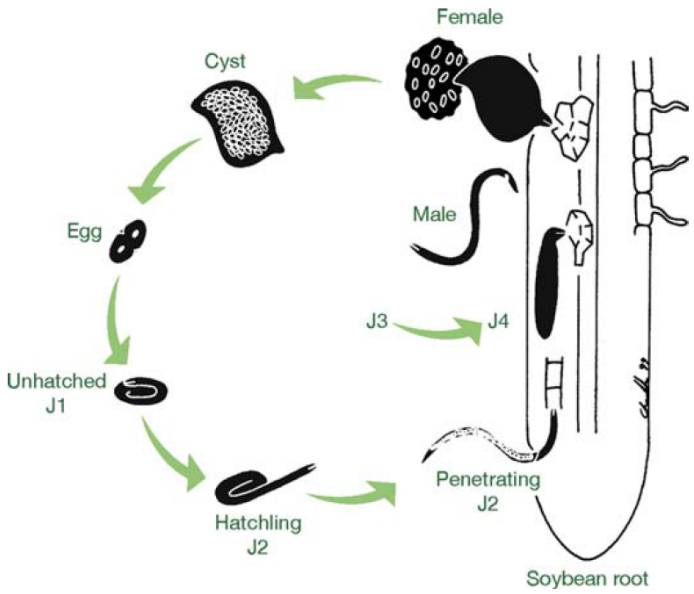

Figure 2.9: Life Cycle of SCN. Not drawn to scale; mature males are 3-4 times the size of juveniles and females can well up to 0.9 mm length cysts. Reprinted with permission from *Annual Reviews* [9].

fall off the soybean root and scatter in the soil around the soybean host roots. The dead cyst is highly robust and resistant to decay [1, 38]. Diapause–an important survival mechanism–will ensure nematode viability during adverse environmental conditions, protecting the eggs for up to nine years until favorable conditions return.

First-stage juveniles (J1) form inside the egg until their first molt, becoming second-stage juveniles (J2) (**Fig. 2.11a**). The initiation of hatching is not well understood, but is believed to be regulated by different combinations of edaphic factors and embryonic J2 readiness. Under favorable conditions, J2s will perforate the eggshell with a hollow needle-like stylet situated at the outer tip of its head [40]. Hatching may be dependent on time, temperature, moisture, oxygen content, and the presence of host root exudates in the soil [37, 40]. Hatching can occur between 16 ^{o}C - 36 ^{o}C at an optimum temperature of about 25 ^{o}C. However, external dependencies can vary even within the same generation of eggs, ensuring a viable reserve of J2s for sudden and dramatic environmental changes [9]. Differential hatching and the robustness of the SCN cyst and eggs are the primary reasons for the difficulty in managing SCN and why completely eradicating SCN has been practically impossible.

In as little as four days, mobile vermiform J2s hatch from the egg, locate and navigate the soil environment to reach the host root via positive chemotaxis towards root exudates [41]. Upon arrival, a J2 will penetrate the host root epidermis, tunnel through the cortex tissues by piercing cell walls with its stylet, and becomes established in the vascular

(a) Gel matrix produced by unfertilized female SCN.

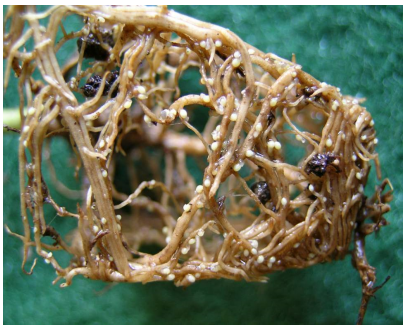

(b) White cysts visible on soybean root.

(c) Visible and browned aging SCN cyst.

Figure 2.10: SCN Cysts on Soybean Roots: **(a)** Females are initially opaque, pale white or yellow and will deposit on average 50-100 eggs into a gelatinous matrix. **(b)** Engorged bodies of fertilized females become so swollen they burst out of soybean roots . **(c)** Aging females cease depositing eggs and darken to a deep brown until they perish and fall off the soybean root. **(a)**: Reprinted with permission from *Annual Reviews* [9]; **(b)** Courtesy of Purdue University. Department of Entomology [39]; **(c)** Courtesy of Iowa State University, Department of Plant Pathology [38]

tissue [42]. Here, the J2 proceeds to develop a feeding site, or syncytium, by secreting a suite of effector proteins which induce dramatic physical and biochemical modifications of targeted vascular cells [42, 43, 44]. The establishment of the syncytium is a highly complicated process that will be elaborated upon further in the following subsection. Initially, the syncytium consists of merely one host cell. However, through a myriad of physiological changes elicited by the secreted effector proteins, adjacent cells will coalesce into the original feeding cell, expanding to incorporate potentially hundreds of cells to form one large feeding site [45]. The syncytium is effectively a metabolic sink from which the nematode intercepts nutrients transported through host tissues.

After feeding for 3-4 days, the J2 will undergo a second molt into a brief (48 hours or less) third stage (J3). At this stage, gender differentiation begins. The development of genitalia continues after a third molt to a fourth-stage juvenile (J4). The female J4 stage lasts for approximately 48 hours, while the male J4 stage lasts for merely 24 hours. As females continue to swell, males, on the other hand, regain their vermiform shape and motility. During their final molt, males exsheath from the J4 cuticle, exit the root, and seek out sedentary females for copulation [9, 44].

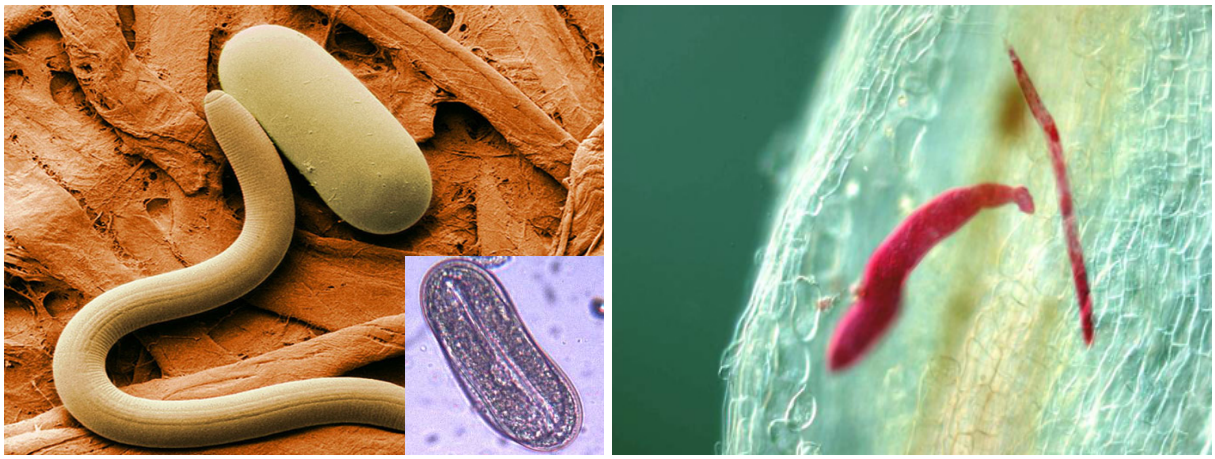

(a) Juvenile SCN and Egg **(b)** J2 Penetrating Root

Figure 2.11: Early Developmental Stages of SCN: **(a)** Large image shows a J2 SCN and an egg magnified 1000 ×. Inset: SCN Egg containing a J1 nematode magnified 200 × **(b)** Two acid fuchsin stained J2s infiltrating the vascular tissue (yellow) of a soybean root. The nematode to the left has been feeding indicated by its swollen size compared to its sibling on the right. **(a)** Courtesy of Agricultural Research Service (ARS) Electron Microscropy Unit [46]). Inset: Courtesy of Purdue Plant and Pest Diagnostic Lab [47]. **(b)** Courtesy of Kris N. Lambert; reproduced from Lambert *et* Bekal [48].

2.2.3 Host-Nematode Interactions during Infection

As J2s migrate into the procambial tissues of the root some damage is inflicted by the physical stabbing by the protractile stylet (**Fig. 2.12a**). However, the vast majority of sustained damage is incurred during the establishment of the syncytium when the nematodes manipulate plant cellular machinery and intercept metabolites thereby depriving the host of energy and nutrients [49]. The J2 accomplishes this by releasing a suite of effector proteins which the host responds to by altering its respiration and photosynthesis [43]. The release of these effector proteins trigger a chain of molecular events and transform host root cells into enlarged, multi-nucleated, metabolically overclocked feeding cells (**Fig. 2.12b**).

While about 70% of effector proteins are novel with undiscovered functions, many of the characterized proteins fall into functional families, including: cell wall degrading enzymes (CWDEs), plant growth regulating and signaling peptides (CLEs), phytohormone mimics, and auxin transport proteins (**Fig. 2.13**) [43, 45]. Microarray analyses of the plant model organism *Arabidopsis thaliana* revealed SCN infection elicited notable changes in gene expression for proteins involved in cell structure, metabolic pathways, protein synthesis, signal transduction, stress response, and transcription [52, 53]. Examples of suggested, yet unconfirmed, functions of these effector proteins include the suppression of plant defenses

(a) SCN J2 Stylet Piercing ISC.

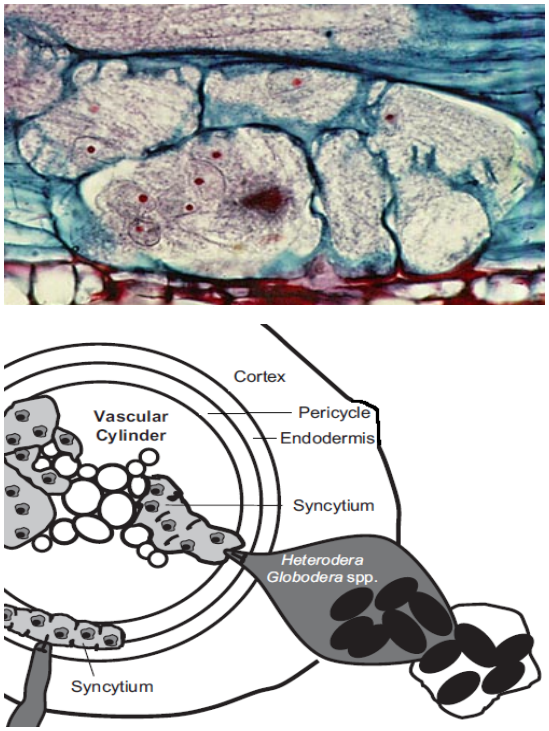

(b) Multi-nucleated Syncytium

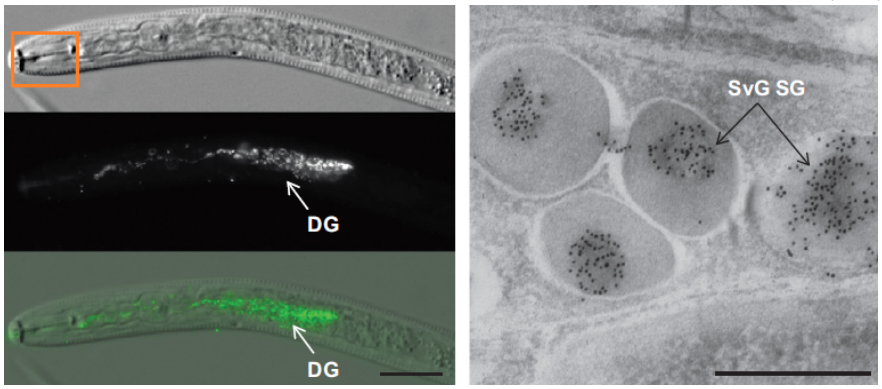

(c) Immunolabelling of effector proteins in preparasitic juveniles.

Figure 2.12: J2 ultrastructures crucial to feeding cell development. **(a)** An electron micrograph of soybean root section 18h after SCN infection. J2 feeding from its ISC via its stylet (St). The expanded rough endoplasmic reticulum (RER) with extensive cisternae (Cs) and plastids (Pd) are visible. The inset shows nematode secrections (NS) which appear as dark granular mass. **(b)** *top* A developing multi-nucleated syncytium showing residual and partially digested cell walls. The enlarged nuclei are stained red. *Bottom* Illustration showing typical location of *Heterodera spp.* syncytia within the procambia vascular tissues. **(c)** *Right*: SCN effector proteins labelled with anti-Hg33E05 antibody are visible within the dorsal glands (DG) and are secreted through the stylet highlighted by the orange box. *Left:* Secretory granules (SG) in *Meloidogyne incognita* within a subventral gland cell (SvG). Scale is 25 μm. **(a)** Reproduced from Endo [50]; **(b *top*)** courtesy B.Y. Endo; Reproduced from Davis *et* Tylka [51]; **(b *bottom*, c)** reproduced with permission from *John Wiley and Sons* [43].

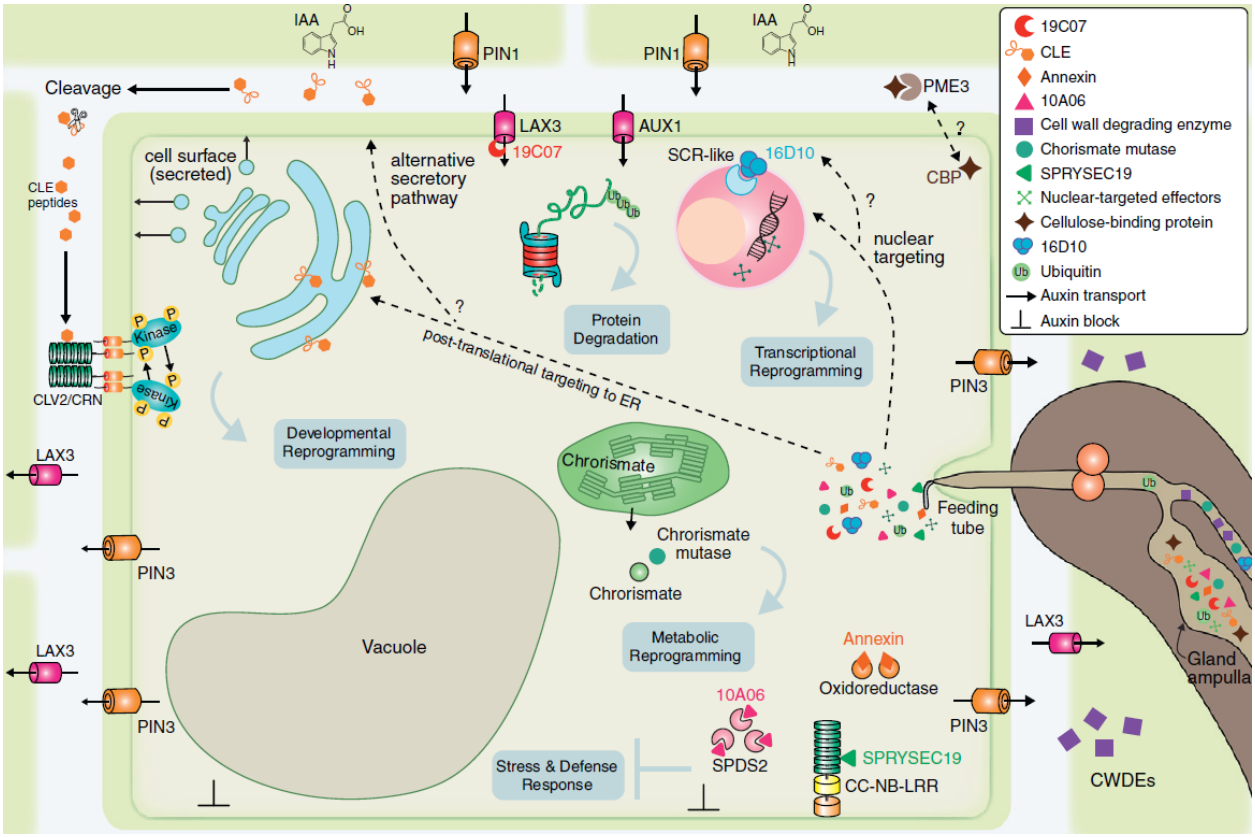

Figure 2.13: Cyst nematode effector proteins manipulate plant cellular mechanisms. Figure highlights: PIN1s are inhibited in the basipetal direction to facilitate the accumulation of auxin in the ISC. PIN3s are activated to transport auxin radially to facilitate the incorporation of adjacent cells. Nematode effectors also target the AUX1/LAX families to increase auxin influx towards the nematode. Nuclear-target effectors contain nuclear localization signals for transport into the plant nucleus. Reproduced from Gheyson *et* Mitchum [45].

and cellular reprogramming to increase the rate of metabolic activity [43]. For instance, J2s were found to have polymorphic expression of chorismate mutases (CMs) which catalyze the conversion of chorismate to prephate in the shikimate pathway [54]. However, this pathway exists in plants, but not animals. Most likely, the secretion of CM by SCN is intended to manipulate endogenous production of plant hormones, aromatic amino acids or other shikimate successors [49]. Alternatively, the presence of CM polymorphisms in various virulent strains points to a role in SCN virulence [54]. The complexity of the host response to parasite effector proteins has stimulated a new and exciting area of research that may shed light on alternative mechanisms for SCN resistance, and present opportunities for deeper understanding of plant cell biology. Detailed explanations of experimentally isolated effector proteins are given by Gheyson *et* Mitchum [55].

The formation of the syncytium begins with the J2 selecting a single parenchymal or

cortical vascular cell that becomes the initial syncytial cell (ISC) [56]. The J2 pierces the ISC with its stylet in two phases: the feeding-preparation period and the feeding period. Though the purpose of the feeding-preparation period is still a subject of investigation, the cytoplasm and vacuole of the ISC are partially emptied. The J2 withdraws and reinserts its stylet into the ISC and begins secreting effector proteins. The effector proteins are produced from the subventral and dorsal pharyngeal glands and are injected through the stylet (**Fig. 2.12c**). Protoplasts of neighboring cells fuse when plasmodesmata widen, while CWDEs, including cellulases (β endoglucanases), and pectinases hydrolyze cell walls of neighboring procambial cells [45, 55]. Differentiated xylem cells are not incorporated and create a barrier to the syncytium [56].

During this time, the nematode allows the protoplasm to continue to proliferate, resulting in a denser, electron-rich cytosol. The dissolution of cell walls and condensed plastids causes several anatomical changes. The nuclei experience hypertrophy and become irregular in shape while losing a small amount of heterochromatin. The primary vacuoles diminish in size while many smaller vacuoles appear. Plastids and mitochondria proliferate rapidly, taking up to 0.5% and 0.7% more area, respectively [56]. Meanwhile the rough endoplasmic reticulum (RER) extends its lumen and increases the surface area of its major cisternae. Each of these changes supports the core function of the syncytium– efficient and rapid metabolic activity to accumulate solutes and metabolites for the nematode. On the other hand, syncytial cell walls are fortified to withstand increased osmotic pressure by constructing new layers and isolating the syncytium symplastically [49, 55, 56].

While fortifying the syncytial cell walls, the nematodes also need to manipulate transport of nutrients into the cytosol. One crucial mechanism that has been demonstrated recently in a close relative of SCN, the sugar beet cyst nematode, *Heterodera schachtii*, is the redirection of auxin transport [57]. This is carried out through manipulating the polarities of AUX1/LAX and PIN transmembrane auxin-transport families which control the auxin influx and efflux, respectively [43, 57]. The accumulation of auxin in the syncytium has been shown to be critical in its initiation and expansion; *pin1* soybean mutants were found to have 40% fewer cysts than infected wild-type soybeans [57]. A proposed model for this process has been elegantly described by Gruenwald *et al.* [57].

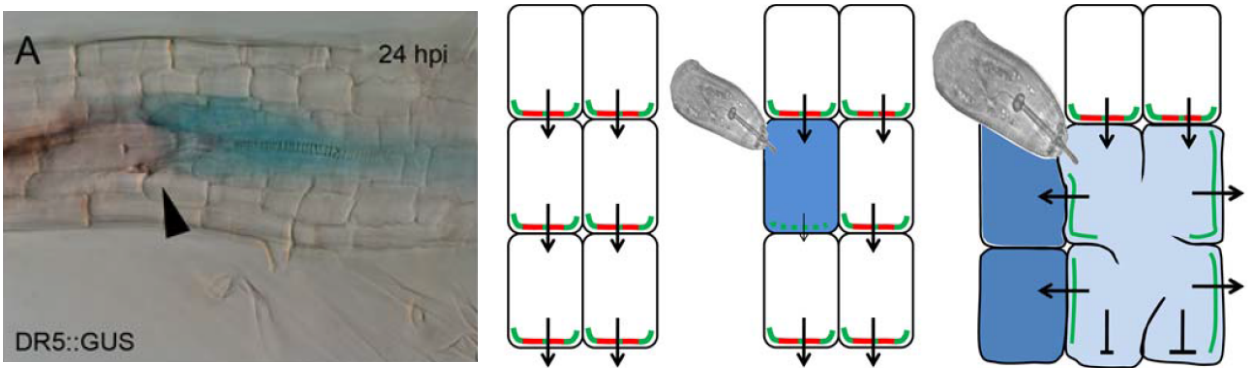

(a) Auxin activity in ISC

(b) Potential mechanism for PIN-mediated auxin transport

Figure 2.14: SCN direct auxin accumulation in syncytia: **(a)** Auxin activity indicated by the DR5 reporter and β-glucuronidase (GUS) within the ISC. The black arrowhead points to the SCN J2 head. **(b)** A proposed mechanism for PIN-mediated auxin transport for accumulation in the syncytium. Both figures reproduced from Grunewald *et al.* [57].

2.3 Current Methods of SCN Management are Inadequate

Currently, no practical solutions have been found that completely eliminate SCN from infected fields. Once SCN becomes established, soybean farmers are forced to managed their fields as though it were a chronic condition requiring indefinite care in order to preserve their profit margin. As in all decision-making situations, adoption of pest management practices are dictated by the economic theory of opportunity cost. Farmers, whose livelihoods depend on profits from soybeans, are at constant odds with the threshold of input costs and fluctuating soybean market values at the center of their business. Intuitively, from the standpoint of the SCN life cycle, one might suggest a long-term solution may be to replace the production of soybeans with non-host crops for several consecutive years. However, it is economically impractical for soybean producers to absorb the expenses of producing less profitable crops. This restriction is an added difficulty in the pursuit of cost-effective management and detection programs.

Many methods exist for controlling SCN though only the most widely deployed integrated management program (IPM) consists of rotating SCN-resistant soybean cultivars and non-host crops. Alternative methods include the application of chemicals including nematicides, seed treatments, applying organic amendments such as manure, biological control (biocontrol) using antagonistic microorganisms, soil suppression, winter weed management and cultural practices such as late season planting and cover cropping [37, 39, 58, 59, 60]. However, most of these proposed solutions perform inconsistently, leaving many US soybean organizations hesitant to recommend them [38, 39, 61, 62]. Fumigation agents and seed treatments are produced commercially, but are costly and

are even ineffective under certain conditions [1]. Biocontrol agents are currently being investigated and show promise, but as of the time of this writing no widely accepted commercial products for SCN have been developed. The following subsections discuss crop rotations, resistant cultivars, and biocontrol in more detail as the first two are currently widely used and the latter more promising.

2.3.1 Symptoms and Diagnosis of Infected Fields

One of the challenges in dealing with SCN is it often goes unnoticed or misdiagnosed due to the pest's underground life-cycle and the similarity of aboveground symptoms to other plant pathologies. Often, SCN does not cause any obvious aboveground symptoms while still inducing yield losses [35]. When symptoms do arise, usually plants are worsened by a secondary affliction, such as nutrient deficiencies (i.e., potassium, nitrogen, and iron), drought stress, and other diseases [9]. Symptoms that are exhibited are nonspecific to SCN including stunted growth, and leaf chlorosis (**Fig. 2.15**). On the other hand, soybean farmers are advised to vigilantly scout for belowground symptoms between 4-6 weeks after planting. During this time female SCN cysts are likely to appear on the soybean roots and stunting of roots may also be apparent [61]. Limited knowledge about SCN prevalence often results in poor utilization of disease management plans. In the meantime, soybean producers can suffer yield losses for several years without taking notice. Regular soil testing for both undiagnosed and diagnosed fields is therefore highly recommended for expedient diagnosis and informed disease management [39, 61, 63].

Figure 2.15: Aeriel view of SCN infected experimental fields showing varying levels of stunting and yellowing. Reproduced from Kurle *et al.* [63].

Egg assays and HG Type tests from field soil surveys can yield useful information beyond diagnosing SCN epidemics. In general, the standard protocol involves collecting multiple soil plugs per uniformly spaced n-acre cells, isolating cysts, releasing and counting the SCN eggs per volume (typically 100 cc or 250 cc) of soil also known as egg

densities [37]. SCN egg densities have been shown to be relatively good predictors of yield loss [64, 65]. The population density of SCN at the time of initial diagnosis for a particular field is called the *action threshold*. The action threshold is used to develop a customized management strategy and acts as a benchmark for further action should SCN numbers surpass it [9]. Furthermore, GPS tagging of sample sites can allow commercial and public testing agencies to map population densities over the field area (**Fig. 2.16**). Mapping information can be crucial for SCN management strategies because SCN population distributions are incredibly patchy [9, 64]. With a more detailed picture of the nature of their infestation, soybean farmers could more strategically prioritize areas of high nematode density or more confidently determine whether their management practices are indeed effective.

HG (*Heterodera glycines*) Type tests are used to determine the particular virulence (nematode growth success on resistant plants) phenotype(s) of the population (**Table 2.1**) [63]. The HG classification scheme is used to identify which of seven distinct sources of SCN-resistance in soybeans are still susceptible to the population. This is useful for making resistant cultivar recommendations from 100s of available SCN-resistant cultivars.

Table 2.1: Indicator lines for HG type classification of genetically diverse populations of SCN. PI = Plant Introduced. Reproduced from [66].

Number	Indicator Line
1	PI 548402
2	PI 88788
3	PI 90763
4	PI 437654
5	PI 209332
6	PI 89772
7	PI 548316

First, a bioassay is conducted in a greenhouse; SCN collected from the field are grown on cultivars from each of the seven SCN-resistant germplasm lines [31, 67]. Female SCN are counted for a measure known as the Female Index (FI, **2.1**) is used to evaluate the indicator lines (i.e. sources of resistance) on which the population is virulent:

$$\text{FI} = \frac{N_x}{N_s} \times 100 \tag{2.1}$$

Where N_x = average number of females on cultivar x, and N_s = average number of females on the susceptible control cultivar. The lower the FI, the more resistant the indicator line is to the tested population. Knowing the HG Type of an SCN population

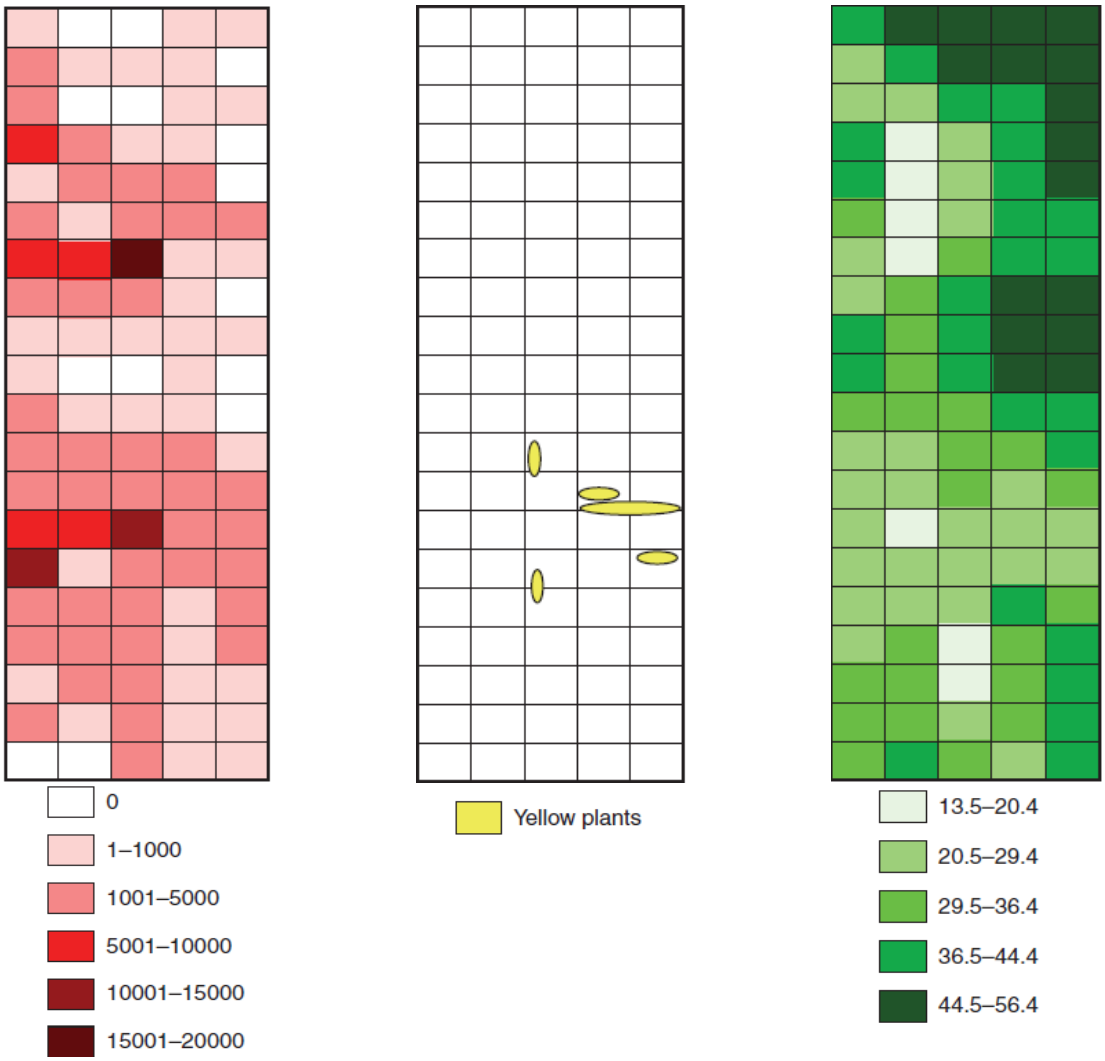

(a) SCN eggs (count/100 cc soil) **(b)** Stunting and chlorosis **(c)** Soybean yield (BU/acre)

Figure 2.16: SCN distribution and soybean yield are uncorrelated with aboveground symptoms. Reprinted with permission from *Annual Reviews* [9].

can not only help producers choose effective SCN-resistant varieties and evaluate the resistance strength over time [9, 37, 63]. Employing a regular program of soil sampling, though it raises the input costs of producing soybeans, is a vital tool for controlling SCN epidemics and contributes significantly to the success of the crop in the long run.

2.3.2 Current Management Strategies

In general, SCN management strategy is twofold: apply methods that suppress SCN proliferation, and maintaining strong plant vigor in order to preserve yields despite suffering from parasitism. The latter portion involves ensuring ample nutrients and water, adequate drainage, and control of other pests, weeds, and plant diseases [59, 63]. The aim is that promoting vitality of the soybeans will compensate for damage caused by persistent parasitism enough to continue to yield sizable and numerous seeds. Improving crop health however does little if anything to reduce SCN population densities; nematode suppression tactics, such as crop rotations and resistance are utilized in parallel [58, 60].

Commercially available soil fumigants, such as those containing methyl bromide (MBr) are effective in reducing SCN populations, though their results are dependent on many factors including: soil type, rainfall, and drainage [68, 69]. Thus, it is difficult for producers to predict whether fumigation will be cost-effective. Another limitation is the acute toxicity of their active ingredients; their use is tightly regulated due to human and environmental health concerns [69, 70, 71]. Because they are highly damaging, broad-spectrum, and are used in significant quantities, these fumigants need to be applied up to three weeks before planting during which the soil may need to be tarped to prevent releasing toxic chemicals into the atmosphere [72]. During this time, it is almost certainly eliminating beneficial soil microbes as well. Therefore, soil fumigants are a high-risk option and are recommended only under emergency situations; a field is heavily compromised by numerous pests and sounder methods are unlikely helpful in a short time frame [39, 63, 72].

Other population control tactics such as inorganic and organic soil treatments may also be employed, but typically only to augment crop rotations and resistant cultivars. Suppressive soils in general do not allow “the pathogen [to] establish or persist, [establish], but [cause] little or no damage..." even if the pathogen is persisting, but controlling edaphic factors and reinforcing competitive or antagonistic soil microbiota [59]. However, the broader ecological principles are still being investigated and the performance of management practices such as tilling have been found to perform inconsistently depending on the soil type and the endemic microbial community of the field [73, 74, 75]. SCN may never be eliminated from a field, but vigilant management and monitoring can keep populations low and yields relatively high.

2.3.3 Crop Rotations with Resistant Cultivars

Rotations are an effective means of SCN management that remove the source of sustenance for the nematodes by replacing soybean for a non-host crop at least one growing season. The number of juveniles and eggs decline initially in the absence of a host, leaving behind dormant cysts [66]. When soybeans are planted in the following rotation, the SCN population will rebound to either a smaller or greater extent if resistant or susceptible soybeans are planted, respectively [76, 77]. In severe situations, it can take several years of rotations to reduce population numbers below *damage thresholds*[1] [66].

In many Midwestern states (Iowa, Illinois, Indiana, Missouri,and Minnesota), rotations most commonly alternate between resistant cultivars and corn (**Fig. 2.17**) [39, 61]. However prolonged use of cultivars from the same resistance germplasm (for instance PI 88788) can result in SCN populations adapting to those sources of resistance, thereby reducing the effectiveness of that germplasm [4, 78]. To maintain the effectiveness of resistant germplasms, producers are advised to alternate between three different cultivars to obstruct SCN adaption to one particular resistance [9, 16, 38, 63]. Variations of crop rotations with resistant cultivars can improve yields by up to 30-50% and reduce egg densities by 10-28% [76, 79, 80]. Additionally, this IPM is economically trivial and remains the most effective method soybean producers use to control SCN.

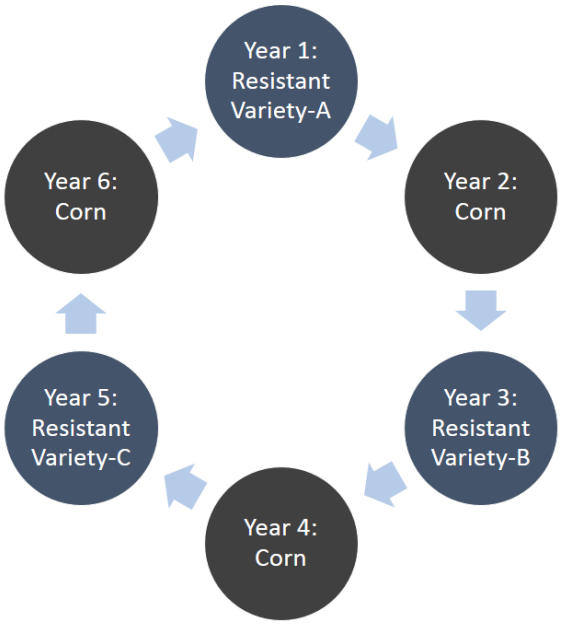

Figure 2.17: Example of a 6-year crop rotation scheme.

[1]The level of SCN infestation at which yield losses are expected. The exact number varies from region to region. This is distinguished from the *action threshold*, the level of SCN infestation that is first detected. At the action threshold, growers are encouraged to develop a long-term strategy to reduce future losses.

2.3.4 SCN Biopesticides

Although there no widely accepted commercial biocontrol agent currently exists, biocontrol is increasingly being looked at as a promising component for integrated SCN management and as an alternative to currently registered chemical nematicides. The application of commercial chemical agents to modify soil properties (e.g. pH, ion levels, and salinity) such that the environment becomes obstructive to SCN propagation has often resulted in substantial negative consequences including the collapse of non-target populations such as insect pollinators and the accidental exposure to humans through food [3, 81]. Likewise, the use of nematicides is expensive and controversial in terms of environmental impact and long-term effectiveness; a prodigious amount of the agent is needed for adequate coverage and is only justifiable for severely infested fields [38, 39, 62]. Furthermore, many states are imposing increased restrictions on nematicide application and the end-use destinations of treated seeds to reduce exposure to humans, animals, and the environment [82, 83, 84]. The unpleasantness of these chemical pesticides provides impetus to seek out sustainable, more environmentally benign alternatives. Nature has built-in regulatory agents for ecosystem population densities. Predators, parasites, and microbial agents can be artificially introduced as surrogate enemies of target pests. When these "biopesticides" become established, they can exert long-term regulation of pest population densities with relatively little active management [3].

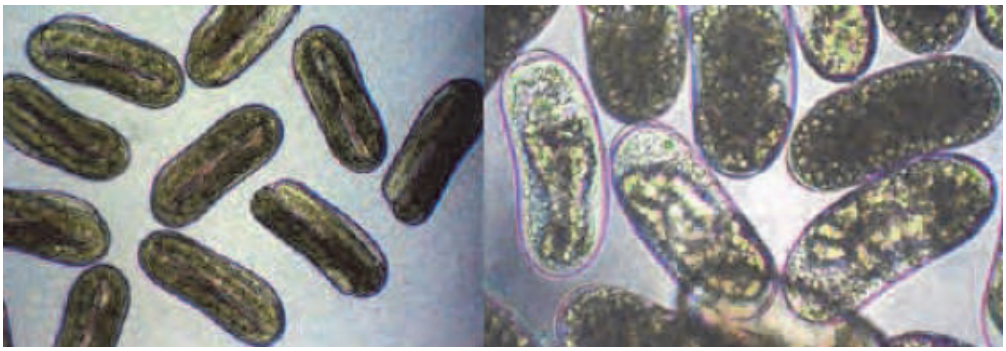

Figure 2.18: Effect of fungal culture filtrates on the development of embryonated eggs. *Left:* Mature healthy SCN eggs containing J2 embryos after 10 days of incubation. *Right:* Abnormal eggs 10 days after treatment with filtrate from a *Lecanicillium* AaF42 hybrid strain. Reproduced from Koike *et al.* [85].

Microorganisms isolated from SCN eggs and cysts have been shown to be antagonistic or parasitic and successfully reduce SCN populations in greenhouse experiments . These biocontrol agents can harm SCN in the following ways: trapping or predation, endoparasitism of vermiform SCN, parasitism of cysts and eggs, production of toxins, and competitive and noncompetitive inhibition [58]. Examples of nematophagous fungi

harmful to SCN are *Fusarium spp.*, *Hirsutella spp.*, *Paecilomyces lilacinus*, *Lecanicillium*, and *Arthrobotrys spp.* [58, 85, 86, 87]. Fewer species of bacteria have been identified as potential biocontrol agents for SCN, such as *Pasteuria spp.* and *Bacillus spp.* both of which are endospore-forming parasites of multiple SCN life stages. Most studies focus on strains *Pasteuria penetrans* which show promising levels of SCN suppression. However, many of these organisms have difficulty colonizing SCN populations, are difficult to culture at a commercial scale, or experience a significant delay until antagonistic activities begin [58, 87].

Currently, a few experimentally tested commercial biocontrol products are available such as Poncho®/VOTiVO® (Bayer CropScience), NemOut™ (ProPhyta), and Clariva™ pn (Syngenta®). Though NemOut and Poncho® /VOTiVO® were not developed specifically for SCN, studies have shown that both are able to suppress vermiform life-stages and reduce the Female Indexes in greenhouse and field microplots [88, 89]. NemOut™uses the egg-parasite fungus *P. lilacinus* strain 251 (PL251) and is mainly marketed for suppressing the cotten pest, *Rotylenchulu reniformis* or reniform nematode. Another commercial product using PL251, MeloCon™ WG (Certis USA, LLC) is sold as a general biocontrol agent for most plant-parasitic nematodes including *Heterodera spp.* [90, 91]. Poncho®/VOTiVO® uses *Bacillus firmus* strain GB-126 (GB126), as its active agent. As opposed to PL251, GB126 does not directly antagonize SCN. Instead, GB126 compete with SCN for space surrounding soybean roots for up to 12 weeks while also consuming root exudates that SCN are believed to rely on to locate roots [92]. A Bayer CropScience-funded pot trials study corroborated that GB-126 can reduce SCN cyst populations in the soil by 84% and juveniles by 91% [89]. Clariva™ Complete Beans are a soybean seed product coated with a mixture of nutrients, chemical pesticides, and *Pasteuria nishizawae* (*P. nishizawae*) endospores. *P. nishizawae* are obligately parasitic bacteria that attach to the cuticle of SCN J2s, germinate upon the start of SCN feeding on soybean roots, and disentegrate the SCN host by the time the SCN reach adulthood [93]. Syngenta found in its own field trials that the Clariva™ Complete Beans improved yields by 4.1% over resistant cultivars treated with an insecticide/fungicide check [94].

2.4 Considerations for Biocontrol of Pest Populations

2.4.1 Introduction of a Control Agent: Concerns for Non-Target Effects

Biological control is increasingly becoming a key component in IPM for food production. Advocates point to its limited environmental effects as well as its ability to counterbalance the growing resistance of pests to chemical control agents and its potential to lead to the withdrawal of these chemical agents [95]. The goal of biological control is a sustained reduction of a target pest species to mitigate or control its negative impacts to an ecologically or economically acceptable level. By using a natural, sometimes non-indigenous[2], enemy as a control agent, the method is often described as a promising environmentally benign alternative to other methods such as the use of chemical control agents [81, 98].

However in practice, past implementations of biological control for conservation purposes or pest control have sometimes resulted in disastrous, irreversible, and unintended consequences [99]. Many early projects involving invertebrate agents and pests relied heavily on broad 2-species interaction concepts while giving community, biogeographic, and ecosystem effects only cursory considerations [96]. Louda *et al.* provide an extensive reexamination of 10 biocontrol case studies in which the introduction of a biocontrol agent results in devastating ripple effects throughout a native ecosystem [99]. The repercussions of ignoring the complexities of ecosystem dynamics has provided numerous valuable insights into the cost-benefit considerations revolving around biocontrol-related decisions. Progress in reducing non-target effects can also be attributed to the improved legal infrastructure by government agencies, biocontrol decision-making and project monitoring moving from the hands of private entities to government agencies, or international groups assisted by available scientific expertise, better understanding of threats to the local ecology, economy, or food security imposed by a target pest, and increased monitoring of biodiversity in a growing number of ecosystems [97].

An important consideration for minimizing the risk of harmful ecological impacts during the introduction of an agent is to choose an agent with high host specificity. In these cases, the model for two-species interactions will be more representative [96]; the predator population will be positively correlated with the target population and therefore

[2]The introduction of a native enemy control agent of an exotic pest constitutes *classical biocontrol* whereas the introduction of a non-native enemy to attack a native pest is termed *neoclassical biocontrol* or *new-association biocontrol* [96, 97].

its geographic range will be limited to the range of the pest. Microbial agents[3] (such as bacteria, fungi, and viruses) have been demonstrably successful against arthropod pests in agro-ecosystems [95, 100].

2.4.2 Commercial Considerations for Biocontrol Products

Biocontrol product development, or the prospect of production, is often compared with the analogous process for chemical control agents [59, 95, 96, 101]. Bale *et al.* discuss significant cost-benefit advantages of biocontrol product development versus its chemical counterpart, especially in cases leading to pesticide resistance. Both types of products are estimated (or in the case of chemical pesticides, averaged) to take approximately 10 years from the extensive research and development, US Environmental Protection Agency approvals, to product release. On the other hand, the development of biocontrol agents is estimated to cost much less than the development of pesticides–$180 million for a new insecticidal chemical (tested amongst $>$3 million ingredients) versus $2 million for an agent (out of 3000 microbial candidates) [95].

However, commercializing biocontrol agents presents numerous unique challenges from the mass production of chemical pesticides. Scaling up a microbial agent may only require large amounts of unspecific media in which case contamination of cultures may be an issue. Other organisms need to be cultured within their prey; scaling up the production of the prey organism creates further challenges that increase with greater biological complexity of the prey [101]. Another challenge is the limited shelf life of biocontrol products which is typically within days or weeks [95]. Naturally, this presents significant difficulties maintaining the effectiveness of the organisms during transport and storage the product before use.

Furthermore, the output of biocontrol products may have initially been slow due dominance of chemical pesticides in the pest control market. As environmental regulations and consumer demand for environmentally-friendly products have deflated the chemical pesticides market, large corporations (such as Monsanto, Syngenta, and Bayer Crop Sciences) are moving to fill subsequent gap with biocontrol products. Another prior roadblock that is increasingly becoming moot is patenting biocontrol products [95]. Wild-type biocontrol agents are unpatentable themselves. However, genetically modified organisms are patentable as well as indirectly related technologies involved in the package, storage,

[3] As opposed to macrobial agents, such as nematodes, predatory insects against other arthropods, herbivorous insects against weeds, and parasitoids [95].

and application of the organism[4]. As the framework for commercializing and using biocontrol products continues to mature, companies will be able to bring increasingly more products to market.

2.5 Nematode Viruses

Despite the relative abundance and diversity of nematodes and viruses, nematode-infecting viruses are not well studied. This is likely due to relatively limited research focus and general clinical applications of nematode pathogens. Plant-pathogenic nematodes have been known to vector plant-infecting viruses by consuming virus particles while feeding from the roots of infected plants and transmitting the particles when they move to new plant hosts [5]. Nematode-transmitted viruses belong to two taxonomic groups: nepoviruses and tobraviruses, which are transmitted by the nematode families *Longidoridae* and *Trichodoridae*, respectively [102, 103]. However, these previously reported findings did not observe virus replication within the nematode vectors.

Though it was believed that viruses infecting nematodes were common given their vast abundance, diversity of morphologies, range of known hosts, and plastic responses to host immune systems, no virus had ever been recorded parasitizing nematodes [104]. That is, until a 2005 study conducted by Lu *et al.* artificially infected *Caenorhabditis elegans* (*C. elegans*) to demonstrate the potential of nematodes as model organisms for genetic studies of antiviral response in eukaryotic hosts [105]. Félix *et al.* were the first to describe natural nematode-infecting viruses found *C. elegans* and its close relative *Caenorhabditis briggsae* (*C. briggsae*). Both isolates were found to be closely related to members of the *Nodaviridae* family. These novel viruses opened the doors to studying viral infections in a convenient whole animal model organism, *C. elegans* [106].

The discovery of the first plant parasitic nematode viruses was made by Bekal *et al.* in laboratory SCN lines that had inexplicably collapsed. Four distinct negative-sense ssRNA viral genomes were found [7]: SCN nyavirus (ScNV), SCN rhabdovirus (ScRV), SCN phlebovirus (ScPV), and SCN tenuivirus (ScTV)–which were named for their closest relative according to BLASTX phylogenetic analysis. These viruses were present in both egg and J2 stages suggesting vertical transmission occurs (**Fig. 2.19**). Horizontal transfer from males to females during sexual reproduction has also been observed [KN Lambert, personal communication]. Tenuiviruses, and phleboviruses are part of the *Bunyaviridae* family, which are commonly entomopathogens. Some bunyaviruses have already been

[4]Assuming the technologies are sufficiently unique from previous patents.

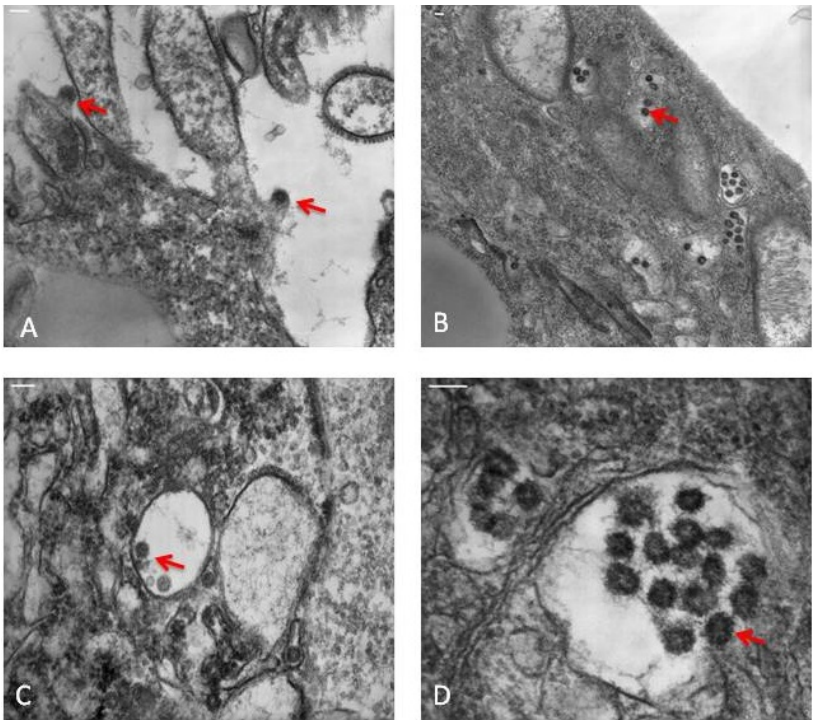

Figure 2.19: Transmission electron microscopy images of an SCN female co-infected with all five viruses, though it is impossible to discern which virus corresponds to which particle. Particles are marked by red arrows and from images A-D measure 70, 50, 70, and 80nm in diameter, respectively. Particles in B-D can be seen budding from the cell. Courtesy of Sadia Bekal.

incorporated into commercial biopesticides for controlling specific agricultural insect pests; [3, 101].

The first positive-sense SCN virus (ScV5) was also discovered by Bekal *et al.* and was found to be distantly related to flaviviruses and pestiviruses [8]. ScV5, as well as the other SCN viruses have been detected in greenhouse and field nematodes, suggesting they are common in nematode populations. However, since the discoveries are so recent, physiopathologies, and epizootiology of these viruses in the field is unknown. It is also likely given the geographic range of SCN in the US that many more elusive SCN viruses exist with a wide range of pathologies.

The pathologies of the aforementioned five SCN viruses have yet to be investigated. It is still unknown which of the viruses is responsible for collapsing SCN laboratory cultures. The viruses were identified from inbred nematode cultures sampled over four years, indicating sustained infections occurred over several generations. ScV5 is expected to be the most likely candidate for a biocontrol agent due to having a positive-polarity single-stranded genome that would be immediately infectiousness. On the other hand, rhabdoviruses cause diseases in a wide phylogenic spectrum of hosts, including

vertabrates, plants, and arthropods [107, 108, 109] . In the context of biocontrol, it will be important to understand the symptoms and reproductive costs to SCN, the impacts of cohabiting pathogens, and transmission rates across genders and transmission modes.

2.6 Host-Pathogen Coevolution

Theoretical and experimental approaches in biocontrol are based from a cross-pollination of epidemiological and ecological frameworks [110]. Both areas are arguably more developed and better understood than biocontrol. The public health concerns regarding saving human lives from and containing devastating infectious diseases[5] has driven the need to understand the mechanisms of disease spread in epidemiology. Conservation concerns have greatly driven the need to understand how intraspecies interactions, and dramatic augmentation of trophic levels effect the population dynamics of a species of interest. Furthermore, the high rate of phenotype changes of pathogens *vis-a-vis* the adaptive arms race against their hosts motivates the integration of ideas from evolutionary ecology. Thus, numerical investigation of the introduction of a microbial agent into a pest population incorporates modeling the long-term pest population dynamics with disease spread and virulence evolution within these populations.

The system of equations most frequently adapted from to describe populations in biological systems are the Lotka–Volterra predator–prey model (**2.2**). The prey and predator are represented by x and y respectively while the constants α, β, γ, and δ represent growth, predation, and death constants.

$$\frac{dx}{dt} = x(\alpha - \beta y) \tag{2.2a}$$

$$\frac{dy}{dt} = -y(\gamma - \delta x) \tag{2.2b}$$

With microbial biocontrol agents, however, the basic epidemic system of equations–the Susceptible-Infected-Recovered (SIR) type models–are more appropriate [111, 112]. (**2.3**) make up the basic framework of SIR modeling. $S(t)$, $I(t)$, and $R(t)$ represent compartmentalized portions of the total population $N(t)$, i.e. $N = S + I + R$. S represents the number of susceptible individuals, I represents the number of infected individuals and R represents the number of recovered individuals [6]. Finally, β^* represents the rate of

[5]Infectious diseases are illnesses caused by an infectious agent (pathogen) that can spread between individuals [111].

[6]This assumes that once an individual is cured from a disease, they will be immune from that point

transmission [7], while ρ represents the rate of recovery by an infected individual.

$$\frac{dS}{dt} = -\beta^* IS \tag{2.3a}$$

$$\frac{dI}{dt} = \beta^* IS - \rho I \tag{2.3b}$$

$$\frac{dR}{dt} = \rho I \tag{2.3c}$$

The SIR model is often improved upon to fit to real-world data and the mechanisms of disease spread for certain pathogens. Some additions include ordinary differential equations describing the population of a vector, vaccination behaviors, and reinfection of a "recovered" individual. Rock *et al.* give a detailed review of many mathematical extensions used in conjunction with the SIR model for a variety of infection diseases [111].

2.6.1 Virulence Theoretically Evolves Towards an Optimum

In theory, pathogens, including viruses, face an adaptive tradeoff between fecundity and host resistance in what is commonly known as the trade-off theory. This phenomenon is driven by the host's own adaptive tradeoff between the costs of resistance (energetic or otherwise) and risk of infection [110, 113, 114]. Exploitation of the host improves the pathogens transmissibility, but at the cost of the host's survival and therefore the time available for transmission. The virulence–transmissibility tradeoff has been demonstrated empirically in malaria models (*Plasmodium spp.*): transmission and virulence are positively correlated until the benefit of increased transmission no longer outweighs the concomitant increase in host mortality [11, 113, 115].

Following the SIR paradigm, a definition of fitness emerged called the *basic reproductive ratio*, R_0 (**2.4**):

$$R_0 = \frac{\beta S}{b + v + \rho} \tag{2.4}$$

where β is the transmission rate, S is the number of susceptible hosts, b is the baseline mortality rate of the host, ρ is the recovery rate at which the infected hosts are cleared

onward.

[7] In some texts, β^* is referred to as the *rate of infectivity* or the rate of change in infected individuals within a population. To distinguish this β^* from the definition of transmission rate for empirical studies as well as for SCNSim– defined as the portion of viral burden successfully transferred to the new host–we will denote our transmission rate simply as β.

of the pathogen, and d is the mortality rate of infected hosts [113, 116]. Generally, R_0 is the rate of new infections emerging with respect to the rate of depletion of the existing infections through death or recovery of the host, or through the loss of a viable pathotype. If the rate of depletion is higher than the rate of emergence, the epidemic will attenuate while the opposite is true if the rate of emergence is higher than or equal to the rate of depletion (**2.5**).

$$R_0 \begin{cases} < 1 & \text{the epidemic will go extinct} \\ \geq 1 & \text{the epidemic will persist} \end{cases} \tag{2.5}$$

R_0 is therefore often used to characterize the fitness of the pathogen at the epidemic level. In theory, pathogens will evolve to maximize R_0, that is, to maximize their rate of disease spread and their duration of infection [11]. However, because R_0 is defined from the SIR model, the same assumptions apply: pathogen adaptive dynamics occur in much shorter time scales than their evolutionary dynamics, and host populations are at or near maximum capacity. Pathogens with high mutation rates, such as RNA viruses, violate the former assumption [117]. Examples from empirical studies are reviewed below.

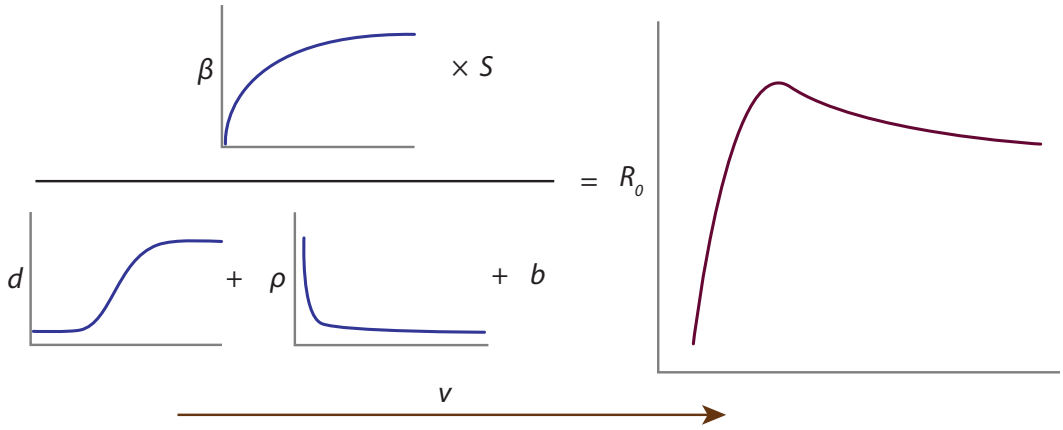

Figure 2.20: Tradeoff hypothesis for the evolution of virulence represented graphically. Pathogens are hypothesized to evolve to maximize fitness (R_0) which exists at some intermediate virulence (x-axis). Adapted from Mackinnon *et al.* [118].

The canonical case study in support of the tradeoff hypothesis is the application of the myxoma virus (MYXV) to control invasive *Oryctolagus cuniculus* (European rabbit) populations in Australia. When MYXV was first introduced in the 1950's, myxomatosis rapidly spread across the entire geographic range of the rabbit and elicited a case fatality rate (CFR) of 99.8% [119]. However within two years, the CFR of the most prevalent strains dropped between 90-99% and over the following 30 years persisted between 70-95% [119, 120]. Phylogenetic analyses by Kerr *et al.* determined the average mutation

rate of MYXV throughout that period was 9.6×10^{-6} nucleotide substitutions per site–comparatively high for a dsDNA virus [120, 121].

Serial passage experiments (SPE) are a frequently used approach to monitor pathogen adaptation. In general, SPEs consist of a culture of pathogens acclimated to a particular host which are then passaged to a new and slightly modified (e.g. containing a resistance gene) host culture [122]. For instance, Messenger *et al.* found after 8 passages of alternating vertical and horizontal transmission between *E. coli* hosts, bacteriophage F1 exhibited increased virulence alongside decreased fecundity [123]. In a review of SPEs, Ebert found that SPEs generally supported the tradeoff hypothesis albeit some inconsistencies found in relatively few studies [122].

Futhermore, host population structure has been shown to affect the levels of optimal virulence in theoretical and experimental studies [113]. A well-studied system in this regard is malaria, which has been studied using SPEs and in the field: *Plasmodium falciparum* (*P. falciparum*) is the most antagonistic species humans and *Plasmodium chabaudi* (*P. chabaudi*) is used in laboratory mouse studies [115, 118, 124]. In general, the *Plasmodium spp.* behave according to the tradeoff hypothesis–virulence and transmissibility are initially positively correlated until the mouse immune response adapted to the infected. However unlike myxomatosis, where host mortality drives virus natural selection, malaria in humans rarely results in high mortality rates with CFRs as low as 1% [118]. Morbidity is a more important measure than mortality in systems like human-malaria. Incorporating morbidity in the basic reproductive ratio is challenging, however, due to its highly variable severity and impact on the individual-level.

Host population spatial structure has been known to have an effect on the optimal levels of virulence [113, 125]. Mackinnon *et al.* speculated on the impact of the role of mosquito vectors on the evolution of virulence, transmissibility, and persistence[8]. Vectored parasites may experience an upward shift in optimal virulence since more virulent infections would lower host defenses against vectors and therefore increase transmission. On the other hand, this impact may be limited in endemic regions where CFR is low. Human patients can have long asymptomatic periods which are unlikely to lead to changes in host behavior or vulnerability. This upward shift may occur during a period of acute disease, but this timeframe is relatively shorter than the asymptomatic period. Infected humans who may ultimately survive impose a burden to the rest of the population by contributing to the spread of malaria throughout the asymptomatic and symptomatic infectious periods [115].

Boots *et* Sasaki published one of the first spatially explicit models to study the impact

[8]Persistence is synonymous with the clearance rate ρ, but is aligned with the parasite's perspective[118].

of host population structure on virulence evolution [126]. Their model was an SIR-based time-series system of equations, which included spacial interactions in a 150×150 lattice. Their study revealed population density or population connectedness plays a role in instigating virulence evolution. Above a *critical connectivity*, low-virulent infections experienced a moderate increase in virulence [126]. Here, transmissibility is optimized between local extinction and the probability for long distance transfer to a new population cluster. Below the critical connectivity, the epidemic remains at low virulence and leads to decreased transmissibility and more isolated population clusters. Though in theoretical studies point to the importance of spatial structure of host populations in evolutionarily stable virulence solutions, data from real-world systems remain scant [127, 128].

One of the main criticisms of the tradeoff hypothesis is its simplicity. The mechanisms of adaptation can be complex and nuanced, such as those resulting from phenotypic plasticity and epigenetics. There is also tremendous variations in virulence amongst the ever-growing number of host-pathogen systems [123]. On one hand, diseases such as Ebola, HIV, and Rabies are almost certainly fatal in humans. Rabies and Ebola are particularly striking cases because of their apparent lack of virulence evolution despite a long period of coexistence with numerous communities around the world.

An experimental study with *Drosophilia melanogaster* (*D. melanogaster*) and a pathogenic sigma virus, DMelSV, the *D. melanogaster* provides an example where tradeoff was not observed [108]. An immune-sensitive strain of DMelSV was unable to overcome the resistance gene *ref(2)P* in a population of 30% resistant *D. melanogaster*. After introducing the insensitive DMelSV counterpart, the insensitive DMelSV completely replaced the population of DMelSV. A possible reason provided for the inability for the sensitive DMelSV to overcome *ref(2)P* is there is a fitness cost for the virus to achieve that capability. When sensitive and insensitive DMelSV were pitted against each other in a susceptible population of *D. melanogaster*, the sensitive viruses had a 20% greater transmission rate over the insensitive type [108]. Thus, in this scenario, the pressures from the energetics of immune-avoidance may be greater than the pressures from host immune activation or host mortality. More studies with more host replicates and virus isolates are needed to explore and confirm this phenomenon.

2.6.2 Driving Forces of Host and Pathogen Evolution

In addition to host population structure and immune-avoidance, there are many possible mechanisms that drive virulence evolution. Local adaptation[9], availability of resources to offset cost of evolving resistance, costs of inducing a response[10], tritrophic interactions (e.g., pathogen-host-plant), host heterogeneity, within-host competition, and many other molecular-level or population-level opportunity costs factor into the shape and nature of virulence evolution [100, 110, 113]. Galvani reviews in more depth some general effects of different factors and selection pressures on virulence evolution [110].

Because RNA viruses undergo rapid evolution, a new framework of understanding the evolutionary dynamics was recently established called *quasispecies theory* [129]. RNA viruses exist as a quasispecies, which are a multidimensional probability cloud of genetically-distanced single nucleotide polymorphisms (SNPs) stemming from a single master sequence (**Fig. 2.21a**). Because of their dynamic gene pool and high degree of genetic diversity, RNA quasispecies will evolve to achieve the greatest overall fitness. To achieve this, a high frequency of SNPs will evolve to mutation rates bordering on a critical mutation rate μ_{crit} which puts the quasispecies on the edge of extinction and maximized evolvability (**Fig. 2.21b**) [130]. Thus, virulence evolution is suggested to be a consequence of achieving an optimum fitness dependent on μ_{crit}.

[9] Pathogen individuals exhibit higher fitness in their native locus than in other distant populations at same site.

[10] To clarify, resistance refers to the host's ability to inhibit growth of the pathogen once infected and response refers to the host's immune activation [113].

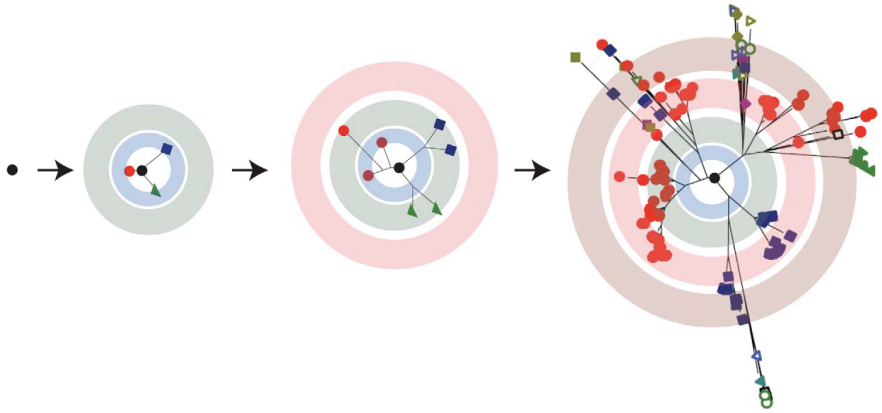

(a) An expanding mutant repertoire over a few generations represented as concentric rings.

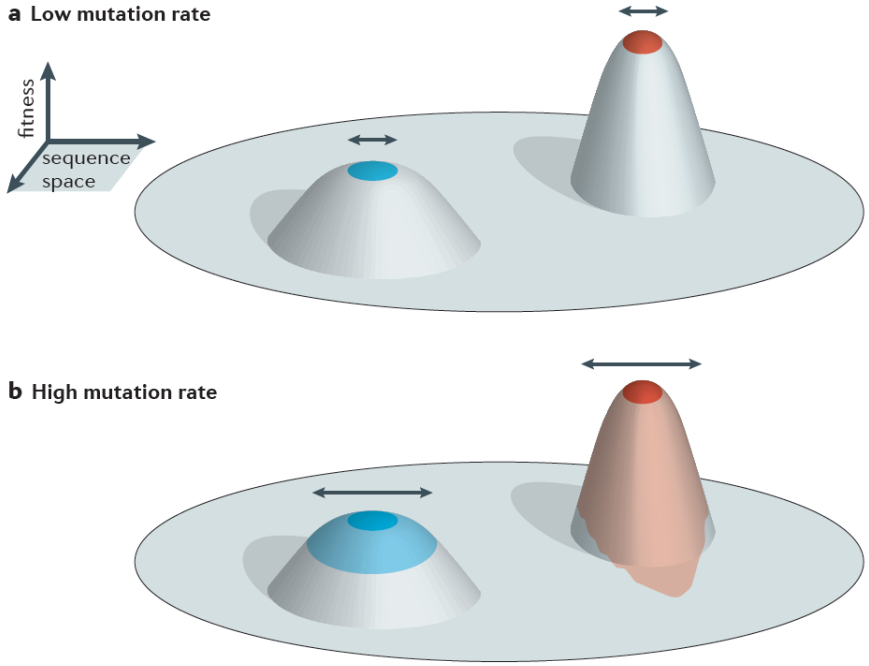

(b) Fitness distribution of quasispecies with low (top) and high (bottom) mutation rates

Figure 2.21: RNA virus quasispecies evolution is driven by highly error-prone replication. **(a)** Reproduced from Lauring *et* Aldino [129]. **(b)** Reproduced with permission from *Nature Publishing Group* [130].

Chapter 3

Objectives

The overall objective of this study was to explore the potential of SCN-pathogenic viruses as SCN biocontrol agents and determine which virulence properties are critical for SCN suppression. Because of potential difficulties regarding adequate experimental time scales, the nature of the SCN life cycle, and its high survivability, we have chosen to conduct this investigation *in silico* with our stochastic host-pathogen model, SCNSim. With SCNSim, we can expeditiously generate data over several years under ideal or non-ideal conditions with a wide range of viruses. In its current state, we used the model to draw broad conclusions surrounding the population kinetics of SCN inflicted with a viral outbreak. In the future, we aim to continuously improve the model by incorporating new information regarding the SCN viruses as it is uncovered as well as develop a nematicidal soybean seed treatment using the one or more of the viruses and integrating them with existing seed coatings.

The specific goals of this project were:

1. Simulate virus evolution in virus-nematode-soybean system.
2. Determine which virulence factors–transmissibility, mutation rate, durability, infection rate, virulence, and viral load–contribute most to SCN suppression.
3. Determine notable trends with virulence over time at different combinations of virus properties.

Chapter 4

Methodology

4.1 Model Description

The SCN simulation (SCNSim) framework employs a discrete time simulation methodology to track the evolution of nematodes and their viral pathogens as they infect a single soybean plant. The nematodes are abstracted as state-based agents; they display numerous phases in their life cycle as they hatch, grow, mate and reproduce. Their survival is predicated upon a “health" parameter that is incremented as they feed upon the plant and decremented as they progress through their life cycle. Viral infections in the nematodes are parameterized by their intensity or “viral loads" (L), transmissibility (β), durability (D), and virulence (v) as described in greater detail below. The environment object implements stochastic temperature variation which can be set to either ideal greenhouse conditions (practically constant temperatures), or to mimic Champaign County, IL using monthly data available from the Illinois State Water Survey (ISWS) [10]. The soybean class creates soybean objects within the typical soybean planting season (early April to late August). Soybean objects are characterized by age, health, and size the latter two of which are negatively impacted by SCN parasitism and positively affected by optimal temperatures (80^o F). Finally, the soybeans can be set for yearly planting or alternate years as in the case of crop rotations.

Meanwhile a virus outbreak, characterized by unique combinations of scale-free virulence properties, coevolves and propagates with the SCN population. Each initial property is given random variation in the model to create a population of viruses described by a normal distribution of the properties (**Table 4.1**). Viruses are transmitted according to dynamic *transmission rates*, β, which are used as probabilities for the Bernoulli process that governs the disease transition. This stochastic event applies to both vertical transmission from females to eggs, and horizontal transmission from males to females during mating.

SCNSim uses Monte Carlo methods to simulate the random nature of viral evolution as well as direct the population kinetics of the infected SCN. The diversity of viruses will increase according to a *mutation rate*, μ. In the simulation arena, this means the distribution of virulence properties will change over time according to the probability distribution determined by μ. The viruses infect a fraction of the initial SCN population

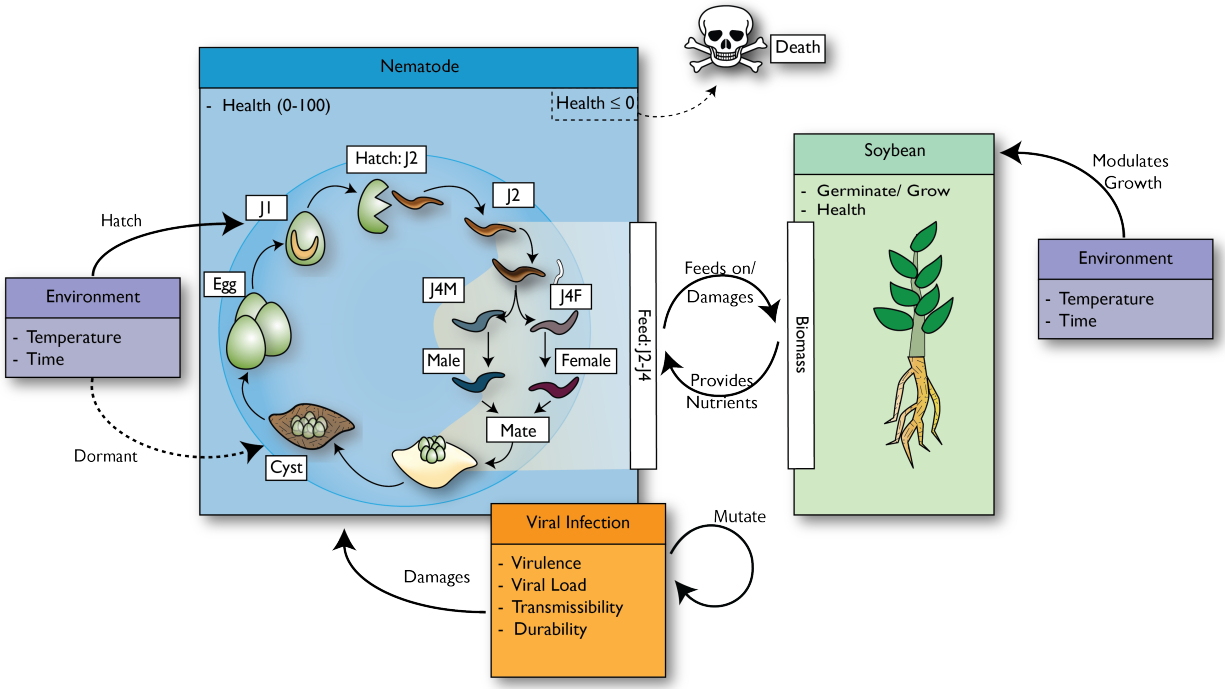

Figure 4.1: Object organization of SCN simulation. A nematode abstract class generates a population of nematode agents based on the kinetic environment, health of the host soybean crops, and the nature of the viral pandemic. Dotted lines indicate states that develop under unfavorable conditions.

defined as the *initial prevalence* i_0. As time progresses, the viruses decrement nematode health at a rate strongly correlated with the viruses mutating *virulence*, v, and *viral load*, L. A *durability*, D, factor describes the longevity of the viral infection. In SCNSim, D increases viral load. The combined effects from the dynamic virus properties and environmental conditions control the rate of growth the nematode population.

4.1.1 The Nematode Agent

During the growing season, the SCN agent carries out multiple simultaneous operations to progress nematode populations through the stages of nematode life cycle **(Fig. 4.1)**. Though SCNSim has an adjustable initial population of 10 cysts per soybean with each cyst capable of producing up to 500 eggs with random variation. Each transition between states is determined by the SCN agent's response to the environment and its own health. **Table 4.2** outlines the major environmental set points that dictate the periods of nematode growth.

Health is measured on a percentile scale with 100% being completely healthy while

Table 4.1: SCNSim initial virus properties.

Property	Symbol	Range	Definition	
			in vivo	*in silico*
Viral Load	L	$0-1$	Amount of viral particles per host	Scalar multiplier to nematode health decrement
Virulence	V_0, v	$\mathbb{R} > 0$	Pathogen damage inflicted on host	Multiplier to Viral Load
Transmissibility	β_0, β	$0-1$	Rate of infection of susceptible population	Proportion of viral load sexually transmitted from infected male to a recipient female
Prevalence	i_0, i	$0-1$	Disease prevalence in a population	Fraction of initial population infected
Durability	D	$0-1$	Longevity of virus particles.	The complement is an amplifying constant on increasing viral load.
Mutation Rate	μ	$0-1$	Proportion of progeny generation with significant genetic variation	Probability of virus properties undergoing mutation

when nematode health reaches 0%, they die. Starvation during the hatched J2 state and infection cause nematodes to lose health percentage points at varying ranges depending on the length of the starvation period and the severity of the viral infection. On the other hand, parasitizing soybeans replenishes health at a fixed rate of 5% per day. Nematodes with adequate health percentages are considered by SCNSim to be “healthy" enough to advance to their next state and will advance given the success of unfair stochastic Bernoulli trials. This probability of success equals the health percentage of the nematode at the time of its transition; the healthier the nematode is, the more likely it is to survive to the next molt. A failed outcome suggests the nematodes were unfit to continue maturing or reproduce and are moved to the dead state.

Table 4.2: SCNSim environmental set points based on figures in Schmitt *et al* [1].

Model Compartment	Parameter Description	Value
SCN Life Cycle Laws		
	SCN eggs per cyst	300-500 [1]
	Minimum hatching temperature	61 ^{o}F
	Maximum hatching temperature	97 ^{o}F
	Cyst dormancy initialize temperature	$<$ 68 ^{o}F
	Probability of hatching from egg sac	0.2[2]
	Probability of hatching from cyst	0.002 [2]
SCN Life Stages		
	Egg state	1-5 days
	J1 state	1-2 days
	Unhatched J2	1-3000 days
	Hatched J2	1-4 days
	J3	3-4 days
	J4 male	5-6 days
	J4 female	3-4 days
	Adult male	1-21 days
	Adult female	2-60 days
	Range of mating	1-21 days
	Gestation period	3-5 days
	Egg Sac	1-3000 days
	Cyst	1-3000 days
Soybean Growth		
	Minimum germinate temperature	55 ^{o}F
	Soybean germinate date	115 days (about April 25th)
	Soybean harvest date	240 days (about August 28th)
	Optimal soybean growth temperature	80 ^{o}F
SCN Parasitism		
	Minimum soybean age for parasitism	20 days post germination[3]
	Maximum soybean age for parasitism	100 days post germination[3]
	Feed rate	5%

SCN parasitism on soybean crops only occurs only after the J2 state which is reached after successful transitions from the egg $\rightarrow$ J1, J1 $\rightarrow$ J2, J2 $\rightarrow$ `Hatching`, and J2 $\rightarrow$ `root penetration`. While soybeans are present and temperatures are between the hatching

[1] According to *Biology and Management of Soybean Cyst Nematode* 2nd *ed.*, a female cyst growing in optimal conditions may produce up to 600 eggs. However, the averages found in fields has been reported to be much lower, ranging between 60 and 200, depending on the location [44].

[2] If hatching is allowed by environment.

[3] Soybeans typically take 20 days to produce root exudates that attract SCN. After 100 days, soybeans are usually within reproductive maturity and root development slows while a woody epidermis prevents new SCN from penetrating.

temperatures SCN will continue to feed off the soybean host, develop, and eventually reproduce. At the J4 stage, the nematodes are split by gender via a 50% stochastic coin flip. The J4s transition once more before mating. Mature females are fertilized with a probability of success equal to their health percentage and are simultaneously filled with up eggs. Any infection the male carries will be partially transmitted to the female. If a female is already infected, her viral burden is compounded. The total resulting burden is then divided equally amongst the eggs.

SCN females will transition from egg sacs to dormant, egg-containing cysts between growing seasons or if temperatures drop below 68^{o}F. Eventually, the cysts will release SCN juveniles in the next spring when favorable conditions return. This dormant cyst phase can persist for up to 3000 days or up to 8.2 years. Here in the model, we assume the metabolism in the dormant phase occurs at a negligible rate and viruses do not mutate or cause damage. Finally, at each sampling point, SCNSim outputs the means and standard deviations of the nematode population distribution including values for each nematode state as well as means and standard deviations of the dynamic virulence properties and means of environmental variables.

4.2 Assumptions and Caveats

"Essentially, all models are wrong, but some models are useful"

–George E.P. Box [131]

Without using explicit mathematical models, SCNSim is capable of computing several years worth of time-series data of infected SCN populations in relatively little computational time. At the time of this writing, relatively little is known about the epidemiology of the SCN viruses, including: their pathogenesis, transmission rates, mutation rates, and etiologies. Thus, broader definitions were needed to describe their *in silico* counterparts and several assumptions were made. Those assumptions are:

- **Viruses are only pathogenic to SCN; no mutualism, symbiosis, or commensalism occurs.** We also ignored competition between viruses for host cellular resources.
- **Viruses begin inflicting damage immediately after infection**. Many real-world viruses, such as HIV, have an asymptomatic incubation period that can last for between a few days to many years.
- **Contact patterns between viruses and SCN are fixed**. In real-world situations, it can be presumed the different modes of transmission have independent, unequal

success rates. For example, Mubaraka *et al* compared the transmission of influenza virus via aerosols and fomites and found aerosolized virus-inoculated droplets to be much more successful than fomites in causing an infection in guinea pigs [132].

- **Contact transmission of viruses was ignored**. This is simply because we have yet to observe an occurrence *in vitro* though it could be a common mode of transmission.
- **There is no spatial dimension in SCNSim**. Distances between nematodes are not considered. Thus, metapopulation dynamics do not influence the epizootic.
- **Soybean immune responses to nematode parasitism are not represented**. The only soybean response considered is a reduction in biomass due to nematode parasitism.

4.3 Model Calibration

Given the paucity of data it is presently difficult to precisely gauge how much damage a nematode inflicts upon the soybean plant on any given day, or how much benefit the SCN derives from a feeding. Based on data available from Schmitt et al, we assumed that at the beginning of the year we would expect to see 10 nematode cysts, while the number could grow up to 5000 at the end of the year on a particularly susceptible plant [1].

4.4 Numerical Investigation

Each unique combination of the varying initial conditions for virus properties were simulated with 5 year monitoring durations, and 4 day sampling frequencies (**Table 4.3**). The replicate iterations were then averaged for each combination at each time point. Due to high data volume ($>$1 million data points) and limited processing capability, the total data space was reduced by removing most of the data between crop years (days 1–99, and 256–365). Further data reduction approaches varied depending on the type of analysis. For instance, medians of each non-normally distributed variables were determined for each within-treatment crop year for expedited qualitative analyses.

4.4.1 Statistical Approach

Exploratory data analysis using the Shapiro-Wilk test for normality found that nearly all treatments of 20 independent variables did not follow normal distributions from between

Table 4.3: SCNSim parameters

Simulation Properties		
	Sampling Frequency	4 days
	Iterations	10
	Simulation duration	5 years
Virus Properties		
	Mutation rates	0, 0.1, 0.2, 0.4, 0.6, 0.8
	Virulence	0.1, 0.5, 1, 1.5, 2, 2.5, 4
	Transmissibility	0.5
	Infection Rate	0.2, 0.8
	Durability	0.5
	Viral Load	0.5

one to all virus factor combinations (crop year, infection rate, mutation rate, and virulence) and a significant portion had some level of heteroscedasticity. Therefore, non-parametric significance tests were used, such as the Kruskal-Wallis test, Kolmogrov-Smirnov test, and permutation tests for multi-factorial analysis of variance (ANOVA) using the R package `lmPerm` [133].

Criteria defined below characterizing virus agent effectiveness were tested between different treatments of viruses, or *pathotypes*. Typically, a pathotype describes a group of organisms with the same type of pathogenicity towards a specific host. In our data, we refer to each unique combination of virus properties as a pathotype. Results from the virus treatment simulations were compared to a control simulation which were run similarly *sans* any viral properties. Statistical analyses were performed using R Statistical Software [134, 135, 136, 137].

4.4.2 Dimensionality Reduction

SCNSim produces a dataset of 31 variables, which not only complicates analysis but also exceeds computational limits of many softwares and processing capability of commercially available computer hardware. Scaled principle component analysis (PCA) was performed to simplify the dataset by qualitatively reducing the number of variables using the `prcomp` function in R [134]. The principle components (PCs) that made up the eigensystem subspace accounting for up to 80% of the sample space variation were selected for further testing. Variables were selected to each PC by examining their index of the loadings (IL, **4.1**) as described in Vasco *et* Vieira [138]:

$$IL_{ij} = \frac{u_{ij}^2 \cdot \lambda_i^2}{s_j} \tag{4.1}$$

where IL_{ij} is the index of loading of the i^{th} PC and the j^{th} variable, μ_{ij} is the loading of the j^{th} variable in the i^{th} PC, λ_i is the eigenvalue for the i^{th} PC, and s_j is the standard deviation of the j^{th} variable which is equal to 1 when a scaled correlation matrix is used.

PCA analysis results revealed that principle components 1-4 accounted for 81.34% of the variance in the virus treatments data space (**Table B.2**). Many of the population variables ('J1', 'J2', etc.) were found to be closely correlated and therefore redundant. Variables 'Nematodes' and 'Cyst' were chosen to represent the SCN population, 'Virulence' and 'Transmissibility' were used to describe the viral epizoology, and 'Fraction Infected' and 'Death by virus' were used to describe disease impacts on SCN.

Finally nematode mortality rates attributed to viruses, d, was calculated by dividing 'Death by virus' by 'Nematodes' at each point in time and then taking the percentage (**4.2**).

$$d = \frac{\text{No. Virus - Caused Deaths}}{\text{No. Nematodes}} \times 100\% \tag{4.2}$$

Mortality rate here is distinct from the baseline mortality rate, b, as well as the enhanced mortality rate which is equivalent to the total mortality rate.

4.4.3 Replication Ratio: Modified Reproduction Ratio

We adapted the basic reproduction ratio, R_0 (**2.4**), to the outputs from SCNSim which we renamed the *viral replication ratio*, R_v (**4.3**), to distinguish it from R_0 . Recall the basic reproduction ratio:

$$R_0 = \frac{\beta S}{b + d + \rho} \tag{2.4}$$

where each of the terms is determined in the context of a population initially at maximum capacity and birth rates are not considered. Therefore, with the exception of the mortality rate terms b and d , the total population is relatively unchanging compared to the nematode population in SCNSim. Thus all the terms that make up R_v are normalized to the total nematode population:

$$R_v = \frac{\beta \cdot (1 - i)}{b + d + \tilde{\rho}_{95}} \tag{4.3}$$

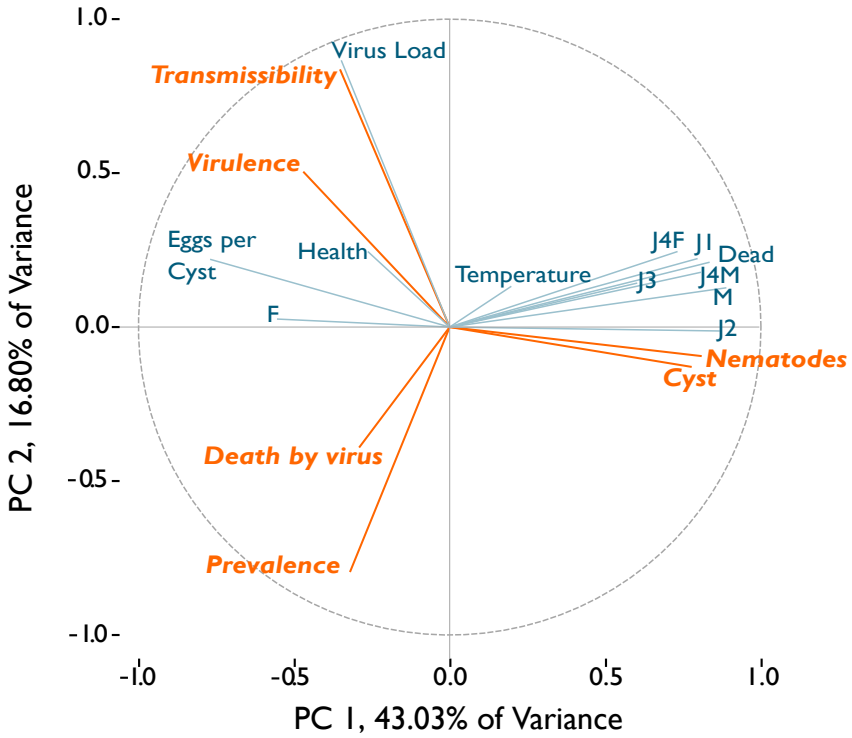

Figure 4.2: PCA correlation circle showing PC1 and PC2 for all predictors. Orange-colored variables were selected for further analysis.

where β is the dynamic transmissibility (as opposed to β_0), i is the *prevalence* or infected portion of the nematode population, b is the *baseline mortality rate* sans any viral infection, d is the *mortality rate* attributed to viral infection, and $\tilde{\rho}_{95}$ is the *avirulent proportion of i*; the proportion of infected nematodes with high ($\geq$95%) health. b was derived by averaging the 10 iterations of the fraction of dead nematodes to live nematodes in the control data while preserving the time-scale resolution.

Since SCNSim was designed without a fitness parameter in mind, it currently does not record the number of cured infections virus infections, we are unable to determine an equivalent recovery ratio ρ to the one used in (**2.4**). Therefore an approximation, $\tilde{\rho}_{95}$, representing the proportion of nematodes with an avirulent infection was created by taking the median of the subset of i where SCN $Health \geq 95$. In future improvements of SCNSim, either ρ or the number of cured viruses will be included in the data output.

R_v was plotted with respect to μ in order to find the *critical mutation rates*, μ_{crit}, at the error threshold. μ_{crit}'s were determined by interpolating the mutation rate at $R_v = 1$ using the slope between the points straddling the threshold. The directionality of the slope at each of these critical mutation rates was also noted.

Chapter 5

Results

"Distinguishing the signal from the noise requires both scientific knowledge and self-knowledge: the serenity to accept the things we cannot predict, the courage to predict the things we can, and the wisdom to know the difference."

–Nate Silver, **The Signal and the Noise**

5.1 Mortality Rate: Nematode Suppression

To evaluate the extent of nematode suppression, final disease mortality rates were compared across multiple factors. None of the pathotypic[1] factors crossed with $V_0 = 0.1$ with combined data from other initial parameters resulted in disease-caused mortalities; all median mortality rates were 0.0% (IQR = 0% - 0%). Thus, in a lot of the following discussion on mortality rates, $V_0 = 0.1$ is omitted where it is not significantly different from the control treatment.

5.1.1 Inundative Release of Viruses Greatly Increases Nematode Mortality

Overall, the $i_0 = 0.8$ treatments had significantly higher mortalities than the $i_0 = 0.2$ treatments with medians at 1.17% (IQR = 0.06% - 2.52%) and 0.12% (IQR = 0.0% - 0.27%), respectively (**Fig. 5.1**, $p < 0.001$, Kruskal-Wallis). The $i_0 = 0.2$ treatments experienced suppressed mortality rates (IQR = 0.01% - 1.17%) even as the prevalence (i) increased above 80% in some treatments. Moreover, the final enhanced mortality rates (diseased and baseline mortality) for pooled data between time and pathotypic factors within $i_0 = 0.2$ were not significantly different from the baseline control mortality rates during the final year ($p = 0.295$, two-sided Wilcoxon rank sum). This suggests at $i_0 = 0.2$ (low release) infections maintained negligible pathogenicity. There is possibly a threshold for i_0 that leads to an effective biocontrol epizootic that lies within $i_0 = 0.8$ and $i_0 = 0.2$. A stochastic

[1] To recapitulate, pathotype refers to the a group of pathogens with the same pathogenicity towards a specific host.

modeling study by Shea *et* Possingham identified the notion that a high release strategy results in greater biocontrol with rules of thumb for [139]. However in this study, we only tested two values for i_0 though it would likely to be helpful to identify an optimal release strategy for SCN in future testing.

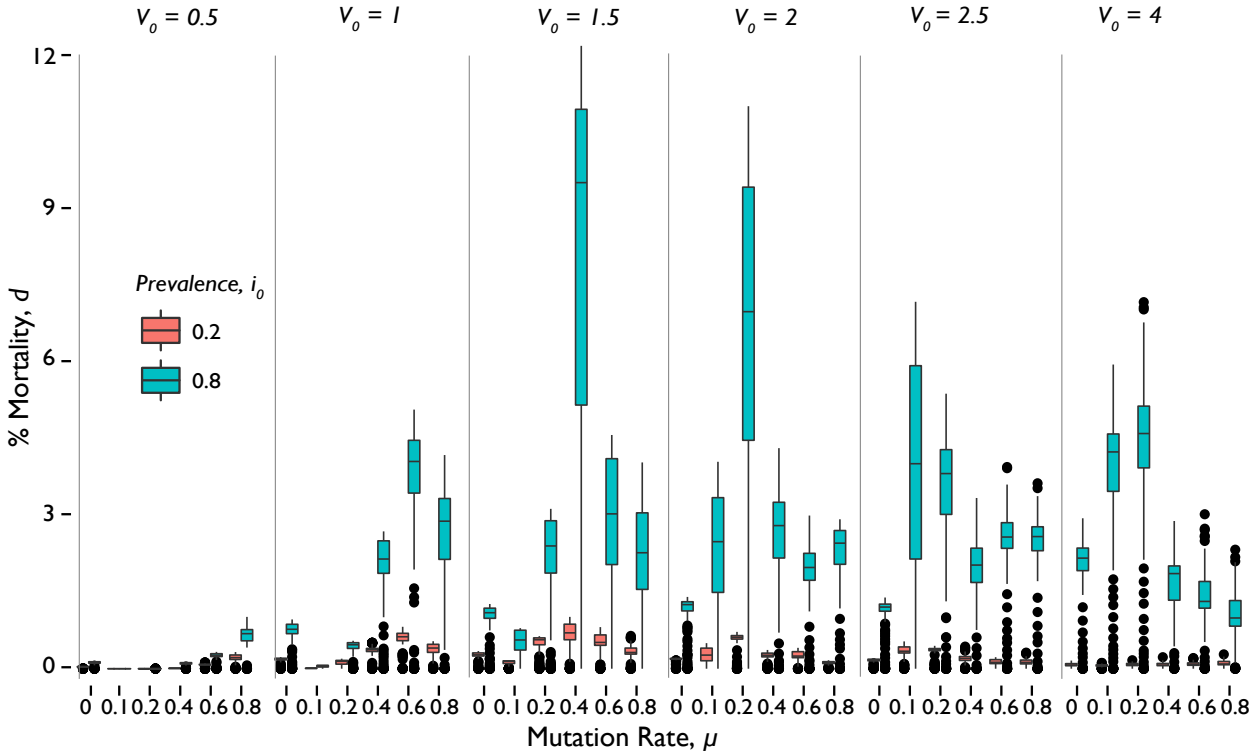

Figure 5.1: SCN mortality rates across mutation rates. Overall, high release treatments resulted in overwhelmingly higher mortalites than the low release treatments ($p < 0.001$, Kruskal-Wallis). The $V_0 = 0.1$ treatment is omitted; no virus-attributed deaths occured within this treatment for any values of μ.

In general, pooled treatments within each i_0 experienced steady declines in i. All combinations within $i_0 = 0.2$ saw a 5-year 11% decrease in i to a median of $i = 0.086$ (IQR =0.008 - 0.605) (p<0.001, Kruskal-Wallis). On the other hand, combinations within $i_0 = 0.8$ saw a significant drop in median i by 16.3% to 0.496 (IQR = 0.233 - 0.903) ($p < 0.001$, Kruskal-Wallis). Between the pooled i_0 treatments, $i_0 = 0.8$ was found to also have significantly higher i than $i_0 = 0.2$ ($p < 0.001$, Wilcox rank sum).

Investigation into viral load and i revealed possible underlying mechanisms for the discrepancy in mortalities between the two i_0s (**Fig. 5.2**). Viral load and i are inversely related with unstable boundary behavior occurring at certain $V_0 \times \mu$ pathotypes. As μ increases, the boundary appears to occur at decreasing V_0s within μ. To illustrate, in $\mu = 0 \times i_0 = 0.8$ the slopes appear to diverge between $V_0 = 4$ and $V_0 = 2.5$ while in

$\mu = 0.6$, the slopes appear to diverge between $V_0 = 1.5$ and $V_0 = 1$.

This unstable boundary behavior is observable in both i_0 treatments. Above this threshold, viral load oscillates at values greater than or equal to its initial value, 0.5, while i decreases over time approaching $(0, 0.5)$. Below this threshold, the data asymptotically approach $(1, 0)$ over time. In the $i_0 = 0.8$ panel, behavior about the threshold is observable in pathotypes $V_0 = 2.5 \times \mu = 0.2$, $V_0 = 2.0 \times \mu = 0.4$, and $V_0 = 1.5 \times \mu = 0.6$. Here, virus load and i have a positively correlated linear relationship that is moving towards the origin with respect to time. In the $i_0 = 0.2$ treatment, the pathotypes "move" very quickly towards each of the aforementioned endpoints compared to those in the $i_0 = 0.8$ treatment.

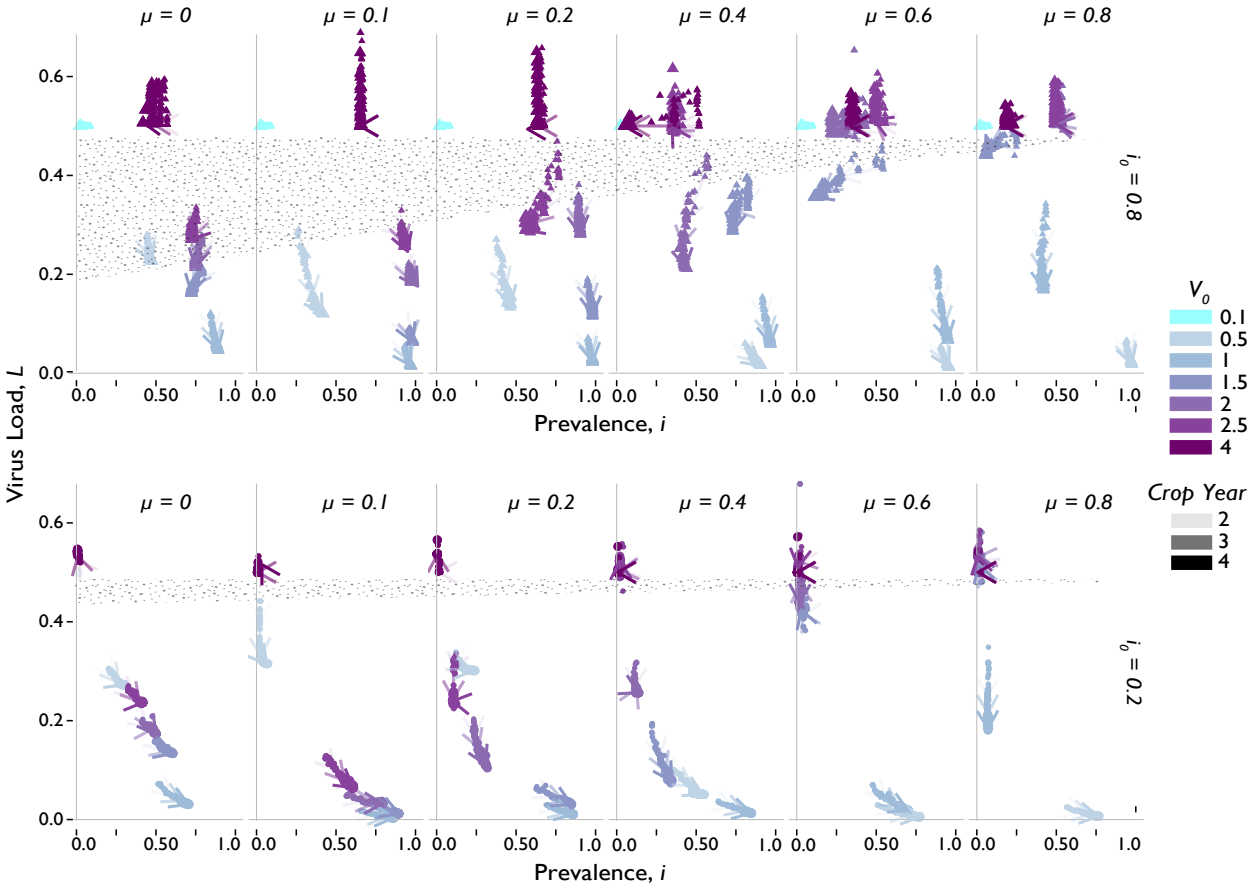

Figure 5.2: An unstable boundary, highlighted by the speckled region, is apparent within the relationship between viral load and prevalence. The top panel belongs to $i_0 = 0.8$ while the bottom figure belongs to $i_0 = 0.2$ with panels for increasing μ from left to right. Arrowhead were superimposed to illustrate yearly vector directions from the beginning to the end of each year. As time increases, the opacity of the arrowheads also increases. Only the last 3 years are shown to illustrate year-year trajectories of each treatment.

Where each pathotype falls in relation to the unstable viral load–i boundary determines

the mechanism for the resulting mortality. The epizootics above the threshold (*sans* $V_0 = 0.1$) become extinguished as highly pathogenic viruses dampen their lifetime transmission as evidenced by the diminished i with sustained viral load. Highly virulent viruses may accomplish this by either killing the adult nematodes over the course of the infection or preventing J1 nematodes from hatching. On the other hand, pathotypes with low virulence below the threshold result in epizootics with diluting viral loads; virus fail to suppress nematode fecundity sufficiently which causes the viruses to distribute thinly over the quickly growing nematode population. Dilution is much more pronounced in a population with fewer infections to begin with. With most of the population uninfected, there are fewer, if any, chances for viruses to accumulate during sexual contact. Meanwhile, the females who are lightly burdened will distribute those few viruses between 100s of new nematodes–now with even lighter viral burdens. Though SCNSim does not model nematode immune response, the effects described here echo those predicted in virulence theory.

5.1.2 Intermediate Pathotypes Were Most Effective Nematode Suppressors

To simplify the discussion on effects of combinations of other virulence factors, the rest of the chapter focuses on the $i_0 = 0.8$ treatment. The $i_0 = 0.2$ treatment generally follows similar trends albeit with offsets of the threshold regions and much more muted nematode suppression.

Fig. 5.3 shows the mortality rates over time across all combinations of $V_0 \times \mu$ pathotypes. As initial μ increases, it is apparent from $\mu = 0$ to $\mu = 0.6$ that the V_0 treatment with the highest nematode mortality decreases. For instance, $V_0 = 4$ is the most lethal pathotype among the $\mu = 0$ viruses, $V_0 = 2.5$ at $\mu = 0.1$, $V_0 = 2$ at $\mu = 0.2$, and so on. The exception at $V_0 = 0.5 \times \mu = 0.8$, where it was expected to demonstrate the highest mortality within $\mu = 0.8$, is indicative of the existence of a minimum initial virulence needed for a virus to develop into an effective epizootic between $V_0 = 0.5$ and $V_0 = 1$. Above this V_0 boundary at $\mu = 0.8$, **Fig. 5.3** suggests V_0 and μ constrain one another and thus exhibit optimal suppression within either factor's intermediate values.

Most of the curves in **Fig. 5.3** appear to exhibit some type of critical points either with a local maximum or approaching quasi-steady state after the 2nd crop season. It is therefore reasonable to speculate that SCNSim models a stable mortality rate for most pathotypes. On the other hand, in the case of $V_0 = 1.5 \times \mu = 0.4$, the maximum occurs relatively later in time (fourth crop season), than other treatments. Since our simulations ended at five

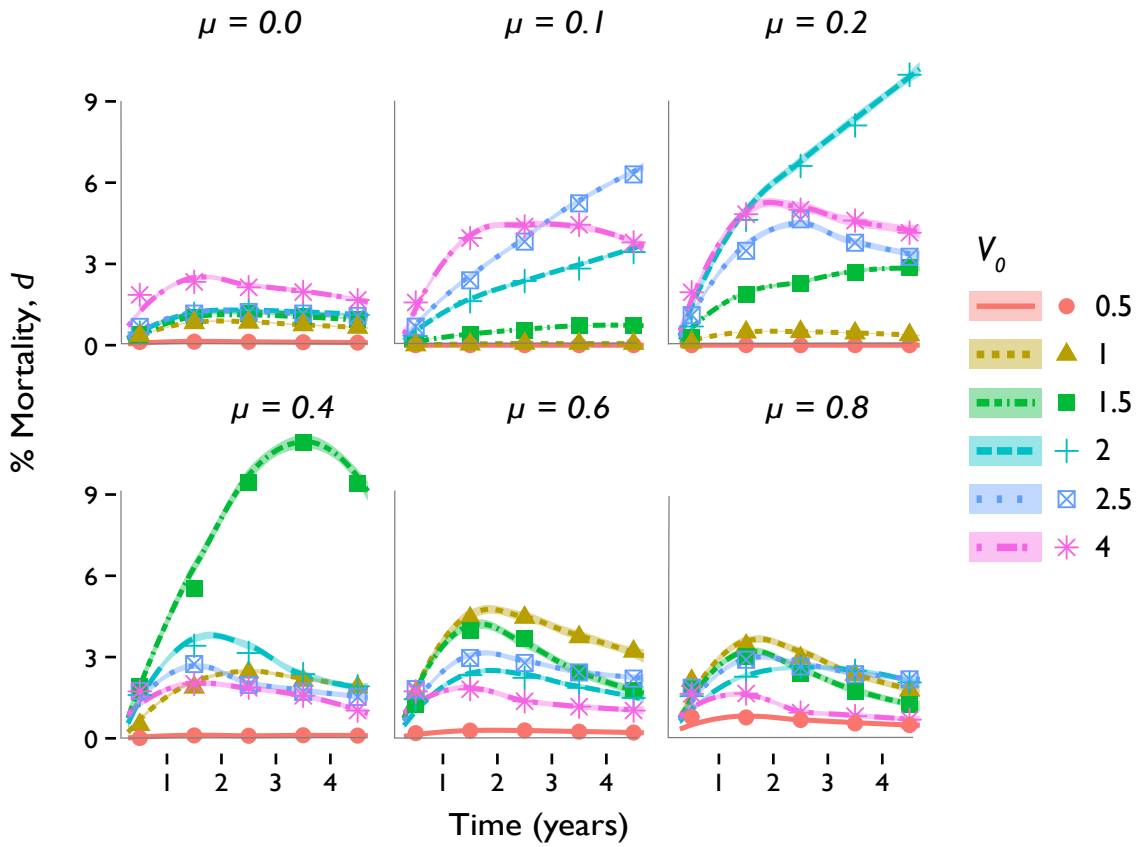

Figure 5.3: Mortality rates over time for each $V_0 \times \mu$ pathotype within $i_0 = 0.8$. $V_0 = 0.1$ is omitted.

years, it is difficult to determine if this pathotype does eventually approach an equilibrium or if the mortality rate continues to drop. Furthermore, the treatments $V_0 = 2.5 \times \mu = 0.1$ and $V_0 = 2 \times \mu = 0.2$ exhibit increasing functions with no saturating or peaking behavior. Therefore, maximums or equilibrium values and when they occur, if they exist, could not be determined within the time scale for this dataset. Nevertheless, given the current time scale, the most successful pathotypes in terms of nematode mortality rate are these intermediate $V_0 \times \mu$ combinations.

The highest mortality rate achieved from all the data was 11.63% (IQR = 4.92% - 10.44%) at the 3rd crop year. This datum is within 1.5× IQR for this treatment indicating it is not an outlier. **Fig. 5.4a** shows the mortality rates over time at $\mu = 0.4$ for selected V_0s. However, the impact on mortality is complicated by interactions between μ and V_0. For both i_0 treatments at $\mu = 0.4$, the decreasing i under low ($V_0 = 0.1$) and high ($V_0 = 4$) indicates that each extreme V_0 pathotype eventually goes extinct in the population; the former could die out as it fails to "catch up" to the nematode population growth rate

while the latter may be crippling nematodes too soon in their life cycle *ergo* prohibiting its own capacity to proliferate.

At critical V_0, prevalence was relatively constant over time

Upon closer examination of $i_0 = 0.8$ within-treatments of $\mu = 0.4$, and between V_0s the behavior of prevalence and time appears diverge at $V_0 = 1.5$, or the seemingly *critical* V_0 for $\mu = 0.4$ (**Fig. 5.4b**). At $V_0 = 1.5$, i appears relatively constant at i_0 until the fourth crop season when the data begins to slowly drop. In the corresponding mortality rate versus time curve, fourth crop season (about 3.5 years into the simulation) is also where the maximum mortality rate occurs (**Fig. 5.4a**). Thus, at the most successful pathotype, i is sustained while mortality increases and the subsequent drop in mortality after the maximum corresponds with a drop in prevalence. Further investigation into the average virulence and transmissibility of viruses with $V_0 = 1.5$ will help determine more certainly whether and how virulence evolution contributed to the waning prevalence in the final crop season.

The two diverging behaviors support our previous conclusions about the epizootiologies for low and high V_0. At $V_0 < 1.5$ (with the exception of $V_0 = 0.1$), i will steadily increase towards $i = 1$ over time. The $V_0 = 0.1$ treatment's prevalence over time follows a similar trend to $V_0 > 1.5$ treatments. For $V_0 > 1.5$, i appeared to initially crash exponentially before saturating at a lower i until the rate of decrease slows or stops. However, in $V_0 = 4$ this pause in decreasing i is followed by a decreasing linear trend towards $i = 0$ after the third crop season. It is difficult (and perhaps meaningless) to speculate how this could be interpreted in a real system. In SCNSim as the $V_0 = 4$ treatment reached the third season, the viruses appear to stop transmitting entirely causing the i to diminish at a rate congruent with the nematode population growth rate (**Fig. 5.4c**).

At critical V_0, transmissibility increased at a nearly constant rate while mortalities accumulated

Fig. 5.4c similarly illustrates β across V_0 treatments over time within $\mu = 0.8 \times i_0 = 0.8$. Interestingly, both the highest and lowest V_0s show the slowest increases in β. Moreover, similar pairs are found between the highest and lowest, and second highest and second lowest V_0s. $V_0 = 0.5$ with a median β of 0.546 (IQR = 0.528 - 0.580), and $V_0 = 2.5$ with a median β of 0.552 (IQR = 0.536 - 0.574) are not significantly different ($p = 0.31$, one-tailed Wilcoxon rank sum). Though $V_0 = 0.1$ and $V_0 = 4$ have nearly identical medians, $\beta = 0.500$ (IQR = 0.500 - 0.500, and IQR = 0.500 - 0.507, respectively), they were not found

to be significantly different ($p < 0.001$, two-tailed Wilcoxon rank sum). The discrepancy between the diverging i versus t and the coupled β versus t behaviors points to differing possible causes for high and low V_0s having attenuated β over time. In the context of previously discussed data, high V_0 treatments may not be able to proliferate due to their reduced lifetime transmission. Low V_0 treatments increase i over time and therefore are evidently transmitting. The relatively slow rate of transmission is potentially due to the nematode population becoming saturated with infections due to the low mortality rate. From **Fig. 5.2**, the likely overall reduction of the infection virulence is due to a rapid decline in virus load. In these low V_0 treatments, with vertical transmission is much more dominant than horizontal transmission, in order for viruses to persist in the nematodes, low β is positively selected.

Meanwhile, the βs of the three intermediate pathotypes, $V_0 = 1$, 1.5, and 2, are all increasing at much faster rates in either logistic or linear fashions. With a rapidly saturating function, β within the $V_0 = 1$ treatment is merely propagating throughout the population while translating to relatively lower mortality rates. This is likely due to the relatively more rapid dilution of viral load through vertical transmission as can be evidenced from **Fig. 5.2**. On the other hand, for the $V_0 = 2$ treatment, though the drop in prevalence is significant initially, the rate of increase for β is sufficient to stabilize the prevalence after the fourth crop season (**Fig. 5.4b**). However, the significant drop in viral load after five years (from 0.50 to 0.20) indicates that vertical transmission is much more dominant than horizontal transmission. Viruses that are selected for in this case will have low virulence to support the low transmissibility; with low lifetime transmission, it would be detrimental for the viruses to further reduce their lifetime transmission with high virulence. The β function for $V_0 = 1.5$ is sandwiched between the others; perhaps being in the most medial position is indicative of an optimum relationship with β over time.

Fig. 5.5a illustrates the same data in **Figs. 5.4a** and **5.4b** from a new perspective: The relationship between mortality rate and i within the $\mu = 0.4$ treatment across V_0s. At $V_0 = 1.5$ the correlation between d and i changes direction within the 5 year period. Up to the 2nd crop year, the correlation is overall positive; mortality rates rise with prevalence. However in the 3rd season, mortality rate plateaus at its maximum. The IQR during that season is 10.44% - 11.14%, only 6.0% of its total range, compared the drop in prevalence which has a corresponding IQR of 0.751 - 0.826, or 72.8% of its total range. Both variables have reached their maxima during this season and begin to crash. During the final year, mortality rate and prevalence are once again positively correlated. However in contrast to the earlier crop seasons, as time increases, both variables decrease linearly at a rate

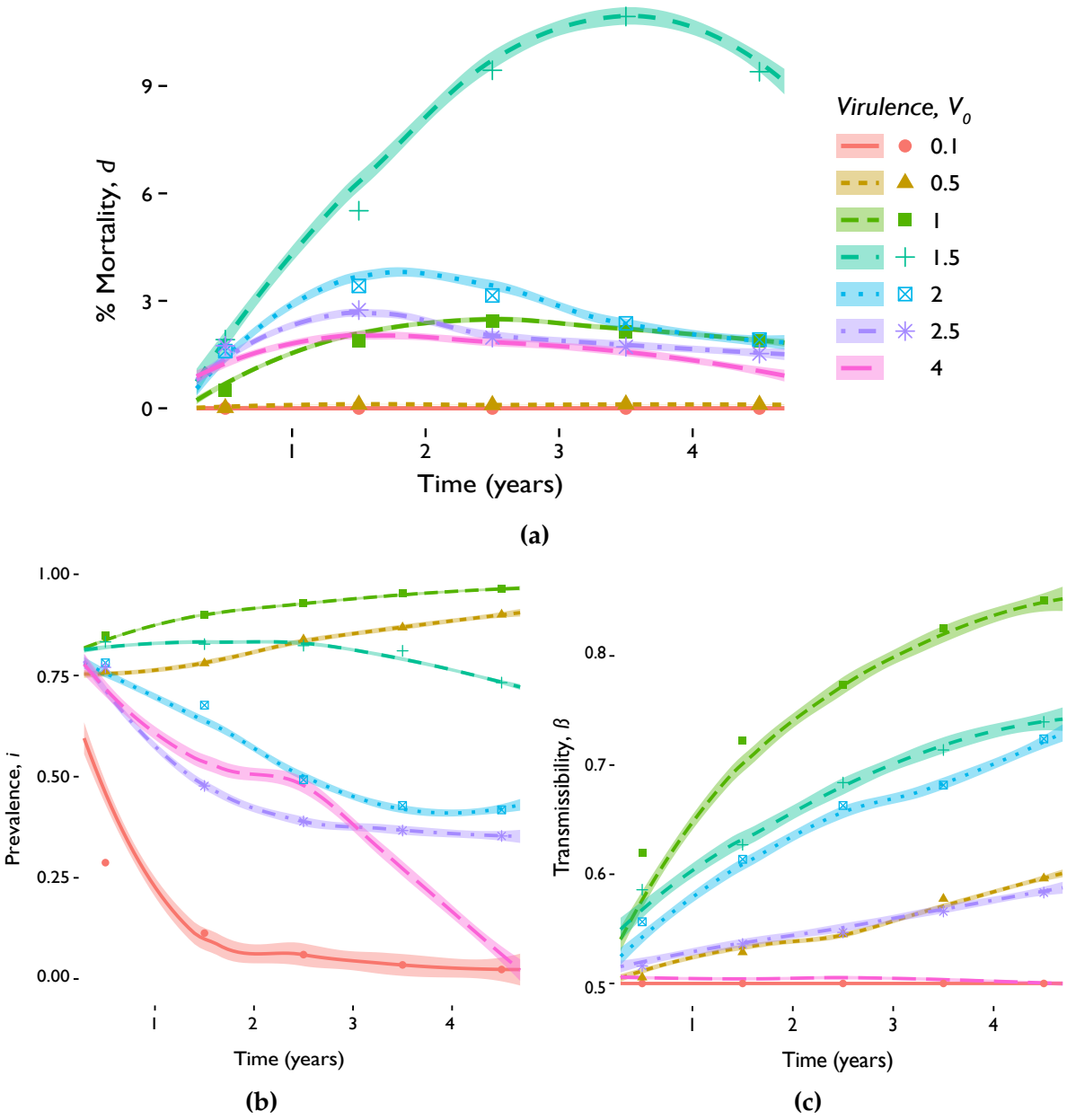

Figure 5.4: SCN suppression over time at $\mu = 0.4$, and $i_0 = 0.8$ across V_0: **(a)** The highest mortality rates occur at intermediate virulences with the maximum at 11.63% in the $V_0 = 1.5$ treatment. **(b)** The $V_0 = 1.5$ treatment exhibits an intermediate disease prevalence while illustrating an inverse relationship between initial virulence and the final i. **(c)** Transmissibility rates remain suppressed over time at $V_0 = 0.5$ and $V_0 = 2.5$. For the remaining three V_0 treatments, there appears to be an inverse relationship between β and V_0. The figures show median points at each crop year as well as LOESS curves.

of 0.95 $^{\%\text{ dead}}/_{\%\text{ infected}}$ ($r^2 = 0.79$). We observed for each pathotype in $i_0 = 0.8$ between V_0s and within μs, there is a point in time at which the mortality rate is at its peak after which it will drop or reach quasi-steady state (**Fig. 5.4a**).

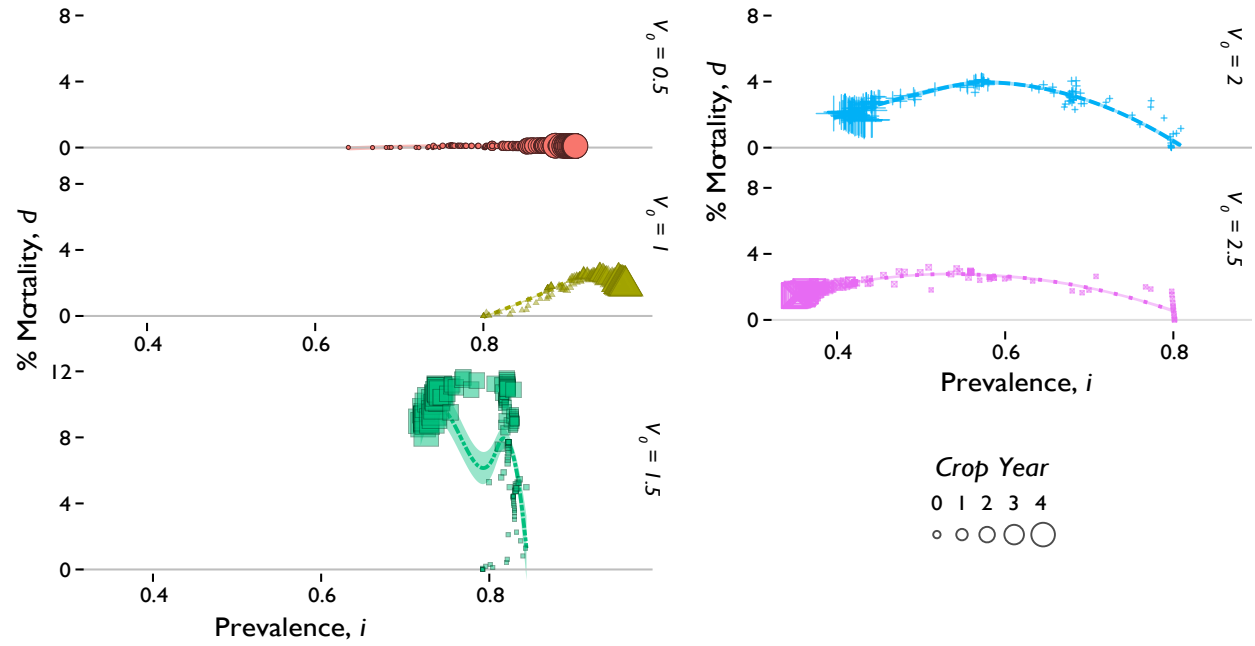

(a)

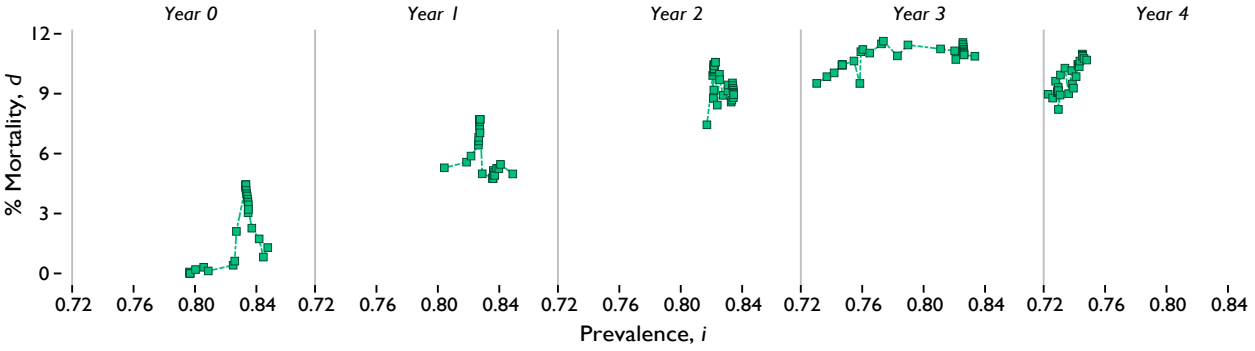

(b)

Figure 5.5: Mortality rates with respect to i at $\mu = 0.4$ and $i_0 = 0.8$. **(a)** Panels are split by decreasing V_0 from top to bottom. $V_0 = 0.1$ and $V_0 = 4$ are both omitted again for visual clarity. $V_0 = 1$ maintained nearly 0% median mortality rate while both $V_0 = 0.1$ and $V_0 = 4$ experienced drops in prevalence to 0 by the final year. **(b)** $V_0 = 1.5$ is split further according to crop years for visual clarity.

5.2 Replication Ratio: Disease Fitness

The replication ratio was used to compare the disease fitness across combinations of virulence factors. According to the tradeoff hypothesis, epizootics with high fitness are expected to have high β and low ν. One-factor analysis determined the factors V_0 and i_0 contributed significantly to the variation in R_v ($p < 0.001$, Kruskal-Wallis) while their interaction effects with initial and final years were not significantly different ($p = 0.332$, permutation test with MANOVA). The $i_0 = 0.2$ IQR for R_v was 1.510 to 1.870 while the $i_0 = 0.8$ IQR for R_v was 0.388 to 0.905. This difference was expected: the $i_0 = 0.2$ viruses have many more susceptible hosts to infect and if transmission is a cost to mortality rate then reinfecting new hosts would lower the overall fitness of the viruses. On the other hand, $i_0 = 0.8$ treatments may be reinfecting each other frequently. The accumulated viral burden leads to higher mortality. Further data analysis corroborates this scenario as the median viral burden for the final year in $i_0 = 0.2$ is 0.276 (IQR = 0.051 - 0.500) while the corresponding $i_0 = 0.8$ viral burden was 0.294 (IQR = 0.140 - 0.5) ($p = 0.007$, Wilcoxan rank sum). Finally, the lowest median R_v was 0.141 which occurred at the final year of the $V_0 = 1$ group in the $i_0 = 0.8$ treatment and the highest median R_v was 2.176 which occurred at the final year of the $V_0 = 2$ group in the low release treatment.

Fig. 5.6 shows that within the V_0 factor the relationship R_v as a function of mutation rate follow approximately sinusoidal patterns. This is especially clear in $V_0 = 0.5$ as the peak and trough are both present within the range of mutation rates. However, the 0.5 virulence treatment is the only group to cross $R_v = 1$ from above the threshold to below with increasing mutation rate. The change in shape of the waveforms between $V_0 = 0.5$ and $V_0 = 1$ indicates the existence of a threshold between the two V_0s. Below this threshold, higher mutation rates leads to the disease dying out. Virus treatments with insufficient starting virulence and high mutation rates may generate a diverse population of harmless viruses; viruses can either persist and do little to no damage or be selected out of the SCN population.

On the other hand, above this threshold, increasing mutation rates improves the fitness of the epizootic. At these higher V_0s, increasing mutation rates could lead to diverse populations of viruses that are damaging, but less so at peak R_v values. Meanwhile in each virulence treatment, the amplitudes generally increase with crop years indicating that as time passes, the effect of mutation rate on R_v is also amplified. The pooled initial and final R_v were found to be significantly different with median initial R_v equal to 1.337 (IQR= 0.386 - 1.536) while final R_v was 1.313 (IQR = 0.618 - 1.862) ($p < 0.001$, Wilcoxan rank sum). The effects on virus fitness appear to be cumulative; viruses with high or low

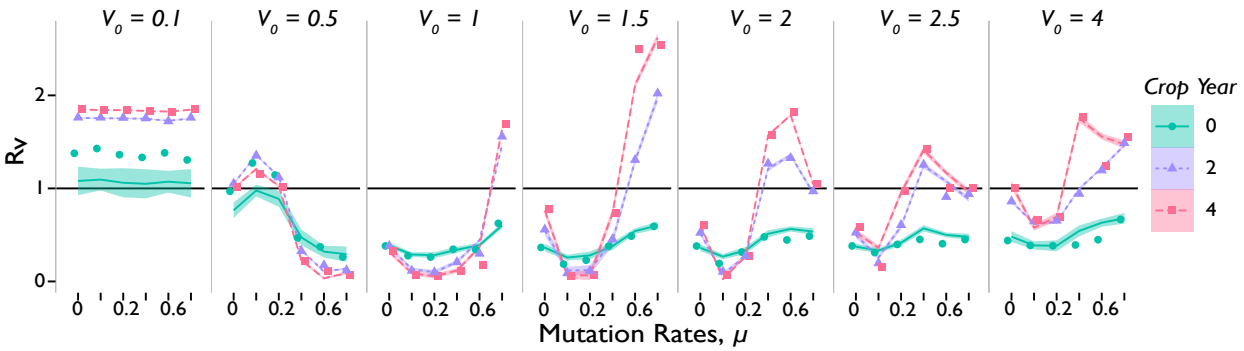

Figure 5.6: Results of R_v with respect to mutation rates reveals behavior near the error threshold $R_v = 1$ within $i_0 = 0.8$. Median R_v values are accompanied by local regression scatterplot smoothing (LOESS) curves with 95% confidence bands. The figure is split into separate panels grouped by initial Virulences while the coloring distinguishes crop years. Crop years 1 and 3 are omitted to improve visual clarity and information density.

fitness will only increase or decrease respectively with time.

Not all treatments cross $R_v = 1$. $V_0 = 0.1$ at either i_0s remains above $R_v = 1$ at all crop years. All initial R_vs at year 0 under high release are above the error threshold. Treatments $V_0 \geq 2$ at high releases remain above the error threshold during all crop years while the opposite is true for the low release treatments. Within virulence factor treatments at different crop years cross the error threshold at similar mutation rates (**Fig. 5.7**). The difference in the vertical offsets between the two release types may indicate the need to adjust the $\tilde{\rho}_{95}$ criteria (**Table 5.1**). For $i_0 = 0.2$ strategy, $\tilde{\rho}_{95}$ could be redefined at a higher health (for example, $\tilde{\rho}_{97.5}$) such that the initial $R_v(\mu)$ waveform would be able to cross the error threshold. The opposite could be done for the high release strategy. In the physical arena, this could be interpreted as the lower release strategies needing more virulent pathogens (fewer avirulent infections) to persist than the higher release strategies.

5.2.1 V_0 and μ_{crit} are Inversely Related

Table 5.1 lists the values of the critical mutation rates for all possible treatments. Interestingly, with the currently defined R_v, many treatments have two critical mutation rates as demonstrated in **Fig. 5.7**. Because of the difference in vertical offset between the two release factors, the paired critical mutation rates occur at a convex curve for low release and at a concave curve at high release. Though this pattern could simply be a consequence of our definition of R_v (**4.3**), it could also imply an instability in disease fitness between the critical mutation rates. For the low release scenario, critical mutation

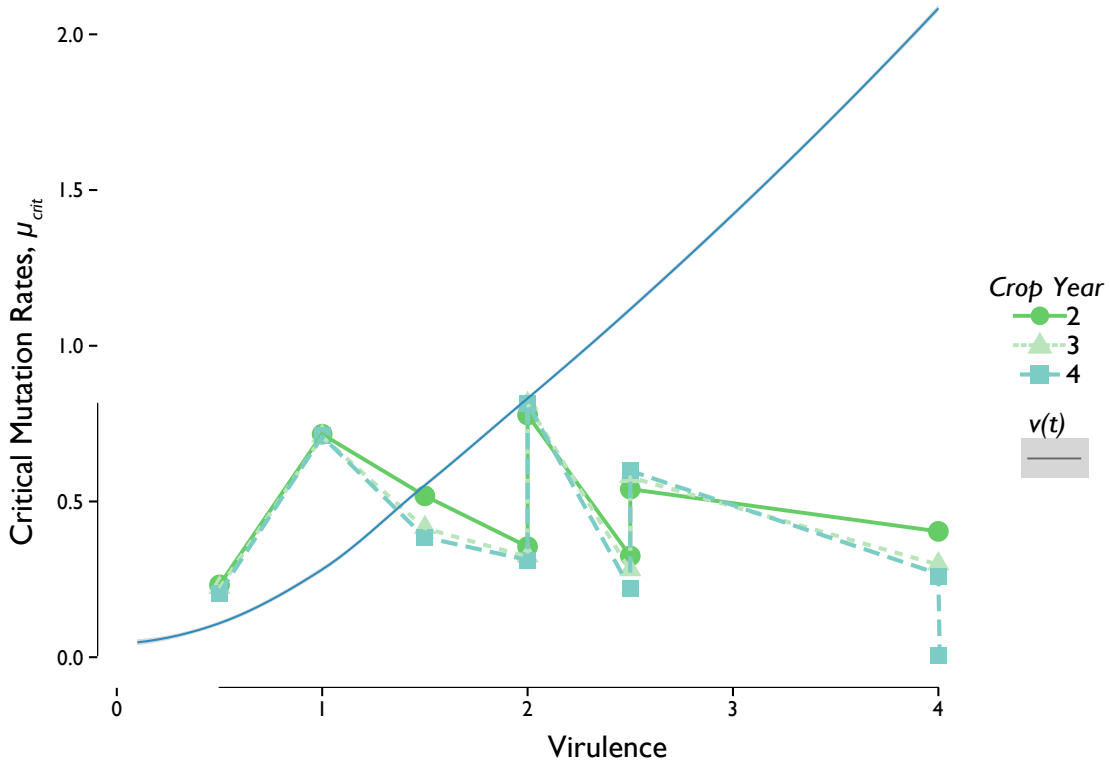

Figure 5.7: Interpolated mutation rates at error threshold. Mutation rates were interpolated using linear regression with 2 or 3 points about $R_v = 1$. A LOESS curve with a 95% confidence band for v is plotted over the mutation rates. Treatments that did not cross $R_v = 1$ are not represented.

rates from a convex curve could mean more highly mutable viruses are more favored for a persisting disease. For the high release scenario, it is more difficult to say which critical point would be more desirable.

5.2.2 High Nematode Mortality Generally Occurs at μ_{crit}

Finally we observed from **Table 5.1** and **Fig. 5.3** that in general, the V_0 pathotype within a certain μ treatment with a μ_{crit} most similar to that initial μ value achieved the highest mortality rates among the other V_0 viruses. For instance, $V_0 = 4$ has a $\mu_{crit} = 0.006$ at the fifth crop season and is also achieving the highest mortality at $\mu = 0$. Likewise, for $V_0 = 1.5$ ($\mu_{crit} = 0.385$ during the fifth crop season) and $V_0 = 1$ ($\mu_{crit} = 0.709$ during the fifth crop season) achieve the greatest nematode suppression in the $\mu = 0.4$ and $\mu = 0.6$ treatments respectively. This observation falls in line with quasispecies theory for RNA viruses which predicts RNA quasispecies will evolve towards the error threshold more so than virulence theory which predicts pathogens in general will evolve to achieve the

Table 5.1: Critical mutation rates interpolated at $R_v = 1$ using linear regression. Parentheses denote the r^2 goodness of fit. Treatments that remained above or below $R_v = 1$ are indicated by a "+" or "–", respectively. Treatments that crossed the error threshold twice are highlighted by the directional arrow symbolizing the slope direction at the intersection corresponding to data in Fig. 5.6.

	Crop Years				
	0	1	2	3	4
$i_0 = 0.2$					
$V_0 = 0.5$	+	+	0.486 (0.97)	0.422 (0.97)	0.373 (0.98)
$V_0 = 1.0$	+	↘ 0.059 (0.87) ↗ 0.379 (0.96)	↘ 0.025 (0.95) ↗ 0.458 (0.96)	↘ 0.004 (0.98) ↗ 0.496 (0.94)	0.519 (0.91)
$V_0 = 1.5$	+	↘ 0.063 (0.95) ↗ 0.164 (0.96)	↘ 0.038 (0.98) ↗ 0.210 (0.98)	↘ 0.026 (0.99) ↗ 0.238 (0.99)	↘ 0.021 (1.00) ↗ 0.258 (1.00)
$V_0 = 2.0$	+	+	↘ 0.083(0.92) ↗ 0.106(0.99)	↘ 0.057(0.98) ↗ 0.118(1.00)	↘ 0.044(0.99) ↗ 0.125(1.00)
$V_0 = 2.5$	+	+	+	+	+
$i_0 = 0.8$					
$V_0 = 0.5$	–	0.248 (0.99)	0.232 (0.99)	0.221 (1.00)	0.206 (1.00)
$V_0 = 1.0$	–	0.776 (0.87)	0.716 (0.99)	0.708 (1.00)	0.709 (1.00)
$V_0 = 1.5$	–	0.648 (0.90)	0.518 (0.84)	0.414 (0.90)	0.385 (0.94)
$V_0 = 2.0$	–	–	↗ 0.355 (0.94) ↘ 0.778 (0.89)	↗ 0.322 (1.00) ↘ 0.812 (0.89)	↗ 0.312 (1.00) ↘ 0.814 (0.95)
$V_0 = 2.5$	–	↗ 0.391 (0.87) ↘ 0.414 (0.65)	↗ 0.325 (0.94) ↘ 0.540 (0.95)	↗ 0.278 (0.96) ↘ 0.578 (0.96)	↗ 0.220 (0.96) ↘ 0.598 (0.98)
$V_0 = 4.0$	–	–	0.404 (0.55)	0.297 (0.82)	↘ 0.006 (0.96) ↗ 0.258 (1.00)

highest R_0 [11, 129]. According to quasispecies theory, this is because virus quasispecies with mutations rates much greater than μ_{crit} will mutate themselves into extinction from lethal mutations while those with mutation rates much less than μ_{crit} will be unable to adapt to a changing environment.

However, $V_0 = 0.5$, 2.0, and 2.5 do not follow this trend. In the case of $V_0 = 0.5$ ($\mu_{crit} = 0.206$ at the fifth crop season), which would be expected to overcome the other V_0 pathotypes within $\mu = 0.8$, this is possibly due to the pathotype's inability to achieve and sustain mortality rates comparable to the other pathotypes. As mentioned earlier, there may be a minimum V_0 less than $V_0 = 1.0$ and greater than $V_0 = 0.5$ required to establish a suppressive epizootic. Since $V_0 = 0.5$ is apparently below this boundary, it may be exempt from the μ_{crit} pattern explained earlier. The inconsistency arising from $V_0 = 2.0$

and 2.5 is less explainable. One possible reason is that both pathotypes in their respective ideal μ treatments have continuously increasing mortality rates within the five-year time frame and neither contain a critical point nor approach equilibrium. Due to the instability of the mortality rates for the two treatments, the nature of their intersections at the error threshold are also unstable. This could potentially point to a weakness in SCNSim, or perhaps with a larger time scale, those two pathotypes would have observable critical points.

5.3 Virulence and Transmissibility: Evolution

5.3.1 Virulence and Transmissibility are Positively Correlated

Fig. 5.8 shows the parametric relationships between β and virulence for each $V_0 \times \mu$ pathotype within $i_0 = 0.8$. Each individual grid reveals a linear and positively correlated relationship between transmissibility and virulence. However, as indicated by the time component, in some pathotypes the relationship is not merely moving in one direction. **Fig. 5.9** highlights three distinct trends found in **Fig. 5.8**. For instance in $V_0 = 2.5 \times \mu = 0.4$, by the final crop season, both β and v have dropped uniformly along the same rate they were rising at during the previous years. For these pathotypes, β and v are behaving as if they are approaching an optimum or simply decreasing after reaching a maximum. Furthermore it appears that despite varying levels of μ, $V_0 = 4$ and $V_0 = 0.1$ remain relatively unchanging, though Kruskal-Wallis hypothesis tests did not support this; $p = 0.002$ and $p < 0.001$, respectively. Regardless, it is evident that the initial conditions have a substantial impact on the temporal lability of β and v.

Fig. 5.8 also visibly confirms a previous finding; greatest nematode mortality is achieved by intermediate pathotypes, which lay on the diagonal of the grid. Within these intermediate pathotypes, β and v are largely increasing throughout the duration of the simulation. This is partly in agreement and partly contrary to the tradeoff hypothesis: At low values β and v are positively correlated, however as $v \to \infty$, no saturating behaviors are observed in β [115]. This may be due to the absence of modeling the host immune response in SCNSim. Thus, the main selection pressure for the viruses is to adjust their β and v in order to keep up with the nematode population growth rate. If an immune response was included in the model, we could expect the viruses becoming more virulent in order to counteract the strengthened immune response as long as the transmission rate remained saturated [113].

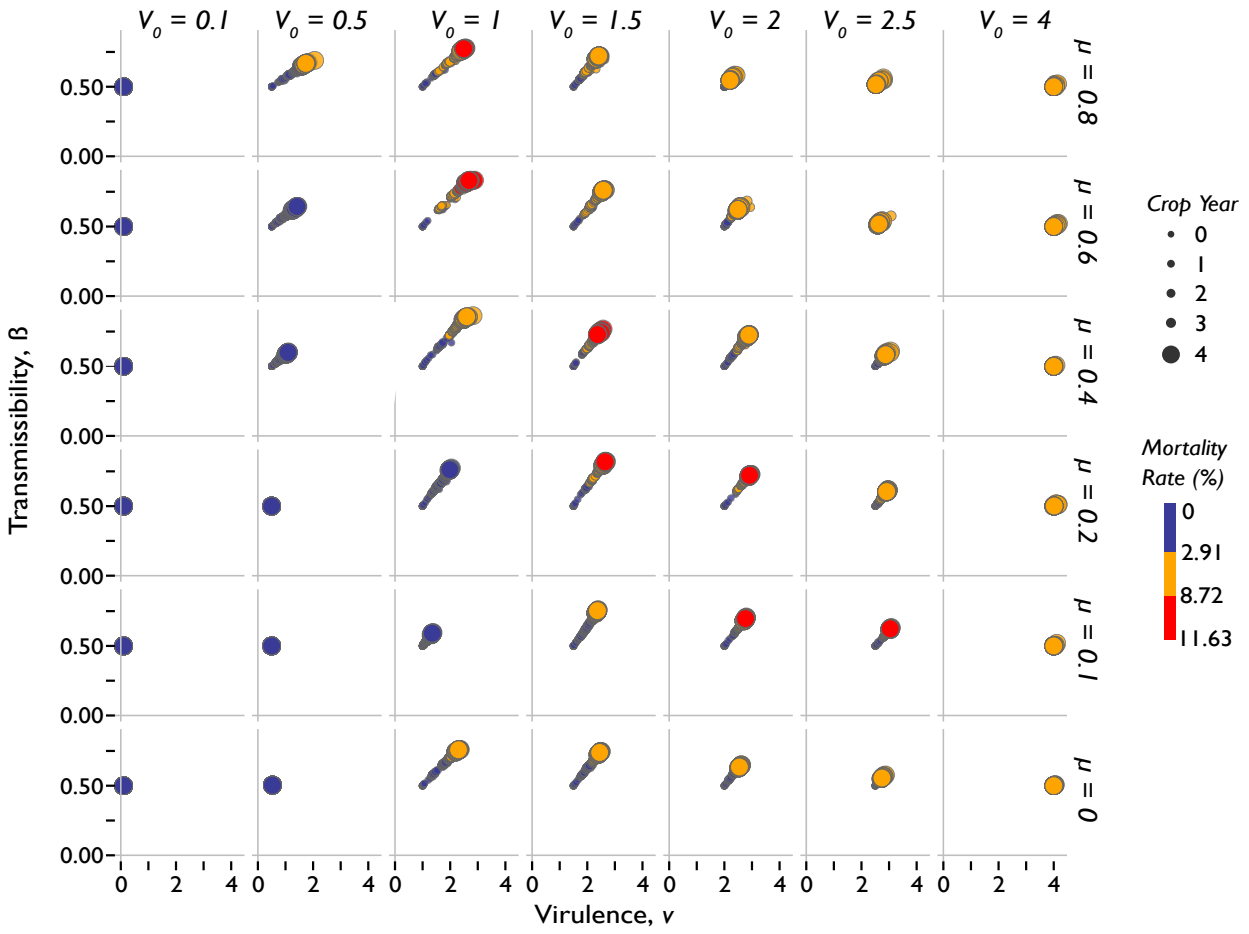

Figure 5.8: Infection mortalities over time across treatments by mutation rates and virulences for $i_0 = 0.8$. The grid layout is marked by columns with increasing mutation rates from left to right and rows with decreasing Virulences from top to bottom. The degree of SCN mortality is distinguished with increasing redness: red (25% highest death rates), yellow (middle 50% death rates), and blue (lowest 25% death rates). The area of the points is also proportional to the crop year in which they take place.

5.3.2 Medial Pathotypes Exhibit Stable Behaviors

In order to discern the stability of virulence trends, data from one variable were plotted with respect to another variable within a $V_0 \times \mu$ grid. This was meant to create figures similar to phase plane diagrams. Each subspace was plotted sequentially over time to maintain the direction of the trend. However, for some variable pairs discussed further below, the relationships appeared to be nonlinear and qualitative stability analysis is believed unreliable for those initial conditions.

Typically, the procedure following this issue is to numerically linearize the data and analyze the phase plane diagram at the critical points. Obtaining eigenvalues from the Jacobian of the system of equations can then classify types of stability at said critical

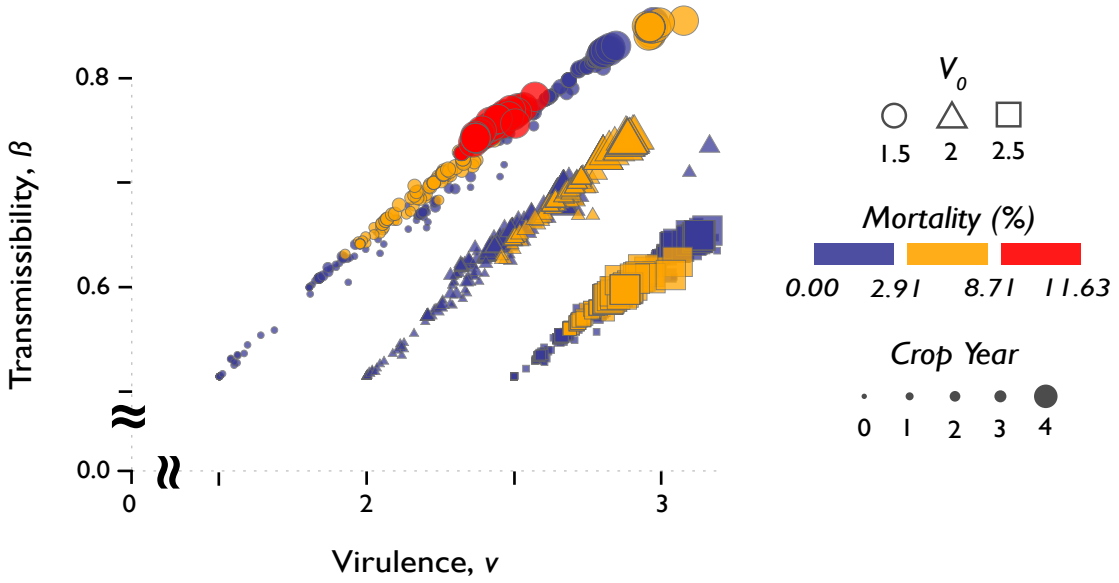

Figure 5.9: Transmissibility versus virulence across three distinct V_0 pathotypes from $\mu = 0.4$, $V_0 = 1.5$, 2.0, and 2.5. These are isolated treatments from **Fig. 5.8**. The colors are indicative of mortality rate; blue represents values 25 % or less of the maximum mortality rate (11.63 %), yellow represents values 25% - 75% of the maximum, and red represents values between the maximum and 75% of the maximum.

points. However, the discrete nature and SCNSim, and the complicated and changing nature of the relationships between variables of interest prevented this approach. For instance, at some V_0 and μ threshold, the data from disease fitness or mortality rate and β appeared to have nonlinear relationships. Thus, discriminating between which virus treatments should be linearized and following subsequent steps is unlikely to be worthwhile. Therefore, with the objectives of this project being qualitative in nature, I proceeded with a qualitative approach.

Fig. 5.10 is a pseudo-phase-portrait diagram comparing mortality rates over β across each combination of pathotypes within $i_0 = 0.8$. Arrows were superimposed to illustrate the vector field for the long-term trends. An encircling pattern is observable within the center-most pathotypes from $V_0 = 1 \times \mu = 0.2$ to $V_0 = 2 \times \mu = 0.4$. This encircling pattern is indicative of a type of stable point. An unfortunate drawback of lacking explicit mathematical models is we are unable to perform the simple linear algebra calculations needed to characterize this stable point.

Speculating from general behaviors of dynamical systems, the most likely type of stability this system exhibits is a spiral sink. Within the general classes of stable behaviors for dynamical systems, there were two possibilities: a spiral sink, and a center [140].

Systems that exhibit centers will have a stably oscillating long-term relationship between the two variables. From previous observations in **Figs.** **5.4c** and **5.4a**, the intermediately virulent and mutable pathotypes generally exhibit stable long-term behaviors and do not oscillate. Thus, we can presume that the modeled system behaves as a spiral sink at intermediate initial conditions.

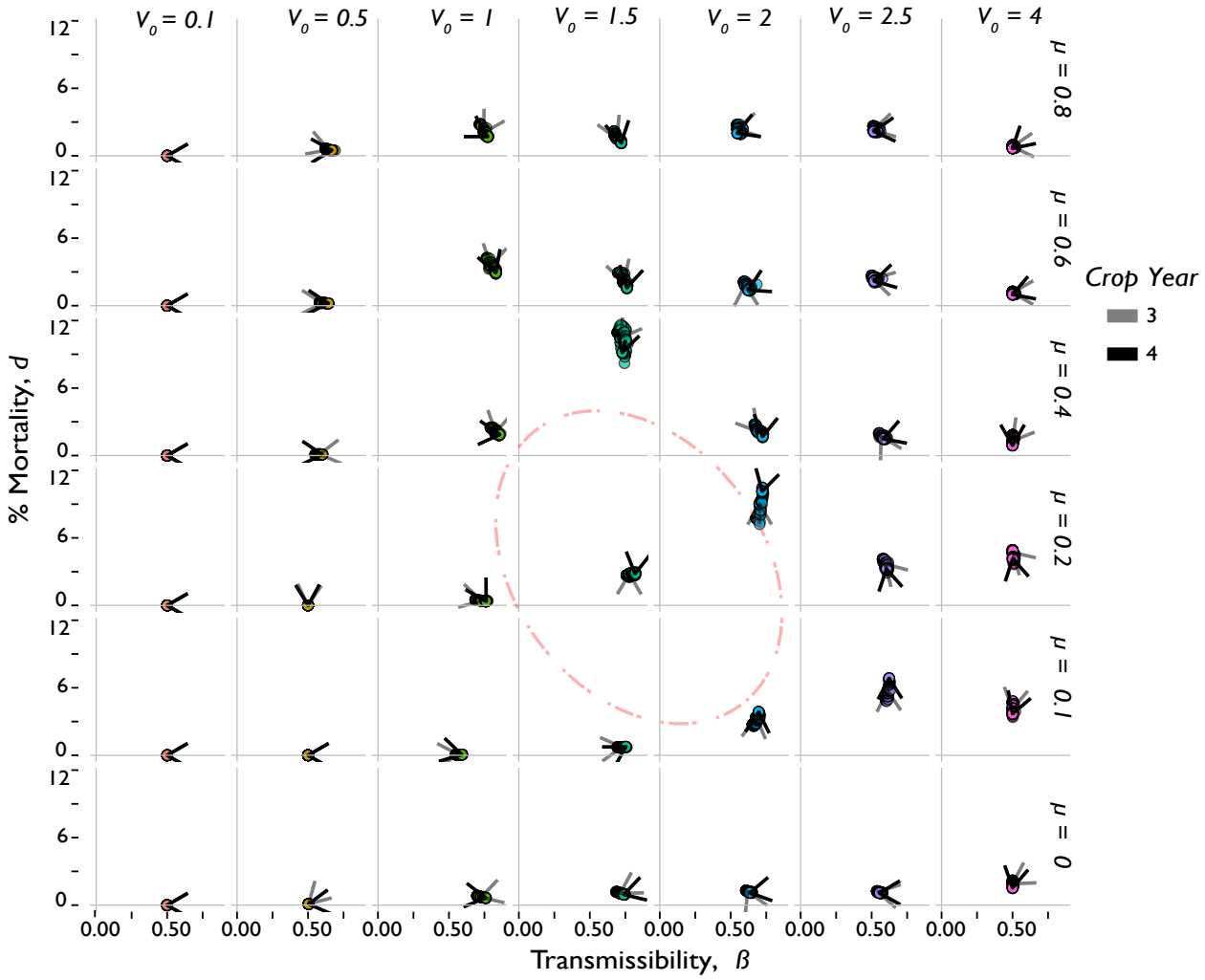

Figure 5.10: Stability of pathotype mortality rates within $i_0 = 0.8$. The dotted circle encompasses pathotypes that appear to be encircling a stable solution in a behavior similar to a spiral sink

Chapter 6
Discussion

"The guide is definitive. Reality is frequently inaccurate."

–Douglas Adams, **The Hitchhiker's Guide to the Galaxy**

SCNSim clearly encapsulates the importance of understanding evolvability in the context of biocontrol. Initial virulence parameters are critical in determining the degree of nematode suppression, and the nature of transmission and virulence evolution. In accordance with the tradeoff hypothesis, we predicted that viruses at low or high states of virulence would perform more poorly than those at intermediate levels. However, though our mortality rate results agreed with theory, the mechanisms differed: We were unable to show a tradeoff between high virulence and transmissibility as $v \to \infty$ [113]. This could be due to the nature of SCNSim; the dataspace may be beyond the region of evolvability. If the 15% range allowed for parameter mutation were increased perhaps then the tradeoff would be observable. We demonstrated the high growth rate of nematodes coupled with the even distribution of viral burden through vertical transmission was a key selection pressure on marginalizing R_v. High vertical transmission of viruses to potentially hundreds of nematode progeny was an especially intense pressure for viruses with low starting virulences which were unable to suppress nematode reproduction.

In SCNSim the contribution of nematode population growth to virus evolution is likely overestimated. Because SCNSim was calibrated such that the nematode population would reach maximum capacity after ten years, in this study's five year simulation the nematode population was allowed to expand relatively uninhibited. If there were a population cap programmed, we would have expected to see greater baseline mortality rates and lower overall health. The lower nematode health in females would translate to fewer surviving J2; those that do survive would have an increased viral load from vertical transmission. This would likely lead to an upward shift in virulence and transmission rate evolution. Furthermore, if SCNSim incorporates a nematode immune response, we could see an even greater upper limit for rising virulence.

Most models of virulence evolution assume the upper limit to virulence is host death. However, in SCNSim we have programmed additional limitations based on stochastic events driven by the nematode *Health* parameter. Though these probabilities may need

to be calibrated in the future, these stochastic events serve to give morbidity a role in virulence evolution. As Mackinnon *et* Read discuss in their review, many common systems such as *P. chabaudi* and influenza rarely result in mortalities, with case fatalities as low as 1% [115]. Because morbidity manifests at the individual level, this is a crucial advantage of agent-based modeling over the SIR mathematically explicit models.

Our fitness parameter R_v results were partly consistent some studies such as those by Mackinnon *et al.* who showed *Plasmodium spp.* evolved to maximize R_0 [115, 124]. In this study, viruses regardless of their initial parameters amplified their initial R_v position. If R_v is initially ≥ 1, the viruses would become more positive over time. In some of the reverse cases where $R_v < 1$, viruses would become more fit in later years, though the remaining pathotypes became even less fit over time. However, a high R_v is not necessarily desirable for biocontrol. From our results, it appears the most desirable pathotypes exist at the $R_v = 1$ threshold with mutation rates at μ_{crit}. If the viruses described by Bekal *et al.* behave according to quasispecies theory, as they are likely to as error-prone RNA viruses, the most frequently occuring viruses should be at approximately μ_{crit} and $R_v = 1$ [129].

The parameters tested in this study were chosen for the investigation of virulence evolution in SCN hosts and were not necessarily true to the SCN system. One of these deliberate deviations was to model annual soybean planting as opposed to rotating crops in alternating years. Withholding soybean hosts every other year would have also served to suppress nematode expansion. In the context of biocontrol however, it is important to acknowledge the impact actual farming practices have on the epizootiology of the virus-nematode system. According to our model, viruses reached their peak mortality rates after the 2^{nd} or 3^{rd} crop season. However, in the real-world, where we expect infectious activity to attenuate during non-host planting seasons, these peak mortalities are likely to be delayed. This is concern can be worsened if the viruses turn out to be unstable during nematode dormancy. Over time, the effectiveness of these viruses would be greatly diminished before they could be expected to manage nematodes.

New commercial biocontrol products are suggested to be applied every planting season by their manufacturers most commonly as seed treatments. The cumulative effects of regular inundatory application and persistence of the viral epizootic would likely have much more positive results than the one-time application simulated in this study. Therefore, if viruses become commercially available as a seed treatment for SCN management, as they already are for many insect pests, their effectiveness would be greater improved than our study's results predict [100].

Five viruses were discovered by Bekal and colleagues as one of the first documented cases of nematode viruses [7, 8]. These viruses are believed to be natural enemies of

SCN, though it is impossible to tell with the current available information the degree to with they impact a field population of SCN. From the sample data, it is estimated 10% of SCN in Champaign, IL are infected with some if not all five viruses simultaneously [8]. This low prevalence may explain why SCN are successful despite the presence of natural pathogens. Our results demonstrated a possible threshold in initial prevalence for the establishment of a successful biocontrol epizootic. Though we did not investigate this further, we know that this minimum prevalence is greater than 20%.

This is one of only a few studies using agent-based modeling in a biocontrol or virulence evolution study. With a complex system such as the virus-SCN-soybean system, it would be extremely difficult to apply continuum-based models such as those adapted from the SIR paradigm. While SCNSim is currently a bit too crude to be useful for the confident selection of a virus biocontrol agent, it has provided us with some valuable insights for desirable virus characteristics. We have also identified weakness that can be readily improved upon as discussed below.

6.1 Recommendations for Future Work

One of the current major weaknesses in SCNSim stems from the lack of empirical data from these novel SCN viruses. Specifically, we do not know which viruses are more pathogenic, their pathophysiology, transmission rates for each transmission mode, their host range, etc. What symptoms manifest from SCN virus infection? What are the fitness consequences of virulence for the viruses? For instance, modeling and empirical studies have shown that specialist pathogens evolve higher virulence than generalists [113, 141]. Boots *et* Sasaki found in their spatially explicit model that pathogens will evolve higher levels of virulence in highly connected communities [126]. What can we expect from the highly heterogeneous population structure of SCN? On one hand, SCN metapopulations are thought to be relatively static. On the other hand, SCN can be spread as contaminated soil is transported within and without fields via agricultural equipment and vehicles [1]. These are all aspects of virulence that will be critical for improving our model of virulence evolution.

With regards to modeling SCN, it would be desirable to incorporate a nematode immune response and be able to follow changes in immune adaptability. We could consider nematode genetic diversity with analogous properties to those we assign to viruses, such as: mutation rates, recovery rate, feeding rate, reproductive success, etc. As SCN is also a pathogen to soybeans, it may even be worthwhile to incorporate a more complex SCN-soybean interaction. Furthermore, we could add complexity to the model

by including soil moisture and pH which has shown to impact SCN population growth [9]. However like the viruses, to more accurately consider these we would need more reliable empirical data.

The SCN life cycle, soybean planting cycles, and varying climates throughout major soybean growing regions provide ample opportunities to increase the complexity of the model. However with all models, there is a tradeoff between computational time and predictive accuracy. Certainly there will be a critical point after which increasing the model complexity does not markedly improve its utility. As it is at the time of this writing, SCNSim is demonstrably useful for generalizing the evolution of virus characteristics though it will need further improvements in order to be more relevant to the novel SCN viruses described in Bekal *et al.* [7, 8].

Chapter 7
Conclusion

SCNSim, an agent-based model, has shown to be a promising approach to study complex host-pathogen systems and is likely to improve as empirical data on SCN virus pathogenicity arises. Currently SCNSim is capable of providing general guidelines to selecting viral agents for biocontrol. However, there are still complexities in the real-world system that once incorporated can allow SCNSim to become a powerful predictive tool. The major conclusions from this thesis project can be summarized as follows:

1. High initial prevalence significantly improves nematode mortality
2. Most suppressive pathotypes have intermediate mutation rates and virulence
3. Initial virulence and critical mutation rates are negatively correlated
4. Transmissibility and virulence are positively correlated and follow a linear relationship given viruses are selected upon by nematode death and fecundity
5. Mortality rates reach stable solutions at medial pathotypes

Agent-based modeling appears to be an underutilized tool for theoretical studies in virulence evolution. In systems where the assumptions of the SIR model fall short, individual-based models are still able to construct complex patterns on the population level. From our results, two interesting speculations emerge: constraining virus properties to achieve a fitness close to $R_v = 1$ may be a helpful guideline for designing virus-agents, and the influence of vertical versus horizontal transmission on long-term efficacy is an important consideration to weigh against nematode growth rates. SCNSim can be used to direct molecular-based methods for designing and testing biocontrol candidates and can be used to guide post-release monitoring of evolutionary changes.

Chapter 8

References

[1] D. P. Schmitt, R. D. Riggs, and J. A. Wrather, *Biology and management of soybean cyst nematode*, 2nd ed., D. P. Schmitt, R. D. Riggs, and J. A. Wrather, Eds. Schmitt & Associates of Marceline, 2004.

[2] S. R. Koenning and J. A. Wrather, "Suppression of soybean yield potential in the continental united states by plant diseases from 2006 to 2009." November 2010, Online, Plant Health Progress, doi:10.1094/PHP-2010-1122-01-RS. [Online]. Available: http://www.plantmanagementnetwork.org/pub/php/research/2010/yield/

[3] F. Hunter-Fujita, P. R. Entwistle, H. F. Evans, and N. E. Crook, *Insect Viruses and Pest Management*, F. Hunter-Fujita, Ed. John Wiley & Sons, 1998.

[4] T. Niblack, A. Colgrove, K. Colgrove, and J. Bond, "Shift in virulence of soybean cyst nematode is associated with use of resistance from pi 88788," January 2008, Online, doi:10.1094/PHP-2008-0118-01-RS. [Online]. Available: http://www.plantmanagementnetwork.org.proxy2.library.illinois.edu/pub/php/research/2008/virulence/

[5] D. Brown, W. Robertson, and D. Trudgill, "Transmission of viruses by plant nematodes," *Annu. Rev. Phytopathol.*, vol. 33, pp. 223–249, 1995.

[6] M.-A. Felix, A. Ashe, J. Piffaretti, G. Wu, I. Nuez, T. Belicard, Y. Jiang, G. Zhao, C. J. Franz, L. D. Goldstein, M. Sanroman, E. A. Miska, and D. Wang, "Natural and experimental infection of *Caenorhabditis* nematodes by novel viruses related to nodaviruses," *PLOS BIOLOGY*, vol. 9, no. 1, JAN 2011.

[7] S. Bekal, L. L. Domier, T. L. Niblack, and K. N. Lambert, "Discovery and initial analysis of novel viral genomes in the soybean cyst nematode," *J. Gen. Virol.*, vol. 92, pp. 1870–1879, AUG 2011.

[8] S. Bekal, L. L. Domier, B. Gonfa, N. K. McCoppin, K. N. Lambert, and K. Bhalerao, "A novel flavivirus in the soybean cyst nematode," *Journal of General Virology*, vol. 95, pp. 1272–1280, 2014.

[9] T. L. Niblack, K. N. Lambert, and G. L. Tylka, "A model plant pathogen from the kingdom animalia: *Heterodera glycines*, the soybean cyst nematode," *Annual Review of Phytopathology*, vol. 44, pp. 283–303, 2006, pT: S; NR: 105; TC: 25; J9: ANNU REV PHYTOPATHOL; PG: 21; GA: 092VV; UT: WOS:000241126300013.

[10] Illinois State Climatologist's Office, "Monthly data for station 118740 (urbana)," 2014, Illnois State Water Survey, Champaign, IL. [Online]. Available: http://www.isws.illinois.edu/data/climatedb/choose.asp?stn=118740

[11] S. Alizon, A. Hurford, N. Mideo, and M. van Baalen, "Virulence evolution and the trade-off hypothesis: history, current state of affairs and the future," *J. Evol. Biol.*, vol. 22, pp. 245–259, 2009.

[12] National Agricultural Statistics Service, Agricultural Statistics Board, and United States Department of Agriculture, *Agricultural Statistics 2012.* USDA, 2012, ch. III: Statistics on Oilseeds, Fats, and Oils, pp. III–13 to III–21.

[13] Economics Research Service, "Feed grains yearbook 2014," USDA, Tech. Rep., 2014.

[14] M. J. Messina, "Legumes and soybean: overview of their nutritional profiles and health effects," *Am J Clin Nutr*, vol. 70, pp. 439–450, 1999.

[15] High Quest Partners and Soyatech, LLC, "How the global oilseed and grain train works," U.S. Soybean Export Council, Tech. Rep., 2011.

[16] L. G. Croppings, *Pest Management in Soybean*, L. Croppings, M. Green, and R. Rees, Eds. Elsevier Applied Science, 1992.

[17] K. Giller and G. Cadisch, "Future benefits from biological nitrogen fixation: An ecological approach to agriculture," *Plant Soil*, vol. 174, pp. 255–277, 1995.

[18] G. Varvel and W. Wilhelm, "Soybean nitrogen contribution to corn and sorghum in western corn belt rotations," *Agronomy Journal*, vol. 95, pp. 1220–1225, 2003.

[19] C. F. Yamoah, G. E. Varvel, W. J. Waltman, and C. A. Francis, "Long-term nitrogen use and nitrogen-removal index in continuous crops and rotations," *Field Crops Research*, vol. 57, pp. 15–27, 1998.

[20] D. Rodriguez-Navarro, I. M. Oliver, M. A. Contreras, and J. Ruiz-Sainz, "Soybean interactions with soil microbes, agronomical and molecular aspects," *Agronomy for Sustainable Development*, vol. 31, pp. 173–190, 2011. [Online]. Available: http://www.scopus.com/inward/record.url?eid=2-s2.0-79952590018&partnerID=40&md5=fd1f410739ca4b5ed7af43e06212715c

[21] R. F. Wilson, *Soybean: Market Driven Research Needs*. Springer Science+Business, 2008, ch. 1, pp. 3–15.

[22] *2014 Soy Products Guide*, United Soybean Board, 2014.

[23] American Soybean Association, "Soy stats 2012," 2012, American Soybean Association, 12125 Woodcrest Executive Dr., Suite 100, Saint Louis, MO 63141. [Online]. Available: http://soystats.com/archives/2012/non-frames.htm

[24] Omni Tech International, "Life cycle impact of soybean production and soy industrial products," United Soybean Board, Tech. Rep., 2010.

[25] USDA PSD Online Statistics, "Soybean area, yield, and production," January 2014, USDA Foreign Agricultural Service. [Online]. Available: http://apps.fas.usda.gov/psdonline/

[26] M. Rosier, "The importance of soybean as a market for agricultural chemicals," in *Pest Management in Soybean*, L. Copping, M. Green, and R. Rees, Eds. Springer Netherlands, 1992, pp. 1–9. [Online]. Available: http://dx.doi.org/10.1007/978-94-011-2870-4_1

[27] M. A. Mikel, B. W. Diers, R. L. Nelson, and H. H. Smith, "Genetic diversity and agronomic improvement of north american soybean germplasm," *Crop Science*, vol. 50, pp. 1219–1229, 2010.

[28] First Call P.R. Newswire, "Monsanto company to acquire delta and pine land company for $1.5 billion in cash," August 2006, Monsanto. [Online]. Available: http://monsanto.mediaroom.com/index.php?s=27632&item=76619

[29] J. A. Wrather and S. R. Kroenning, "Soybean disease loss estimates for the united states, 1996-2010," August 2013, University of Missouri Agricultural Experiment Station. [Online]. Available: http://aes.missouri.edu/delta/research/soyloss.stm

[30] J. A. Wrather and S. R. Kroenning, "Estimates of disease effects on soybean yield in the united states 2003 to 2005," *Journal of Nematology*, vol. 38, pp. 173–180, 2006.

[31] T. Niblack, G. Tylka, P. Arelli, J. Bond, B. Diers, P. Donald., J. Faghihi, V. Ferris, K. Gallo, R. Heinz, H. Lopez-Nicora, R. Qualen, T. Welacky, and J. Wilcox, "Standard greenhouse method for assessing soybean cyst nematode resistance in soybean: Sce08 (standardized cyst evaluation 2008)," *Plant Health Progress*, vol. Online, 2009.

[32] National Agricultural Statistics Service, Agricultural Statistics Board, and United States Department of Agriculture, *Agricultural Statistics 2005.* USDA, 2005, ch. III: Statistics on Oilseeds, Fats, and Oils, pp. III–13.

[33] "Consumer price index history table," January 2014, US Department of Labor, Bureau of Labor Statistics. [Online]. Available: ftp://ftp.bls.gov/pub/special.requests/cpi/cpiai.txt

[34] North Carolina Agricultural Experiment Station, United States. Agricultural Research Service. Field Crops Research Branch, United States. Agricultural Research Service. Horticultural Crops Research Branch, and United States. Plant Pest Control Branch, *Soybean Cyst Nematode*, U. A. R. Service, Ed. USDA Agricultural Research Service, 1956, vol. 22-29.

[35] J. Wang and T.L, "Soybean cyst nematode reduces soybean yield without causing obvious aboveground symptoms," *Plant Disease*, vol. 87, pp. 623–628, 2003.

[36] B. Sipes, D. Schmitt, and K. Barker, "Fertility of three biotypes of *Heterodera glycines*," *Phytopathology*, vol. 82, pp. 999–1001, 1992.

[37] T. Niblack, "Soybean cyst nematode management reconsidered," *Plant Disease*, vol. 89, pp. 1020–1026, 2005.

[38] Department of Plant Pathology, Iowa State University, "Soybean cyst nematode," January 2014, Iowa State University. [Online]. Available: http://www.plantpath.iastate.edu/scn/node/53

[39] J. Faghihi and V. R. Ferris, "Soybean cyst nematode–e-210-w," in *Field Crops*. Purdue University Entomology Extension, 2012.

[40] P. Jones, G. Tylka, and R. Perry, *Physiology and Biochemistry of Free-Living and Plant-Parasitic Nematodes*. CABI Publishing, 1998, ch. 8: Hatching, pp. 181–212.

[41] M. Papademetriou and L. Bone, "Chemotaxis of larval soybean cyst nematode, *Heterodera glycines* race 3, to root leachates and ions," *J. Chem. Ecol.*, vol. 9, no. 3, pp. 387–396, 1983.

[42] V. M. Williamson and R. S. Hussey, "Nematode pathogenogenesis and resistance in plants," *The Plant Cell*, vol. 8, pp. 1735–1745, 1996.

[43] M. G. Mitchum, R. S. Hussey, T. J. Baum, X. Wang, A. A. Elling, M. Wubben, and E. L. Davis, "Nematode effector proteins: an emerging paradigm of parasitism," *New Phytologist*, vol. 199, pp. 879–894, 2013.

[44] S. Koenning, *Biology and Management of Soybean Cyst Nematode*. Schmitt & Associates of Marceline, 2004, ch. Population Biology, pp. 73–110.

[45] G. Gheyson and M. G. Mitchum, "How nematodes manipulate plant development pathways for infection," *Current Opinion in Plant Biology*, vol. 14, pp. 415–421, 2011.

[46] Beltsville Electron and Confocal Microscopy Unit, "Soybean cyst nematode (*Heterodera glycines*)," 2009, Online, ARS-USDA. [Online]. Available: http://emu.arsusda.gov/typesof/default.html

[47] Plant & Pest Digital Library, "Soybean cyst nematode," December 2008, Purdue University. [Online]. Available: http://www.ppdl.org/dd/id/SCN-soybean.html

[48] K. N. Lambert and S. Bekal, "Introduction to plant-parasitic nematodes," 2002, The Plant Health Instructor, dOI: 10.1094/PHI-I-2002-1218-01. [Online]. Available: http://www.apsnet.org/edcenter/intropp/PathogenGroups/Pages/IntroNematodes.aspx

[49] G. Noel, *Biology and Management of Soybean Cyst Nematode*. Schmitt & Associates of Marceline, 2004, ch. 8: Soybean Response to Infection, pp. 131–151.

[50] B. Y. Endo, "Ultrastructures of initial responses of susceptible and resistant soybean roots to infection by *Heterodera glycines*," *Revue de Nematologie*, vol. 14, pp. 73–94, 1991.

[51] E. Davis and G. Tylka, "Soybean cyst nematode disease," 2000, The Plant Health Instructor, dOI: 10.1094/PHI-I-2000-0725-01. [Online]. Available: http://www.apsnet.org/edcenter/intropp/lessons/Nematodes/Pages/SoyCystNema.aspx

[52] R. Khan, N. Alkharouf, H. Beard, M. MacDonald, I. Chouikha, S. Meyer, J. Grefenstette, H. Knap, and B. Matthews, "Microarray analysis of gene expression in soybean roots susceptible to the soybean cyst nematode two days post invasion," *Journal of Nematology*, vol. 36, pp. 241–248, 2004.

[53] D. Puthoff, D. N. N. Rodermel, and T. Baum, "*Arabidopsis* gene expression changes during cyst nematode parasitism revealed by statistical analysis of microarray expression profiles." *Plant Journal*, vol. 33, pp. 911–921, 2003.

[54] S. Bekal, T. L. Niblack, and K. N. Lambert, "A chorismate mutase from the soybean cyst nematode *Heterodera glycines* shows polymorphisms that correlate with virulence," *Molecular Plant-Microbe Interactions*, vol. 16, pp. 439–446, 2003.

[55] G. Gheyson and M. G. Mitchum, *Cell Biology of Plant Nematode Parasitism*. Springer Berlin Heidelberg, 2009, ch. Molecular Insights in the Susceptible Plant Response to Nematode Infection, pp. 45–81.

[56] M. Sobczak and W. Golinkowski, *Cell Biology of Plant Nematode Parasitism*, ser. Plant Cell Monographs. Springer, 2009, vol. 15, ch. Structure of Cyst Nematode Feeding Sites, pp. 153–188.

[57] W. Grunewald, B. Cannoot, J. Frimi, and G. Gheyson, "Parasitic nematodes modulate pin-mediated auxin transport to facilitate infection," *PLoS Pathogens*, vol. 5, pp. 1–7, 2009.

[58] S. Chen, *Management with Biological Methods*. Schmitt & Associates of Marceline, 2004, ch. Management with Biological Methods, pp. 207–242.

[59] A. G. Stone, S. J. Scheuerell, and H. M. Darby, *Soil Organic Matter in Sustainable Agriculture*. CRC Press, 2004, ch. Suppression of Soilborne Diseases in Field Agricultural Systems: Organic Matter Management, Cover Cropping, and Other Cultural Practices, pp. 132–164.

[60] T. Niblack and S. Chen, *Biology and Management of Soybean Cyst Nematode*. Schmitt & Associates of Marceline, 2004, ch. Cropping Systems and Crop Management, pp. 181–206.

[61] G. L. Tylka, *Soybean Cyst Nematode Field Guide*, 2nd ed., Iowa State University of Science and Technology and Iowa Soybean Association, 2012.

[62] G. Smith, J. Shannon, L. Sweets, W. Wiebold, J. Wrather, D. Edwards, P. Donald, G. Noel, J. Orf, and R. Riggs, "Soybean cyst nematode management guide," 2013, Online, Plant Health Initiative, North Central Soybean Research Program, 5th ed. [Online]. Available: http://www.ncsrp.com/pdf_doc/SCN_Management.pdf

[63] J. Kurle, D. Malvick, B. Potter, and J. Orf, *Soybean Cyst Nematode Management Guide*, University of Minnesota Extension, 2011.

[64] K. Barker, S. Koenning, and D. Schmitt, *Biology and Management of Soybean Cyst Nematode*. Schmitt & Associates of Marceline, 2004, ch. Population density based management, pp. 89–110.

[65] S. Koenning, D. Schmitt, K. Barker, and M. Gumpertz, "Impact of crop rotation and tillage system on *Heterodera glycines* polulation density and soybean yield," *Plant Disease*, vol. 79, pp. 282–286, 1995.

[66] T. Niblack and R. Riggs, *Variation in Virulence Phenotypes*. Schmitt & Associates of Marceline, 2004, ch. Variation in Virulence Phenotypes, pp. 57–71.

[67] J. Shannon, P. Arelli, and L. Young, *Biology and Management of the Soybean Cyst Nematode*. Schmitt & Associates of Marceline, 2004, ch. Breeding for Resistance and Tolerance, pp. 156–180.

[68] J. L. D. Bruin and P. Pedersen, "Soybean cultivar and planting date response to soil fumigation," *Agronomy Journal*, vol. 100, pp. 965–970, 2008.

[69] *Telone ™C-35 Soil Fungicide and Nematicide*, Dow AgroSciences, Indianapolis, IN, Noember 2011, product Code: 59176.

[70] Office of Pesticide Programs, "Reregistration eligibility decision (red) for methyl bromide (soil and non-food structural uses)," Environmental Protection Agency, Tech. Rep. EPA 738-R-08-005, 2008.

[71] W. Thomas, "Methyl bromide: Effeffect pest management tool and environmental threat," *Journal of Nematology*, vol. 28, pp. 586–589, 1996.

[72] *Midwest Vegetable Production Guide for Commercial Growers*, University of Illinois Extension, 2014, c1373-14.

[73] G. Noel and L. Wax, "Population dynamics of Heterodera glycines in conventional tillage and no-tillage soybean/corn cropping systems," *JOURNAL OF NEMATOLOGY*, vol. 35, no. 1, pp. 104–109, MAR 2003.

[74] T. Nishanthan, "Ecology of soybean cyst nematode suppressive soils in midwest soybean cropping systems," Ph.D. dissertation, University of Vermont, 2013.

[75] Y. Bao, D. A. Neher, and S. Chen, "Soil disturbance and biocides on nematode communities and extracelextra enzyme activiy in soybean cyst nematode suppressive soil," *Nematology*, vol. 13, pp. 687–699, 2011.

[76] E. A. Adee and T. L. Niblack, "Effect of soybean cultivar moderately resistant to soybean cyst nematode on scn populations and yield," June 2008, Plant Health Progress, doi:10.1094/PHP-2008-0618-03-RS. [Online]. Available: http://www.plantmanagementnetwork.org.proxy2.library.illinois.edu/sub/php/research/2008/scn/scn.pdf

[77] D. Miller, S. Chen, R. Porter, G. Johnson, D. Wyse, S. Stetina, L. Klossner, and G. Nelson, "Rotation crop evaluation for management of the soybean cyst nematode in minnesota," *Agronomy Journal*, vol. 98, pp. 569–578, 2006.

[78] D. Hershman, R. Heinz, and B. Kennedy, "Soybean cyst nematode, *Heterodera glycines*, adapting to resistant soybean cultivars in kentucky," *Plant Disease*, vol. 92, p. 1475, 2008.

[79] J.H. Long, Jr. and T. Todd, "Effect of crop rotation and cultivar resistance on seed yield and the soybean cyst nematode in full-season and double-cropped soybean," *Crop Science*, vol. 41, pp. 1137–1143, 2001.

[80] P. A. Donald, P. E. Pierson, S. K. S. Martin, P. R. Sellers, G. R. Noel, A. E. MacGuidwin, J. Faghihi, V. R. Ferris, C. R. Grau, D. J. Jardine, H. Melakeberhan, T. L. Niblack, W. C. Stienstra, G. L. Tylka, T. A. Wheeler, and D. S. Wysong, "Assessing *Heterodera glycines*-resistant and susceptible cultivar yield response," *Journal of Nematology*, vol. 38, pp. 76–82, 2006.

[81] National Academy of Sciences, *Research Briefings 1987*. The National Academies Press, 1988. [Online]. Available: http://www.nap.edu/openbook.php?record_id=1061

[82] J. Alms, D. Vos, M. Rosenberg, A. Szczepaniec, B. Hadi, and K. Ruden, *South Dakota Soybean Crop Protection Guide: Seed Treatments*, 03rd ed., iGrow, South Dakota State University Extension, 2013.

[83] *The Guide to Seed Treatment Stewardship*, American Seed Trade Association and CropLife America, 3 2013.

[84] *7 USC §1551-1611 Federal Seed Act*, Marketing and Regulatory Programs and Agricultural Marketing Service and Livestock and Seed Program and Seed Regulatory and Testing Branch Std., Rev. 1988, 1998, 1940.

[85] M. Koike, R. Shinya, D. Aiuchi, M. Mori, R. Ogino, H. Shinomiya, M. Tani, and M. Goettel, *Soybean Physiology and Biochemistry*. InTech, 2011, ch. Future Biological Control for Soybean Cyst Nematode, pp. 193–208.

[86] A. Khan, K. Williams, and H. Nevalainen, "Control of plant-parasitic nematodes by *Paecilomyces lilacinus* and *Monacrosporium lysipagum* in pot trials," *BioControl*, vol. 51, no. 5, pp. 643–658, 2006. [Online]. Available: http://dx.doi.org/10.1007/s10526-005-4241-y

[87] P. C. Trivedi and A. Malhotra, *Bacteria in Agrobiology: Disease Management*. Springer, 2013, ch. Bacteria in the Management of Plant-Parasitic Nematodes, pp. 349–378.

[88] M. Terefe, T. Tefera, and P. Skhuja, "Effect of a formulation of *Bacillus firmus* on root-knot nematode *Meloidogyne incognita* infestation and the growth of tomato plants in the greenhouse and nursery," *J. Invertebr. Pathol.*, vol. 100, pp. 94–99, 2008.

[89] D. Schrimsher, "The studies of plant host resistance to the reniform nematode in upland cotton and the effects of bacillus firmus gb-126 on plant-parasitic nematodes," Masters, Auburn University, Auburn, AL, April 2013.

[90] S. Kiewnick, *Recent Developments in Management of Plant Diseases*. Springerlink, 2009, ch. Importance of Multitrophic Interactions for Successful Biocontrol of Plant Parasitic Nematodes with *Paecilomyces lilacinus* Strain 251, pp. 81–92.

[91] "Melocon™wg," 2014, Certis USA, Columbia, MD. [Online]. Available: http://www.certisusa.com/pest_management_products/bionematicide/melocon_biological_nematicide.htm

[92] Bayer CropScience, "Poncho™/votivo™corn and soybean q&a," Online, Bayer CropScience, Research Triangle Park, NC, 2011, http://www.bayercropscience.us/ /media/Bayer

[93] G. R. Noel, N. Atibalentja, and L. L. Domier, "Emended description of *Pasteuria nishizawae*," *Int. J. Syst. Evol. Microbiol.*, vol. 55, pp. 1681–1685, 2005.

[94] B. Callanan and M. Alderfer, "Clariva complete beans manages scn and improves yield in 2013 trial results," February 2014, Syngenta, Greensboro, NC. [Online]. Available: http://www.syngentaebiz.com/htmlRender/display.aspx?page=cpppnews&newsid=179606

[95] J. Bale, J. van Lenteren, and F. Bigler, "Biological control and sustainable food production," *Philosophical transactions of the royal society biological sciences*, vol. 363, pp. 761–776, 2008.

[96] D. Simberloff, "Risks of species introduced for biological control," *Biological Conservation*, vol. 78, pp. 185–192, 1996.

[97] R. van Driesche, M. Hoddle, and T. Center, *Control of PPest and Weeds by Natural Enemies: and Introduction to Biological Control*. Blackwell Publishing, 2008, ch. Non-Target Impacts of Biological Control Agents, pp. 183–200.

[98] F. Geiger, J. Bengtsson, F. Berendse, W. W. Weisser, M. Emmerson, M. B. Morales, P. Ceryngier, J. Liira, T. Tscharntke, C. Winqvist, S. Eggers, R. Bommarco, T. PÃd'rt, V. Bretagnolle, M. Plantegenest, L. W. Clement, C. Dennis, C. Palmer, J. J. OÃśate, I. Guerrero, V. Hawro, T. Aavik, C. Thies, A. Flohre, S. HÃd'nke, C. Fischer, P. W. Goedhart, and P. Inchausti, "Persistent negative effects of pesticides on biodiversity and biological control potential on european farmland," *Basic and Applied Ecology*, vol. 11, no. 2, pp. 97 – 105, 2010. [Online]. Available: http://www.sciencedirect.com/science/article/pii/S1439179109001388

[99] S. Louda, R. Pemberton, M. Johnson, and P. Follett, "Nontarget effects–the achilles' heel of biological control? retrospective analyeses to reduce risk associated with biocontrol introductions," *Annual Reviews in Entomology*, vol. 48, pp. 365–396, 2003.

[100] J. S. Cory and M. T. Franklin, "Evolution and microbial control of insects," *Evolutionary Applications*, vol. 5, pp. 455–469, 2012.

[101] G. G. Khachatourians, "Production and use of biological pest control agents," *Trends Biotechnol.*, vol. 4, pp. 120–124, 1986.

[102] I. Roberts and D. Brown, "Detection of six nepoviruses in their nematode vectors by immonosorbent electron microscopy." *Ann. Appl. Biol.*, vol. 96, pp. 187–192, 1980.

[103] R. Robbins and D. Brown, "Comments on the taxonomy, occurence and distribution of longidoridae (nematoda) in north america," *Nematologica*, vol. 37, pp. 395–419, 1991.

[104] S. Freeman, L. Allison, M. Black, G. Podgorski, K. Quillin, J. Monroe, and E. Taylor, *Biological Science*. Pearson Education, Inc., 2014, ch. Viruses, pp. 711–730.

[105] R. Lu, M. Maduro, F. Li, H. Li, G. Broitman-Maduro, W. Li, and S. Ding, "Animal virus replication and rnai-mediated antiviral silencing in *Caenorhabditis elegans*," *Nature*, vol. 436, pp. 1040–1043, 2005.

[106] K. M. Balla and E. R. Troemel, "*Caenorhabditis elegans* as a model for intracellular pathogen infection," *Cell. Microbiol.*, vol. 15, pp. 1313–1322, 2013.

[107] S. A. Hogenhout, M. G. Redinbaugh, and E.-D. Ammar, "Plant and animal rhabdovirus host range: a bug's view," *Trends Microbiol.*, vol. 11, pp. 264–271, 2003.

[108] B. Longdon, L. Wilfert, and F. M. Jiggins, *Rhabdoviruses: Molecular Taxonomy, Evolution, Genomics, Ecology, Host-Vector Interactions, Cytopathology and Control*. University of Edinburgh, 2012, ch. 8. The Sigma Viruses of Drosophilia, pp. 117–132.

[109] P. Fort, A. Albertini, A. Van-Hua, A. Berthomieu, S. Roche, F. Delsuc, N. Pasteur, P. Capy, Y. Gaudin, and M. Weill, "Fossil rhabdoviral sequences integrated into arthropod genomes: Ontogeny, evolution, and potential functionality," *Mol. Biol. Evol.*, vol. 29, pp. 381–390, 2012.

[110] A. P. Galvani, "Epidemiology meets evolutionary ecology," *trends in ecology and evolution*, vol. 18, pp. 132–139, 2003.

[111] K. Rock, S. Brand, J. Moir, and M. J. Keeling, "Dynamics of infectious diseases," *Rep. Prog. Phys.*, vol. 77, 2014.

[112] F. Brauer, *Mathematical Epidemiology Issue 1945*. Springer, 2008, ch. 2: Compartmental Models in Epidemiology, pp. 19–79.

[113] L. Råberg and M. Stjernman, *Ecoimmunology*. Oxford University Press, 2012, ch. 18. The Evolutionary Ecology of Infectious Disease Virulence, pp. 548–578.

[114] G. E. Demas, T. Greives, E. Chester, and S. French, *Ecoimmunology*. Oxford University Press, 2012, ch. 8: The energetics of immunity: Mechanisms mediating trade-offs in Ecoimmunology, pp. 259–296.

[115] M. J. Mackinnon and A. F. Read, "Virulence in malaria: an evolutionary viewpoint," *Phil. Trans. R. Soc. Lond.*, vol. 359, pp. 965–986, 2004.

[116] R. Anderson and R. May, "Coevolution of host and parasites," *Parasitology*, vol. 85, pp. 411–426, 1982.

[117] T. W. Berngruber, R. Froissart, M. Choisy, and S. Gandon, "Evolution of virulence in emerging epidemics," *PLoS Pathog.*, vol. 9, no. 3, p. e1003209, 2013. [Online]. Available: http://www.plospathogens.org/article/info%3Adoi%2F10.1371%2Fjournal.ppat.1003209

[118] M. Mackinnon, S. Gandon, and A. Read, "Virulence evolution in response to vaccination: The case of malaria," *Vaccine*, vol. 26S, pp. C42–C52, 2008.

[119] F. Fenner and F. Ratcliffe, "Rabbit populations and myxoma virus," *Science*, vol. 150, no. 3700, pp. 1146–1151, 1965.

[120] P. J. Kerr, E. Ghedin, J. V. DePasse, A. Fitch, I. M. Cattadori, P. J. Hudson, D. C. Tscharke, A. F. Read, and E. C. Holmes., "Evoevolution history and attenuation of myxoma virus on two continents," *PLOS Pathogens*, vol. 8, pp. 1–9, 2012.

[121] J. W. Drake, B. Charlesworth, D. Charlesworth, and J. F. Crow, "Rates of spontaneous mutation," *Genetics*, vol. 148, pp. 1667–1686, 1998.

[122] D. Ebert, "Experimental evolution of parasites," *Science*, vol. 282, pp. 1432–1435, 1998.

[123] S. L. Messenger, I. J. Molineux, and J. Bull, "Virulence evolution in a virus obeys a trade-off," *Proc. R. Soc. Lond. B*, vol. 266, no. 1417, pp. 397–404, 1999.

[124] M. J. Mackinnon and A. F. Read, "Immunity promotes virulence evolution in a malaria model," *PLoS Biol*, vol. 2, no. 9, p. e230, 06 2004. [Online]. Available: http://dx.doi.org/10.1371%2Fjournal.pbio.0020230

[125] A. Tack, P. Thrall, L. Barrett, J. Burdon, and A. Laine, "Variation in infectivity and aggressiveness in space and time in wild host-pathogen systems: causes and consequences." *J. Evol. Biol.*, vol. 25, pp. 1918–1936, 2012.

[126] M. Boots and A. Sasaki, "' small worlds' and the evolution of virulence: infection occurs locally and at a distance," *Proc. R. Soc. Lond.*, vol. 266, pp. 1933–1938, 1999.

[127] M. Kamo, A. Sasaki, and M. Boots, "The role of trade-off shapes in the evolution of parasites in spatial host populations: An approximate analytical approach," *Journal of Theoretical B*, vol. 244, pp. 588–596, 2007.

[128] P. Ewald, J. Sussman, M. Distler, C. Libel, W. Chammas, V. Dirita, C. Salles, A. Vicente, I. Heitmann, and F. Cabello, "Evolutionary control of infectious disease: prospects for vectorborne and waterborne pathogens," *Mem Inst Oswaldo Cruz*, vol. 93, no. 5, pp. 567–576, 1998.

[129] A. Lauring and R. Andino, "Quasispecies theory and the behavior of rna viruses," *PLoS Pathogens*, vol. 6, 2010. [Online]. Available: http://www.plospathogens.org/article/info%3Adoi%2F10.1371%2Fjournal.ppat.1001005

[130] A. S. Lauring, J. Frydman, and R. Andino, "The role of mumutation robustness in rna virus evolution," *Nat. Rev. Microbiol.*, vol. 11, pp. 327–336, 2013.

[131] G. Box and N. Draper, *Empirical Model Building and Response Surfaces*. New York, New York: John Wiley & Sons, 1987.

[132] S. Mubareka, A. C. Lowen, J. Steel, A. L. Coates, A. Garcìa-Sastre, and P. Palese, "Transmission of influenza virus via aerosols and fomites in the guinea pig model," *J. Infect. Dis.*, vol. 199, pp. 858–865, 2009.

[133] B. Wheeler, *lmPerm: Permutation tests for linear models*, 2010, r package version 1.1-2. [Online]. Available: http://CRAN.R-project.org/package=lmPerm

[134] R Core Team, *R: A language and environement for statistical computing*, R Foundation for Statistical Computing, Vienna, Austria, 2013. [Online]. Available: http://www.R-project.org

[135] H. Wickham, "The split-apply-combine strategy for data analysis," *Journal of Statistical Software*, vol. 40, no. 1, pp. 1–29, 2011. [Online]. Available: http://www.jstatsoft.org/v40/i01/

[136] H. Wickham, "Reshaping data with the reshape package," *Journal of Statistical Software*, vol. 21, no. 12, pp. 1–20, 2007. [Online]. Available: http://www.jstatsoft.org/v21/i12/

[137] H. Wickham, *ggplot2: elegant graphics for data analysis*. Springer New York, 2009. [Online]. Available: http://had.co.nz/ggplot2/book

[138] M. Vasco and C. Vieira, "Permutation tests to estimate significances on principle components analysis," *Computational Ecology and Software*, vol. 2, pp. 103–123, 2012.

[139] K. Shea and H. Possingham, "Optimal release strategies for biological control agents: An application of stochastic dynamic programming to population management," *Journal of Applied Ecology*, vol. 37, pp. 77–86, 2000.

[140] B. W. Bequette, *Process Dynamics: Modeling, Analysis, and Simulation*. Prentice Hall, 1998, ch. 13. Phase-Plane Analysis, pp. 303–330.

[141] L. Z. Garamszegi, "The evolution of virulence and host specialization in malaria parasites of primates," *Ecology Letters*, vol. 9, no. 8, pp. 933–940, 2006.

[142] R. Sanjuàn, M. R. Nebot, N. Chirico, L. M. Mansky, and R. Belshaw, "Viral mutation rates," *J. Virol.*, vol. 84, pp. 9733–9748, 2010.

[143] R. Lorenz, S. H. Bernhart, C. H. zu Siederdissen, H. Tafer, C. Flamm, P. F. Stadler, and I. L. Hofacker, "ViennaRNA Package 2.0," *Algorithms for Molecular Biology*, vol. 6:26, pp. 1–14, 2011. [Online]. Available: http://www.almob.org/content/6/1/26

[144] Z. Yang and J. P. Bielawski, "Statistical methods for detecting molecular adaptation," *TREE*, vol. 15, no. 15, pp. 496–503, 2000.

[145] A. Banerjee and S. Barik, "Gene expression of vesicular stomatitus virus genome RNA," *Virology*, vol. 188, no. 2, pp. 417–428, 1992.

[146] D. Spadafora, D. Canter, R. Jackson, and J. Perrault, "Constitutive phosphorylation of the vesicular stomatitus virus p protein mmodulate polymerase complex formation but is not essential for transcription or replication," *J. Virol.*, vol. 70, no. 7, pp. 4538–4548, 1996.

Appendix A

Translating experimental data for SCN viruses in SCNSim: A thought experiment featuring ScRV

A.1 Motivation

The previously described agent-based model SCNSim uses abstract numerical definitions of virus parameters to model soybean cyst nematode epizootics. Though helpful for extracting broad trends over several years, the major limitation of SCNSim is the absence of experimental data on the viruses and a subsequent translation of that data in silico. If SCNSim is to be used as a guide for choosing or engineering virus biocontrol agents for SCN management, SCNSim will need to be updated as new developments arise in laboratory studies. Here, we explore deep-sequencing data on one of the four viruses described by Bekal *et al.*, SCN Rhabdovirus (ScRV), in order to determine its mutation rate and develop a translation *in silico* [7].

The *in silico* definition of viral mutation rates is a probability of a successful increase or decrease (within 15% of the value) of all virus parameters. Thus, in this definition, mutation rate strictly results in changes in phenotype, which diverges with the general definitions of experimentally derived mutation rates. In biology, mutation rates are generally defined as mutation per replication per target [121]. Calculated mutations (μ) nearly always include substitutions, and frameshifts and usually include insertions, deletions and other larger changes. In addition to μ, RNA viruses are also described in terms of their mutant frequency (f).

The translation from f to μ depends on the mode replication, linear (μ_{lin}) or binary (μ_{bin}) and the reported μ is the average of the two μs. However, there are a few significant drawbacks to these calculations: average μ is similar to μ_{lin} in some viruses while similar to μ_{bin} in others, f takes into account the whole mutant spectrum; doesn't exclude synonymous mutations and provides no information to the directionality of the mutations over generations given certain selection pressures.

RNA viruses have been reported to have spontaneous mutation rates between 10^{-4}-10^{-6} substitutions per nucleotide per cell infection ([142]). Though this range gives us an idea of how inherently labile RNA replication can be, it's difficult to translate this range into a probability of phenotype change. Furthermore, unlike eukaryotes, RNA mutation rates include mutations throughout the entire genome as opposed to the effective genome, that is, the portion of the genome excluding introns and repeating sequences. Though RNA viruses do not have introns so to speak, they do have non-coding regions and conserved sequences which may experience either neutral or lethal mutations. Both types of mutations would not result in a noticeable phenotype change; one would result in viable viruses similar to the prior generation while the latter would result in non-viable viruses unable to pass on the mutation rate to future generations.

Thus, for the purposes of SCNSim, we should only consider mutation rates that potentially impact the adaptability of the virus–the nonsynonymous mutations. Using ScRV as an example, we can try to solve for the mutation rate using mutation data from deep sequencing J2s. ScRV is a negative-sense (-) ssRNA virus most closely related to Northern Ceral Mosiac Virus (NCMV), a member of Rhabdoviridae [7]. It has a genome size of 12698 bases and five ORFs typical of rhabdoviruses: nucleoprotein (N), phosphoprotein (P), matrix protein (M), glycoprotein (G), and the long protein (L).

A.2 Material and Methods

A.2.1 Acquiring RNA Genome and Mutation Rate data

The ScRV genome was assembled from a cDNA contig library using the CLC Genomics Workbench and comparison to GenBank sequences using BLASTX. Methods are detailed in Bekal *et al.* 2011 [7].

A.2.2 Determination of Regions of Interest for Analysis

In another aspect of this work, the secondary structures of the ScRV genome were predicted using the minimum free energy (MFE)–based program RNALfold (Vienna RNA 2.0) [143]. RNALfold was preferred to RNAfold due to its greater reliability in predicting structrues for large genomes ($>$ 10000 bases). While RNAfold predicts structures for entire genomes, these predictions are less accurate as large RNA strands are decreasingly thermodynamically stable [Ivo L Hofacker personal communication]. RNALfold reconciles the lability of large RNAs by computing locally stable structures within small ($\leq$ 150 bases) and overlapping windows throughout the entire genome genomes. For each fragment, a secondary structure was computed along with its MFE.

A.2.3 $^{Ka}/_{Ks}$ Determination

To explore the nature of the selection pressures on various regions of the genome, the ratio of the frequencies of nonsynonymous mutations (K_a) and synonymous mutations (K_s). The *Ka* and *Ks* values for each region were calculated from ScRV Illumina sequencing data by summing their respective frequencies for each fragment and taking their ratio. The mutation frequencies were normalized to sequence coverage.

A.2.4 Mutation Rate Estimation

In SCNSim, mutation rate, μ, is merely the probability (the variability is fixed) that the mutation will result in a change in phenotype. In general, rhabdovirus N, M, and G proteins are directly involved in infection *ergo* contribute to virulence and transmission. With the given data and ignoring intra-gene complexity, we simplified the probability of a phenotype change as a result of a mutation to be equal to the probability of a nonsynonymous mutation given a substitution mutation occurring in the N, G, or M proteins. To determine μ, plugged in a few known mutation rate values from the literature into (A.1) [121, 142].

$$P(f_a) = P(f_{SNV}) \cdot P(\gamma_i) \sum_{i}^{N,G,M} P(f_a|X_i)P(X_i) \tag{A.1}$$

Where f_a is the frequency of nonsynonymous mutations, f_{SNV} is the frequency of substitution mutations, and X_i is the nucleotide fraction or portion nucleotides of gene i with respect to the genome size.

A.3 Results

The most frequent mutation occurred at the 672nd position found in 20% of reads (11 /55) and was a silent substitution a threonine codon from the the 558th cytosine to uracil. For mutations with greater than 200$\times$ coverage the most frequent mutation found occurred at the 1209th position with 14% frequency (32/228). This was a silent substitution of the 1095th uracil with cytosine–translating to alanine.

Table A.1: A summary of the data of ScRV in SCN J2s. Fractions are the sum of the frequencies of each type of mutation normalized to the coverage at each genome position.

ScRV Genome			
	Genome Size	G	12698 bases
	Fraction of NCRs including leading and lagging strands	X_{NCR}	0.0407 (517 ÷ 12698)
	Fraction of ORF 1, Nucleoprotein	X_N	0.1366 (1735 ÷ 12698)
	Fraction of ORF 2, Phosphoprotein	X_P	0.0697 (885 ÷ 12698)
	Fraction of ORF 3, Matrix protein	X_M	0.0482 (612 ÷ 12698)
	Fraction of ORF 4, Glycoprotein	X_G	0.1862 (2364 ÷ 12698)
	Fraction of ORF 5, Long protein (RdRP)	X_L	0.5186 (6585 ÷ 12698)
Mutation Frequencies			
	Frequency of indels	f_i	0.0287 (24.17 ÷ 840.66)
	Frequency of substitutions	f_{SNV}	0.9713 (816.49 ÷ 840.66)
	Frequency of missense	f_a	0.6591 (538.18 ÷ 816.49)
	Frequency of transversions	f_{tv}	0.6580 (537.27 ÷ 816.49)
	Frequency of transitions	f_{ts}	0.3420 (279.22÷ 816.49)

RNALfold identified 1890 structures along the ScRV genome . Fig. A.1 shows the $^{Ka}/_{Ks}$ results of the RNALfold fragments. Roughly, the biological counterpart of the *in silico* mutation rate is the probability of nonsynonymous mutation taking place in the N, M or G ORFs. Proteins translated from ORFs 1, 2, and 3 did not find a close match on BLASTX [7]. According to BLASTX matching, and the relatively low occurance of nonsynonymous mutations, it is likely that ORF 5 translates the L protein (Table A.2) [7].

On the other hand, from preliminary analyses of selection pressures, it appears unlikely that ORF 4 transcribes the G protein due to the low $^{Ka}/_{Ks}$ values throughout. In a gene involved in host cell infiltration such as one that translates the G protein, we would expect to see higher $^{Ka}/_{Ks}$ values which would indicate the virus is able to adapt to host cell defenses. However in our results illustrated in Fig. A.1, ORF 4 appears to be undergoing negative selection [144].

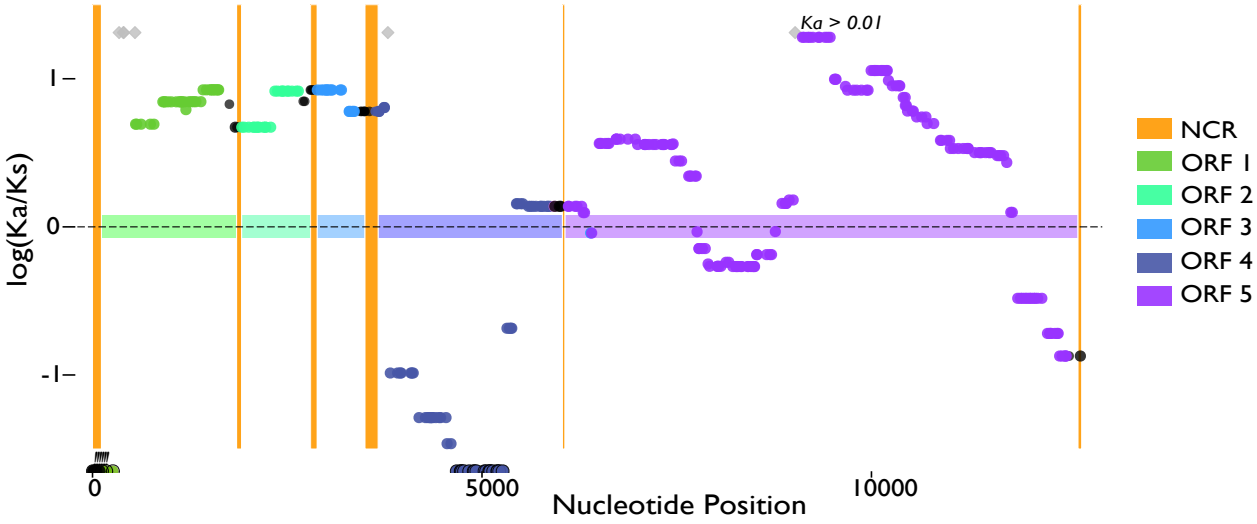

Figure A.1: Selection pressures across ScRV Genome. Fragments above the $\log(K_a/K_s) = 0$ line likely experienced positive selection, while those underneath experienced negative selection. Each point represents one of the 1890 fragments selected from RNALfold. Orange bars highlight NCRs while black points indicate fragments within or overlapping with an NCR. Points accented with exclamation marks have $K_s = 0$ as well as $K_a = 0$.

A possible alternative for ORF 4 would be it encodes the P protein instead; together with the L protein, the P protein constitutes the RNA-dependent RNA polymerase (RdRP) in rhabdoviruses [145]. The structure of RdRP is crucial to its function which in turn is crucial to viral replication; if the P or L protein did not have conserved regions, the viruses would experience lethal mutations. Yet when Bekal *et al.* reported the predicted properties of ScRV proteins, ORF 4 was closely matched to glycoamylase from *Candida albicans* [7]. Thus, below we estimated μ as if ORF 4 encoded either the G protein or the P protein.

Table A.2: Mutation frequencies by component.

Component	$f_a \vert X_i, f_{SNV}$	$f_i \vert X_i$	$f_{SNV} \vert X_i$	f_{tot}
N	143.54	3.95	214.01	217.96
P	64.62	3.43	81.31	84.74
M	49.13	1.25	60.1	61.35
G	113.53	1.13	154.77	155
L	167.35	0.74	203.71	204.45
NCR	0	13.67	102.6	115.27

Table A.3 shows the final estimations for μ. Drake *et al.* reported the range of substitution mutations per nucleotide per cell (s/n/c) was between 10^{-4} to 10^{-6} for RNA viruses [121]. Thus, μ was estimated using each reported endpoint as well as using the average nucleotide substitution rate for vesicular stomatitus virus (VSV) [142].

Table A.3: Estimation of μ from ScRV assuming ORF 4 translates to G and P.

Assumption	μ s/n/c	$P(f_a)$ s/c	Including indels	Ref.
ORF 4 codes G				
	10^{-4}	0.327	0.317	[121]
	3.5×10^{-5}	0.114	0.111	[142]
	10^{-6}	0.00327	0.00317	[121]
ORF 4 codes P				
	10^{-4}	0.224	0.218	[121]
	3.5×10^{-5}	0.0783	0.0761	[142]
	10^{-6}	0.00224	0.00218	[121]

A.3.1 Conclusions

The range of the estimates for μ varied widely since the reported range for RNA viruses encompassed two orders of magnitude. If we presume the estimated μs are representative, the estimates using the high frequency end point would translate to moderately mutable viruses in SCNSim. Meanwhile, it is immediately apparent from the results in the main study above that if the values 0.00327 and 0.00224 estimated from the lowest mutation frequency more accurate that ScRV would result in harmless epizootics.

However, these results remain inconclusive as a number of pivotal factors are ignored. For instance, the impact of a single basepair mutation even within an ORF is non-uniform; some mutations may result in silent mutations while others may improve the adaptability of the virus and still others may be lethal. Knowing the tertiary protein structures and identifying active sites would help us better understand where substitution mutations would have greater impacts.

With three ORFs unmatched to known proteins in BLASTX, it is difficult to confidently determine the order of the common rhabdovirus proteins. It's uncertain why, if ORF 4 translates the G protein, the overall region experienced negative selection. However, Spadafora *et al.* has reported in a study using VSV that although mutations altering single amino acids in the P protein active sites results in defective P-L polymerase complexes, the P protein was still active in RNA synthesis [146]. Thus, there maybe some flexibility in the P protein that allows for positive selection without completely nullifying its activity. On the other hand, it has also been reported 40% of mutations in VSV are lethal [130]. Are perilously high error rates simply a characteristic of RNA viruses? If so, we may need to expand on the effects of mutation in SCNSim to allow for wider parameter changes as well as self extinction. More experimental values within rhabdoviridae are needed to make more informed postulations.

Appendix B

Supplementary Data

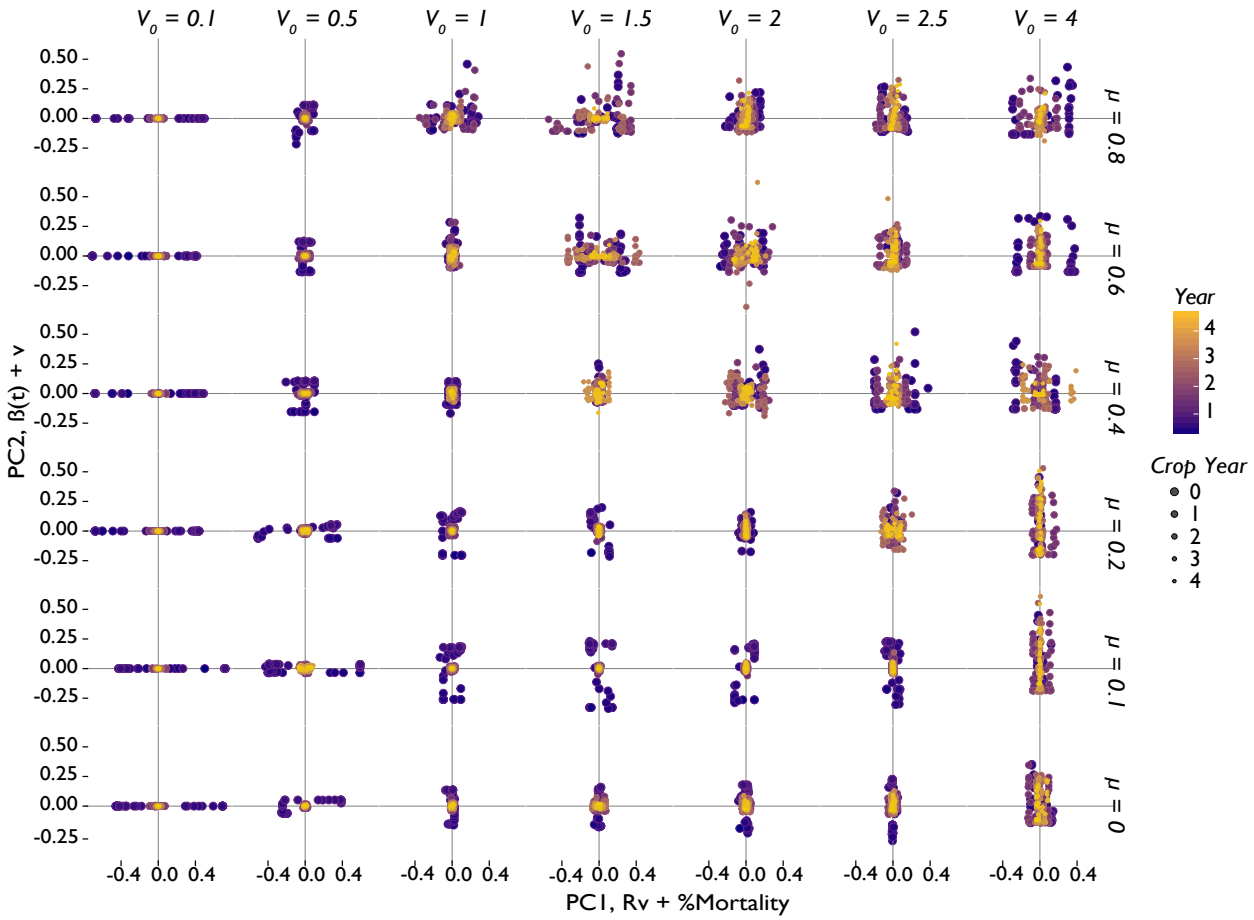

Figure B.1: Principle component scores for $R_v + d$ (PC1) against scores for $\beta + v$ (PC2) over a $\mu \times V_0$ grid. Decreasing point size and lightening point color is indicative of increasing time. A change in pattern is observable across the diagonal: to the left of the diagonal (mostly low V_0 and high and low μ), PC1 appears to contribute much more than PC2, on the diagonal (intermediate V_0 and μ)the spread appears minimal, and on the right of the diagonal (mostly high V_0 and low and high μ) origin-centered, and periodic behavior is observed with a stronger influence from PC2 in the low μ pathotypes.

Table B.1: Table of loadings for components 1-7 of original data set.

	PC1	PC2	PC3	PC4	PC5	PC6	PC7
Transmissibility Mean	-0.130	0.494	-0.193	0.078	-0.139	0.058	-0.269
Virulence Mean	-0.174	0.298	-0.189	0.269	0.023	0.125	0.804
Virus Load	-0.129	0.512	-0.169	0.041	-0.032	0.010	-0.234
Nematodes	0.299	-0.056	-0.336	-0.008	0.230	-0.071	0.009
Fraction Infected	-0.118	-0.470	0.158	0.245	0.132	0.076	0.116
Death by Virus	-0.107	-0.231	-0.191	0.453	-0.513	0.235	-0.209
Eggs per Container Mean	-0.284	0.130	0.141	0.136	0.401	0.004	0.117
Cyst	0.287	-0.076	-0.365	0.035	0.231	-0.058	-0.005
Dead	0.308	0.124	0.129	0.103	0.038	0.056	0.026
J1	0.294	0.131	0.180	0.184	0.060	0.053	-0.032
J2	0.320	-0.008	-0.197	0.027	0.193	-0.002	0.000
J3	0.222	0.084	0.339	0.303	-0.047	0.208	-0.042
J4F	0.270	0.145	0.230	0.199	-0.045	0.217	0.080
J4M	0.298	0.105	0.212	0.092	-0.025	0.166	-0.021
M	0.328	0.075	-0.079	-0.193	-0.009	-0.019	0.042
F	-0.205	0.015	0.031	0.358	0.602	0.059	-0.378
Temperature	0.073	0.078	0.171	0.368	-0.144	-0.885	0.027
Health Mean	-0.097	0.145	0.485	-0.385	0.035	-0.002	-0.001

Table B.2: Correlation table from PCA of Virus treatments

Components	Eigenvalues	Percent of Variance	Cumulative Percent
1	7.314	43.027%	43.027%
2	2.854	16.793%	59.820%
3	2.222	13.073%	72.893%
4	1.439	8.462%	81.355%
5	0.924	5.434%	86.789%
6	0.447	2.631%	89.420%
7	0.354	2.088%	91.510%
⋮	⋮	⋮	⋮
17	0.001	0.008%	100%

Table B.3: Scores for components 1-8 of yearly SCNSim dataset

Mutation Rate	Virulence	Infection Rate	Crop Year	PC1	PC2	PC3	PC4	PC5	PC6	PC 7	PC 8
0	0.1	0.2	0	1.056	2.408	3.111	0.027	-0.785	0.612	-0.882	-0.632
0	0.1	0.2	1	3.255	2.671	2.516	0.737	-0.579	-0.089	-0.955	-0.862
0	0.1	0.2	2	1.846	1.588	-0.089	-0.374	0.009	-0.820	-1.084	-0.387
0	0.1	0.2	3	3.562	1.743	-0.345	0.285	0.392	0.110	-1.058	0.274
0	0.1	0.2	4	5.013	1.967	-0.679	1.162	0.916	0.027	-1.070	-0.363
0	0.5	0.2	0	0.457	1.438	2.711	-0.251	-0.549	-0.426	-0.367	-0.688
0	0.5	0.2	1	3.350	1.482	2.848	0.826	-0.278	-0.409	-0.343	-0.965
0	0.5	0.2	2	2.309	0.280	0.513	-0.284	0.216	-0.605	-0.381	-0.394
0	0.5	0.2	3	3.974	0.410	0.370	0.494	0.899	0.431	-0.457	-0.634
0	0.5	0.2	4	4.624	0.342	0.278	2.059	1.551	-0.454	-0.763	-0.119
0	1	0.2	0	0.160	0.143	2.624	-0.601	-0.042	-0.120	0.084	-1.291
0	1	0.2	1	2.842	-0.291	3.151	1.160	-0.160	-1.495	0.211	-0.481
0	1	0.2	2	3.695	-0.847	2.407	0.894	0.303	0.158	0.309	-0.710
0	1	0.2	3	3.760	-1.531	1.006	0.665	0.652	-0.200	0.300	0.294
0	1	0.2	4	5.908	-1.231	1.145	2.082	1.000	-0.261	0.491	-0.351
0	1.5	0.2	0	-0.895	0.074	2.252	-0.611	-0.399	-1.033	0.207	-0.551
0	1.5	0.2	1	2.594	0.294	2.916	0.921	-0.408	-0.292	0.287	-0.955
0	1.5	0.2	2	3.288	-0.186	2.232	1.402	0.002	-0.197	0.161	-0.154
0	1.5	0.2	3	2.870	-1.032	0.124	0.337	0.307	-0.115	0.379	-0.504
0	1.5	0.2	4	4.144	-1.024	-0.403	1.114	0.784	-0.198	0.318	-0.032
0	2	0.2	0	-0.148	0.455	2.413	-0.538	-0.332	-0.462	0.396	-0.766
0	2	0.2	1	2.185	0.438	2.514	0.896	0.322	0.230	-0.023	-0.086
0	2	0.2	2	3.345	0.281	1.935	1.532	0.349	-0.450	0.094	-0.519
0	2	0.2	3	4.230	0.060	1.402	1.981	0.275	-0.489	0.249	0.273
0	2	0.2	4	4.042	-0.663	-0.636	1.008	0.686	-0.653	0.347	0.044
0	2.5	0.2	0	-0.760	1.229	1.937	-0.626	-0.743	-0.237	0.693	-0.580
0	2.5	0.2	1	1.614	0.808	1.658	0.261	-0.338	-0.902	0.434	-0.920
0	2.5	0.2	2	3.434	0.842	1.758	1.218	-0.041	0.413	0.477	-0.364
0	2.5	0.2	3	4.293	0.682	1.343	2.058	0.518	-0.019	0.260	-0.982
0	2.5	0.2	4	5.152	0.532	0.625	2.312	0.520	-0.208	0.472	0.186
0	4	0.2	0	-1.084	2.845	1.780	0.471	-0.474	0.326	1.313	0.145
0	4	0.2	1	1.686	3.238	1.371	1.101	-0.440	0.414	1.190	-0.184
0	4	0.2	2	0.863	2.445	-0.824	0.092	-0.532	-0.921	1.421	-0.221
0	4	0.2	3	3.137	2.943	-0.719	1.355	0.204	0.146	1.291	-0.052
0	0.1	0.8	0	0.063	1.770	2.325	-0.445	-0.751	-0.602	-0.704	-1.177
0	0.1	0.8	1	3.296	2.527	2.516	0.541	-0.484	0.742	-0.896	-0.913
0	0.1	0.8	2	3.090	2.067	1.189	0.832	-0.108	-0.795	-1.126	-0.728
0	0.1	0.8	3	4.138	2.040	0.247	0.641	0.330	0.574	-0.954	-0.246
0	0.1	0.8	4	5.898	2.410	0.402	1.891	0.433	-0.381	-0.976	-0.554
0	0.5	0.8	0	-0.318	0.651	2.539	-0.136	-0.476	-0.931	-0.250	-0.863
0	0.5	0.8	1	3.087	0.966	2.978	1.127	-0.087	-0.351	-0.310	-1.340
0	0.5	0.8	2	3.949	0.535	2.105	1.099	0.439	0.877	-0.361	-0.698
0	0.5	0.8	3	3.610	-0.302	0.308	0.493	0.530	0.179	-0.108	-0.420
0	0.5	0.8	4	3.912	-0.626	-0.639	0.760	1.012	-0.558	-0.167	-0.195
0	1	0.8	0	-1.061	-0.474	2.748	0.102	-0.002	-0.876	0.167	-0.370
0	1	0.8	1	1.384	-0.907	2.728	1.101	-0.358	-0.264	0.103	-0.694
0	1	0.8	2	2.346	-1.511	1.804	1.040	-0.342	0.511	0.206	-0.597
0	1	0.8	3	3.889	-1.636	1.840	1.716	-0.414	1.193	0.257	0.119
0	1	0.8	4	5.647	-1.489	1.661	3.247	0.205	0.128	0.168	-0.109
0	1.5	0.8	0	-2.240	-0.384	2.267	-0.031	0.204	-0.527	0.144	0.223
0	1.5	0.8	1	0.083	-0.632	2.076	1.189	0.105	-0.122	-0.195	-0.170
0	1.5	0.8	2	1.518	-0.828	1.625	1.377	-0.413	1.117	-0.060	0.178

Table B.3: Continued

Mutation Rate	Virulence	Infection Rate	Crop Year	PC1	PC2	PC3	PC4	PC5	PC6	PC 7	PC 8
0	1.5	0.8	3	1.837	-1.093	0.850	1.874	-0.535	0.080	-0.129	-0.526
0	1.5	0.8	4	3.381	-0.971	0.596	2.783	-0.441	-0.059	-0.103	0.130
0	2	0.8	0	-2.899	-0.122	1.996	0.355	0.450	-1.693	0.177	0.126
0	2	0.8	1	-0.272	-0.263	1.926	1.087	-0.091	0.036	0.083	0.515
0	2	0.8	2	-0.329	-0.781	1.110	1.652	-0.102	-0.360	-0.275	0.023
0	2	0.8	3	1.464	-0.731	1.008	2.541	-0.636	-0.691	0.000	-0.139
0	2	0.8	4	2.659	-0.776	0.522	2.946	-0.363	0.478	-0.123	0.040
0	2.5	0.8	0	-3.247	0.543	2.153	0.796	0.808	-0.732	0.293	0.468
0	2.5	0.8	1	-1.426	-0.113	1.662	1.234	0.551	0.003	-0.035	0.742
0	2.5	0.8	2	-0.276	-0.352	1.018	1.366	-0.348	-0.605	0.214	-0.454
0	2.5	0.8	3	0.302	-0.680	0.415	1.997	-0.201	-0.028	0.051	-0.111
0	2.5	0.8	4	0.505	-1.106	-0.877	1.789	-0.292	-0.118	0.151	-0.451
0	4	0.8	0	-5.691	1.504	1.665	2.623	3.490	-0.317	-0.071	0.955
0	4	0.8	1	-3.875	1.582	1.205	2.966	1.507	-1.072	0.459	0.263
0	4	0.8	2	-2.946	1.421	-0.012	2.264	0.332	-0.449	0.878	-0.459
0	4	0.8	3	-2.250	1.297	-0.452	2.625	-0.265	0.036	0.983	-0.416
0	4	0.8	4	-1.208	1.315	-1.049	3.163	-0.882	-0.894	1.199	-0.953
0.1	0.1	0.2	0	-1.056	1.567	1.291	-1.692	-0.120	0.449	-1.123	-0.303
0.1	0.1	0.2	1	0.201	1.347	0.166	-1.169	-0.135	-0.337	-1.110	-0.297
0.1	0.1	0.2	2	1.046	1.313	-0.611	-0.902	0.108	-1.432	-1.212	-0.805
0.1	0.1	0.2	3	3.050	1.566	-0.597	-0.090	0.158	-0.316	-1.005	1.201
0.1	0.1	0.2	4	1.746	0.538	-3.325	-1.373	1.047	-0.757	-1.099	0.124
0.1	0.5	0.2	0	-0.742	1.682	1.433	-1.128	-0.733	-0.845	-0.753	-0.022
0.1	0.5	0.2	1	0.088	0.852	-0.522	-2.470	-0.692	0.022	-0.361	-1.023
0.1	0.5	0.2	2	0.738	0.745	-0.789	-1.092	-0.577	-2.275	-0.365	-0.190
0.1	0.5	0.2	3	1.610	0.032	-2.273	-1.892	0.878	0.167	-0.584	-0.661
0.1	0.5	0.2	4	2.661	-0.358	-3.085	-1.726	0.170	-1.490	0.279	0.130
0.1	1	0.2	0	-0.534	-1.034	2.091	-2.300	-0.443	1.062	0.519	-0.230
0.1	1	0.2	1	2.438	-1.336	2.602	-0.141	0.416	-0.109	0.214	0.083
0.1	1	0.2	2	1.479	-2.342	0.902	-0.807	0.621	-0.199	0.400	-0.808
0.1	1	0.2	3	1.345	-3.022	-0.758	-1.023	1.550	-0.333	0.210	-0.432
0.1	1	0.2	4	2.459	-3.269	-1.525	-1.150	1.419	0.443	0.590	0.409
0.1	1.5	0.2	0	-0.743	-1.153	2.077	-2.161	-0.452	0.072	0.766	-0.161
0.1	1.5	0.2	1	2.748	-1.323	2.745	-0.144	0.763	2.164	0.208	-0.242
0.1	1.5	0.2	2	3.871	-1.664	1.614	0.360	0.673	0.347	0.598	-0.325
0.1	1.5	0.2	3	1.299	-3.300	-1.106	-1.566	0.806	0.739	0.574	0.014
0.1	1.5	0.2	4	1.056	-3.756	-2.320	-0.899	1.148	-1.367	0.517	0.440
0.1	2	0.2	0	-0.044	-0.372	2.702	-0.930	-0.798	-1.146	0.720	0.066
0.1	2	0.2	1	0.178	-1.962	0.975	-1.427	0.202	0.318	0.372	0.282
0.1	2	0.2	2	1.177	-1.995	1.000	-0.011	0.203	-0.888	0.302	0.338
0.1	2	0.2	3	1.897	-2.600	-0.518	-0.234	0.674	-0.463	0.289	0.515
0.1	2	0.2	4	1.493	-3.286	-1.819	-0.375	0.567	-0.567	0.227	-0.355
0.1	2.5	0.2	0	-1.853	0.177	1.349	-1.509	-0.472	-0.370	0.513	-0.137
0.1	2.5	0.2	1	0.150	-0.760	0.918	-1.120	0.028	0.330	0.378	-0.361
0.1	2.5	0.2	2	0.718	-1.439	0.539	-0.415	0.193	-0.383	0.146	-0.255
0.1	2.5	0.2	3	0.406	-2.270	-0.921	-0.587	1.114	0.341	-0.206	0.325
0.1	2.5	0.2	4	1.946	-2.145	-0.791	0.395	0.395	-0.517	0.239	0.785
0.1	4	0.2	0	-1.670	2.497	1.335	-0.524	-0.623	0.222	1.444	0.873
0.1	4	0.2	1	0.641	2.539	0.144	-0.039	-0.115	0.361	1.109	-0.437
0.1	4	0.2	2	0.141	1.882	-1.407	-0.622	0.044	0.378	1.105	0.153
0.1	4	0.2	3	-0.255	1.365	-2.941	-0.824	0.284	-0.546	1.164	0.172
0.1	4	0.2	4	1.830	1.753	-2.870	0.325	0.611	-0.863	1.162	0.731

Table B.3: Continued

Mutation Rate	Virulence	Infection Rate	Crop Year	PC1	PC2	PC3	PC4	PC5	PC6	PC 7	PC 8
0.1	0.1	0.8	0	-0.763	1.278	1.393	-1.411	-0.901	-0.715	-0.683	0.343
0.1	0.1	0.8	1	0.177	1.267	0.180	-0.848	0.073	-1.148	-1.220	-0.947
0.1	0.1	0.8	2	1.558	1.333	-0.414	-0.865	0.628	0.805	-1.346	0.457
0.1	0.1	0.8	3	3.040	1.562	-0.688	-0.260	-0.097	-0.511	-0.710	-0.362
0.1	0.1	0.8	4	2.388	0.875	-2.088	-0.790	-0.062	-1.110	-0.832	0.330
0.1	0.5	0.8	0	-1.908	0.792	1.243	-1.361	-0.213	-0.301	-0.554	0.398
0.1	0.5	0.8	1	0.986	0.355	0.711	-1.642	-0.232	0.552	-0.197	-1.036
0.1	0.5	0.8	2	0.956	-0.677	-0.370	-1.386	0.191	-0.313	-0.150	0.929
0.1	0.5	0.8	3	2.594	-0.920	-0.584	-0.401	0.400	-1.255	0.064	0.293
0.1	0.5	0.8	4	5.777	-0.362	0.807	1.644	1.430	0.666	-0.021	0.310
0.1	1	0.8	0	-0.698	-1.361	2.056	-1.993	-0.253	0.720	0.589	-0.322
0.1	1	0.8	1	0.015	-2.461	0.870	-1.264	0.391	-0.939	0.474	0.186
0.1	1	0.8	2	2.679	-1.957	2.131	0.775	0.542	0.174	0.453	0.736
0.1	1	0.8	3	2.968	-2.582	0.256	-0.225	0.470	-0.687	0.851	0.098
0.1	1	0.8	4	3.385	-3.122	-1.220	-0.327	1.553	0.101	0.593	0.495
0.1	1.5	0.8	0	-1.953	-1.720	1.648	-1.535	-0.065	-0.641	0.486	-0.573
0.1	1.5	0.8	1	-0.865	-2.437	1.176	-0.903	-0.154	-0.386	0.328	0.069
0.1	1.5	0.8	2	0.247	-2.500	1.114	-0.136	-0.822	-0.551	0.551	0.203
0.1	1.5	0.8	3	-1.364	-3.760	-1.867	-1.363	-0.027	-0.727	0.228	-0.347
0.1	1.5	0.8	4	-0.140	-3.697	-1.756	-0.431	0.017	0.145	0.131	-0.561
0.1	2	0.8	0	-2.170	-0.927	1.966	-0.896	-0.515	0.342	0.699	0.637
0.1	2	0.8	1	-2.672	-2.204	0.010	-1.226	-0.433	1.284	0.038	0.163
0.1	2	0.8	2	-2.273	-2.393	0.025	0.634	-1.142	-0.096	-0.119	0.439
0.1	2	0.8	3	-1.794	-2.669	-0.630	1.453	-1.760	-0.962	-0.053	0.792
0.1	2	0.8	4	-1.907	-3.138	-1.330	1.916	-2.028	0.452	-0.462	0.370
0.1	2.5	0.8	0	-2.387	0.162	2.565	0.349	-0.577	-0.568	0.721	1.242
0.1	2.5	0.8	1	-2.619	-1.248	0.872	0.566	-0.706	0.074	-0.057	0.784
0.1	2.5	0.8	2	-2.570	-1.663	0.148	1.434	-1.368	-0.464	-0.127	0.676
0.1	2.5	0.8	3	-2.129	-1.995	-0.274	2.612	-2.008	-0.752	-0.312	0.955
0.1	2.5	0.8	4	-3.722	-3.118	-2.244	1.775	-2.071	0.366	-0.746	-0.746
0.1	4	0.8	0	-7.098	1.069	0.729	1.788	4.233	0.216	-0.422	-0.139
0.1	4	0.8	1	-5.657	0.668	-0.191	0.503	1.900	2.360	0.621	-0.378
0.1	4	0.8	2	-5.361	0.713	-0.781	2.099	0.727	-1.674	0.688	-0.401
0.1	4	0.8	3	-5.282	0.050	-2.039	1.173	0.186	0.500	0.892	-1.210
0.1	4	0.8	4	-5.446	-0.480	-3.059	1.381	-0.435	-0.732	1.021	-1.920
0.2	0.1	0.2	0	-1.491	1.311	1.126	-2.334	-0.450	1.389	-0.920	0.025
0.2	0.1	0.2	1	-0.388	0.949	-0.467	-2.734	-0.994	0.118	-0.702	0.767
0.2	0.1	0.2	2	1.128	1.296	-0.613	-1.184	0.264	0.277	-1.211	0.607
0.2	0.1	0.2	3	1.956	1.074	-1.551	-1.133	0.356	0.054	-1.067	0.211
0.2	0.1	0.2	4	3.769	1.404	-1.434	0.327	0.556	-1.051	-1.084	0.567
0.2	0.5	0.2	0	-1.347	1.386	1.359	-1.429	-0.524	-0.578	-0.648	0.431
0.2	0.5	0.2	1	0.261	0.624	0.790	-0.388	-0.142	-2.750	-0.670	0.390
0.2	0.5	0.2	2	-0.515	-0.436	-1.143	-1.963	0.378	-0.540	-0.522	-0.335
0.2	0.5	0.2	3	3.998	0.658	0.131	0.029	1.097	0.887	-0.658	-0.073
0.2	0.5	0.2	4	3.414	-0.033	-1.277	0.047	0.969	-0.286	-0.293	0.241
0.2	1	0.2	0	-2.550	-1.621	1.169	-2.648	0.009	-0.174	0.173	-0.202
0.2	1	0.2	1	2.067	-1.437	2.419	-0.045	-0.206	-0.830	0.554	0.657
0.2	1	0.2	2	1.932	-2.178	0.869	-0.124	0.207	-2.225	0.516	-0.385
0.2	1	0.2	3	-0.751	-3.651	-1.545	-2.110	0.958	0.208	0.263	-0.197
0.2	1	0.2	4	3.231	-2.728	-0.456	0.559	1.241	-0.616	0.352	0.140
0.2	1.5	0.2	0	-0.965	-0.773	1.833	-1.712	0.088	0.938	0.339	-0.511
0.2	1.5	0.2	1	-1.051	-2.262	0.206	-2.458	-0.464	-0.089	0.484	-0.064

Table B.3: Continued

Mutation Rate	Virulence	Infection Rate	Crop Year	PC1	PC2	PC3	PC4	PC5	PC6	PC 7	PC 8
0.2	1.5	0.2	2	0.617	-2.261	0.521	-0.294	0.171	-0.136	0.150	1.580
0.2	1.5	0.2	3	0.113	-3.071	-0.941	-1.141	0.474	1.366	0.118	-0.198
0.2	1.5	0.2	4	1.464	-3.287	-1.286	-0.119	0.607	0.750	0.029	0.278
0.2	2	0.2	0	-1.299	0.683	1.589	-1.187	-0.008	0.603	0.264	-0.467
0.2	2	0.2	1	0.373	0.064	1.056	-0.397	-0.650	-0.158	0.245	0.206
0.2	2	0.2	2	-0.903	-1.237	-0.973	-1.560	-0.504	0.035	0.102	-0.883
0.2	2	0.2	3	1.019	-1.191	-1.176	-0.400	-0.576	-1.283	0.301	-0.042
0.2	2	0.2	4	0.650	-1.907	-2.007	0.065	0.285	-1.391	-0.348	-0.320
0.2	2.5	0.2	0	-2.457	0.674	0.626	-1.201	-0.494	-1.559	0.263	0.573
0.2	2.5	0.2	1	-0.064	0.874	0.973	-0.036	-0.121	-0.008	-0.085	0.816
0.2	2.5	0.2	2	1.113	0.766	0.327	0.412	-0.778	-1.268	0.354	0.586
0.2	2.5	0.2	3	1.393	-0.160	-1.300	-0.534	0.556	1.114	-0.094	0.795
0.2	2.5	0.2	4	3.404	0.287	-0.628	1.072	-0.125	-0.404	0.281	-0.092
0.2	4	0.2	0	-2.584	1.945	0.279	-1.432	-0.644	0.694	1.444	0.392
0.2	4	0.2	1	0.908	2.616	0.351	-0.409	-0.470	1.068	1.308	0.238
0.2	4	0.2	2	0.313	2.099	-0.957	-0.117	-0.780	-1.689	1.469	-0.183
0.2	4	0.2	3	1.747	2.230	-2.538	-0.842	-0.259	0.032	1.822	0.753
0.2	0.1	0.8	0	-1.974	0.910	1.070	-1.811	-0.823	-0.784	-0.774	-0.394
0.2	0.1	0.8	1	-0.478	1.111	0.109	-1.343	-0.287	-1.143	-1.150	-0.824
0.2	0.1	0.8	2	-0.513	0.778	-1.104	-1.542	-0.259	-1.415	-1.044	-0.215
0.2	0.1	0.8	3	2.083	1.309	-0.970	-0.887	0.068	0.250	-0.902	-0.787
0.2	0.1	0.8	4	4.082	1.633	-1.196	0.056	0.716	0.442	-0.945	-1.142
0.2	0.5	0.8	0	-1.382	0.297	1.217	-1.772	-0.393	-0.273	-0.347	-0.102
0.2	0.5	0.8	1	1.312	0.284	1.350	-0.830	0.073	0.208	-0.381	0.812
0.2	0.5	0.8	2	0.008	-1.231	-1.062	-1.950	0.669	-0.503	-0.278	0.353
0.2	0.5	0.8	3	1.733	-1.319	-1.091	-0.985	1.291	-0.033	-0.275	0.668
0.2	0.5	0.8	4	2.534	-1.989	-2.481	-1.902	1.252	0.713	0.251	0.057
0.2	1	0.8	0	-2.234	-1.605	1.733	-1.635	-0.271	-0.586	0.381	0.160
0.2	1	0.8	1	0.754	-2.011	1.959	-0.172	0.086	0.336	0.158	0.757
0.2	1	0.8	2	1.006	-2.600	0.847	-0.316	-0.362	-0.318	0.563	-0.628
0.2	1	0.8	3	1.975	-2.866	0.003	0.048	0.344	0.199	0.413	0.383
0.2	1	0.8	4	2.004	-3.478	-1.548	-0.210	1.095	0.120	0.235	-0.623
0.2	1.5	0.8	0	-3.053	-1.337	0.949	-2.330	-0.062	1.991	0.491	-0.035
0.2	1.5	0.8	1	-2.277	-1.997	0.721	-0.424	0.218	2.172	-0.503	0.619
0.2	1.5	0.8	2	-2.282	-2.721	-0.268	0.163	-0.441	1.184	-0.482	0.264
0.2	1.5	0.8	3	-4.044	-3.684	-1.917	0.738	-0.608	-1.732	-1.011	-1.233
0.2	1.5	0.8	4	-0.010	-2.930	-0.228	2.466	-1.729	1.909	-0.569	0.503
0.2	2	0.8	0	-3.092	0.259	1.708	-0.138	-0.182	0.231	0.360	1.128
0.2	2	0.8	1	-3.722	-1.319	-0.444	-0.415	-1.114	1.046	-0.216	0.146
0.2	2	0.8	2	-3.720	-1.705	-0.733	1.523	-1.046	1.312	-0.890	0.129
0.2	2	0.8	3	-3.051	-2.077	-0.962	2.649	-2.398	0.276	-0.934	0.328
0.2	2	0.8	4	-4.556	-3.088	-2.694	2.494	-1.783	1.937	-1.661	-1.070
0.2	2.5	0.8	0	-5.842	0.278	0.497	0.194	1.763	-1.382	-0.304	-0.392
0.2	2.5	0.8	1	-5.017	-0.264	0.070	0.993	1.016	-1.206	-0.708	-0.179
0.2	2.5	0.8	2	-2.616	-0.468	0.426	1.292	-1.600	-0.391	0.136	0.590
0.2	2.5	0.8	3	-3.490	-1.531	-1.340	0.312	-0.684	1.025	-0.535	-0.346
0.2	2.5	0.8	4	-2.980	-1.715	-1.817	0.774	-0.760	0.986	-0.795	-0.111
0.2	4	0.8	0	-6.702	0.953	0.623	0.890	3.315	1.013	0.163	-0.248
0.2	4	0.8	1	-5.873	0.978	0.433	2.111	2.289	0.656	0.351	0.038
0.2	4	0.8	2	-5.457	0.420	-1.268	1.341	0.792	-0.501	0.586	-0.715
0.2	4	0.8	3	-5.143	0.010	-2.385	0.311	-0.589	1.034	1.384	-1.453
0.2	4	0.8	4	-5.241	-0.407	-3.115	1.211	-1.523	-1.276	1.439	-2.079

Table B.3: Continued

Mutation Rate	Virulence	Infection Rate	Crop Year	PC1	PC2	PC3	PC4	PC5	PC6	PC 7	PC 8
0.4	0.1	0.2	0	-1.934	1.098	0.584	-2.215	-0.686	-0.802	-1.006	-0.116
0.4	0.1	0.2	1	1.287	1.868	1.229	-0.072	-0.086	-0.493	-1.311	-0.832
0.4	0.1	0.2	2	0.739	0.906	-1.472	-2.587	-0.011	1.610	-0.847	0.616
0.4	0.1	0.2	3	3.103	1.783	-0.155	1.034	0.464	-1.874	-1.308	1.068
0.4	0.1	0.2	4	4.977	1.829	-1.147	0.686	0.629	-0.616	-0.860	0.661
0.4	0.5	0.2	0	-2.355	-0.529	1.119	-2.264	0.096	-0.342	-0.246	-0.165
0.4	0.5	0.2	1	-0.157	-1.436	0.624	-1.987	-0.032	-0.555	0.142	0.301
0.4	0.5	0.2	2	2.870	-0.793	1.714	-0.128	0.092	0.278	0.313	0.300
0.4	0.5	0.2	3	2.922	-1.343	0.605	-0.314	0.586	-0.033	0.282	0.744
0.4	0.5	0.2	4	1.760	-2.528	-1.592	-1.137	1.323	-0.784	0.174	-1.234
0.4	1	0.2	0	-1.107	-0.416	2.174	-0.604	-0.117	-1.539	0.150	-0.058
0.4	1	0.2	1	0.782	-1.778	1.517	-1.083	0.041	0.651	0.295	0.063
0.4	1	0.2	2	0.853	-2.554	0.140	-0.670	0.687	-0.281	0.212	-0.385
0.4	1	0.2	3	3.258	-2.323	0.290	0.214	0.530	-0.076	0.391	-0.384
0.4	1	0.2	4	3.443	-2.712	-0.444	0.995	1.308	-0.039	0.139	1.276
0.4	1.5	0.2	0	-1.264	0.904	1.387	-1.142	0.083	0.688	-0.130	-0.042
0.4	1.5	0.2	1	0.377	0.056	1.139	-0.072	-0.809	-0.378	-0.043	0.517
0.4	1.5	0.2	2	0.361	-1.016	-0.213	-0.611	-0.401	-0.416	-0.011	-0.020
0.4	1.5	0.2	3	0.607	-1.979	-1.801	-1.074	0.129	-0.651	-0.030	0.048
0.4	1.5	0.2	4	3.113	-1.489	-0.770	0.716	0.585	0.649	-0.144	-0.114
0.4	2	0.2	0	-1.088	1.176	1.735	-1.295	-0.858	0.896	0.411	0.945
0.4	2	0.2	1	0.483	0.887	0.824	-0.875	-0.747	-0.428	0.318	0.616
0.4	2	0.2	2	-0.450	-0.236	-1.129	-1.193	-0.566	-1.627	0.248	0.391
0.4	2	0.2	3	4.138	0.930	0.071	0.288	-0.384	0.861	0.592	-0.471
0.4	2	0.2	4	0.554	-0.944	-3.548	-1.999	0.963	1.210	-0.007	-0.617
0.4	2.5	0.2	0	-2.429	1.844	0.487	-1.711	-1.309	-0.694	1.007	0.873
0.4	2.5	0.2	1	-1.278	1.849	-0.628	-0.696	-0.922	-1.579	0.506	0.179
0.4	2.5	0.2	2	1.206	2.481	-0.279	0.762	-0.350	-0.332	0.355	0.287
0.4	2.5	0.2	3	1.196	1.967	-2.068	-0.022	0.375	0.555	0.277	0.343
0.4	2.5	0.2	4	2.679	2.560	-1.739	1.875	0.348	-1.101	0.260	0.813
0.4	4	0.2	0	-1.045	2.549	1.292	-0.993	-1.057	1.438	1.726	-0.285
0.4	4	0.2	1	0.756	2.564	0.265	-0.306	-0.649	0.654	1.408	0.072
0.4	4	0.2	2	0.530	1.865	-1.658	-0.994	-0.374	0.283	1.443	0.438
0.4	4	0.2	3	-0.436	1.123	-3.419	-1.775	-0.418	-0.937	1.555	0.163
0.4	4	0.2	4	3.839	2.406	-1.819	0.897	0.746	1.171	1.223	0.340
0.4	0.1	0.8	0	-0.691	1.568	2.101	-0.521	-0.517	-0.798	-0.833	-0.998
0.4	0.1	0.8	1	0.627	1.344	0.303	-1.745	-0.596	0.477	-0.746	0.093
0.4	0.1	0.8	2	2.875	1.829	0.454	0.319	-0.450	-1.454	-0.733	1.371
0.4	0.1	0.8	3	1.366	0.767	-2.438	-1.586	0.744	-0.723	-1.096	0.766
0.4	0.1	0.8	4	3.565	1.243	-1.887	-0.625	0.275	-0.248	-0.770	0.206
0.4	0.5	0.8	0	-1.917	-1.647	1.669	-2.133	-0.345	-0.325	0.358	0.074
0.4	0.5	0.8	1	-0.513	-2.384	0.899	-1.705	0.229	0.009	0.206	-0.269
0.4	0.5	0.8	2	1.637	-2.193	1.450	-0.103	1.033	1.145	-0.026	0.634
0.4	0.5	0.8	3	1.612	-2.901	-0.146	-0.755	0.136	-0.628	0.722	0.543
0.4	0.5	0.8	4	1.621	-3.473	-1.868	-1.227	1.070	-0.672	0.638	-1.183
0.4	1	0.8	0	-3.017	-1.143	1.114	-1.821	-0.107	0.617	0.213	0.065
0.4	1	0.8	1	-1.546	-1.977	0.713	-0.569	-0.607	0.718	-0.070	0.976
0.4	1	0.8	2	-2.989	-3.181	-0.651	0.233	0.482	0.038	-1.228	-0.171
0.4	1	0.8	3	-1.361	-3.466	-0.932	0.415	-1.287	-0.772	-0.178	-0.032
0.4	1	0.8	4	0.620	-3.298	-0.383	1.485	-0.543	1.560	-0.660	0.329
0.4	1.5	0.8	0	-4.161	-0.087	0.880	-0.607	0.115	0.416	-0.296	0.136
0.4	1.5	0.8	1	-4.167	-0.715	0.141	0.873	-0.235	-0.141	-0.997	0.217

Table B.3: Continued

Mutation Rate	Virulence	Infection Rate	Crop Year	PC1	PC2	PC3	PC4	PC5	PC6	PC 7	PC 8
0.4	1.5	0.8	2	-4.847	-1.718	-1.201	0.873	-0.936	1.117	-1.247	-0.787
0.4	1.5	0.8	3	-4.149	-1.930	-1.588	1.974	-1.528	0.437	-1.339	-0.403
0.4	1.5	0.8	4	-3.745	-2.086	-1.647	3.140	-2.543	-0.397	-1.409	-0.346
0.4	2	0.8	0	-4.474	0.558	0.910	-0.521	0.666	0.016	0.243	0.232
0.4	2	0.8	1	-2.997	0.148	0.054	-0.026	-0.957	0.265	0.067	0.693
0.4	2	0.8	2	-1.485	-0.120	-0.217	0.780	-2.259	0.041	0.149	0.623
0.4	2	0.8	3	-1.183	-0.971	-0.801	1.089	-1.926	-0.830	-0.284	0.809
0.4	2	0.8	4	1.095	-1.133	-1.271	0.888	-1.736	0.983	-0.212	0.407
0.4	2.5	0.8	0	-5.421	0.822	1.364	0.396	2.406	1.381	-0.291	0.254
0.4	2.5	0.8	1	-4.251	0.586	-0.464	-0.275	0.084	0.355	0.004	-0.062
0.4	2.5	0.8	2	-3.571	0.686	-0.998	0.735	-0.383	-1.422	-0.033	0.219
0.4	2.5	0.8	3	-2.401	0.881	-0.820	2.341	-0.156	-1.476	-0.461	0.833
0.4	2.5	0.8	4	-1.903	0.484	-2.373	1.424	-1.394	-1.676	0.570	-0.315
0.4	4	0.8	0	-5.709	1.168	1.056	1.344	2.630	-0.063	0.596	0.442
0.4	4	0.8	1	-4.899	1.045	-0.300	1.368	1.981	0.254	0.075	0.360
0.4	4	0.8	2	-3.423	0.958	-0.417	1.872	0.465	-0.130	0.601	0.593
0.4	4	0.8	3	-1.981	0.757	-1.922	0.246	-1.302	0.521	1.541	-0.207
0.4	4	0.8	4	1.835	2.246	-0.495	2.272	-1.041	-0.853	0.904	-0.726
0.6	0.1	0.2	0	0.737	2.125	2.275	-1.044	-1.343	0.106	-0.381	0.346
0.6	0.1	0.2	1	1.543	1.854	0.858	-0.295	0.463	-0.102	-1.478	0.383
0.6	0.1	0.2	2	-0.027	0.649	-1.970	-2.207	0.091	-1.016	-1.032	0.116
0.6	0.1	0.2	3	0.699	0.612	-2.457	-1.949	0.318	-0.194	-0.975	-0.185
0.6	0.1	0.2	4	3.660	1.563	-1.290	0.663	1.263	0.161	-1.368	-0.417
0.6	0.5	0.2	0	-0.662	-0.533	1.975	-2.017	-0.436	0.378	0.200	-0.111
0.6	0.5	0.2	1	2.319	-0.860	2.242	-0.813	0.142	0.964	0.423	-1.152
0.6	0.5	0.2	2	0.628	-2.359	0.322	-1.418	0.540	-0.473	0.320	-0.120
0.6	0.5	0.2	3	2.652	-2.358	0.000	-0.826	0.613	-0.149	0.657	-0.066
0.6	0.5	0.2	4	3.694	-2.402	-0.209	0.342	1.430	-0.507	0.306	-0.857
0.6	1	0.2	0	-1.730	-0.285	1.114	-2.214	-0.259	0.331	0.358	0.272
0.6	1	0.2	1	1.841	-0.748	2.124	0.489	-0.328	-0.748	0.098	0.934
0.6	1	0.2	2	0.945	-1.993	0.428	-0.298	0.440	0.028	-0.078	-0.380
0.6	1	0.2	3	1.865	-2.457	-0.586	-0.541	-0.757	-1.214	0.720	0.021
0.6	1	0.2	4	2.719	-2.919	-1.534	-0.380	1.006	1.470	0.112	-0.365
0.6	1.5	0.2	0	-1.964	1.786	1.469	0.062	-0.971	-2.418	-0.122	0.243
0.6	1.5	0.2	1	1.182	2.300	1.070	0.156	-1.146	0.934	0.082	-0.800
0.6	1.5	0.2	2	0.834	1.658	-0.533	-0.127	-0.550	0.790	-0.255	-0.233
0.6	1.5	0.2	3	2.428	1.982	-0.795	0.763	-0.665	-0.023	0.015	-0.838
0.6	1.5	0.2	4	1.198	1.180	-3.241	0.240	-0.174	-1.169	-0.152	0.703
0.6	2	0.2	0	-2.406	1.406	0.518	-1.270	-0.550	-0.959	0.037	0.291
0.6	2	0.2	1	0.641	2.160	0.174	-0.658	-0.191	1.991	-0.061	0.246
0.6	2	0.2	2	1.764	2.307	-0.281	0.255	0.042	0.240	-0.088	-0.418
0.6	2	0.2	3	1.225	1.469	-2.481	-1.497	-0.087	2.274	0.390	-0.573
0.6	2	0.2	4	-0.061	0.923	-3.711	-0.367	1.090	0.062	-0.340	-0.501
0.6	2.5	0.2	0	-2.627	1.854	0.300	-1.736	-0.443	0.688	0.383	0.220
0.6	2.5	0.2	1	-0.253	2.146	-0.231	-0.424	-0.069	-0.074	0.064	-0.709
0.6	2.5	0.2	2	1.736	2.276	-0.818	-0.651	-0.591	0.643	0.729	-0.659
0.6	2.5	0.2	3	3.410	2.675	-0.311	1.293	0.559	1.160	0.044	0.485
0.6	2.5	0.2	4	3.456	2.169	-1.647	1.208	0.609	0.387	0.314	0.332
0.6	4	0.2	0	-2.450	2.249	0.821	-0.598	-0.085	0.606	1.168	-0.284
0.6	4	0.2	1	-0.709	2.074	-0.691	-0.792	0.308	0.743	0.885	-0.290
0.6	4	0.2	2	-0.222	1.826	-1.374	-0.630	-0.296	-0.006	1.288	0.160
0.6	4	0.2	3	2.262	2.251	-1.525	0.431	0.632	0.616	1.043	1.339

Table B.3: Continued

Mutation Rate	Virulence	Infection Rate	Crop Year	PC1	PC2	PC3	PC4	PC5	PC6	PC 7	PC 8
0.6	4	0.2	4	3.053	2.001	-3.023	-0.142	0.952	0.551	1.293	-0.394
0.6	0.1	0.8	0	-0.600	1.390	1.619	-1.328	-1.009	-0.409	-0.609	-0.137
0.6	0.1	0.8	1	0.661	1.315	0.128	-1.732	-0.451	0.119	-0.775	0.827
0.6	0.1	0.8	2	-0.516	0.613	-1.333	-1.657	0.439	0.023	-1.348	0.029
0.6	0.1	0.8	3	2.596	1.462	-0.641	-0.405	0.296	0.569	-0.996	-0.626
0.6	0.1	0.8	4	3.183	1.081	-2.253	-1.316	0.215	0.363	-0.619	-0.352
0.6	0.5	0.8	0	-2.302	-1.643	1.425	-2.110	0.111	0.773	0.170	0.075
0.6	0.5	0.8	1	1.529	-1.677	2.364	-0.413	-0.064	0.546	0.424	-0.001
0.6	0.5	0.8	2	1.604	-2.336	1.262	-0.137	0.840	0.652	0.067	-0.294
0.6	0.5	0.8	3	2.591	-2.625	0.448	0.390	1.092	0.335	0.217	0.280
0.6	0.5	0.8	4	3.484	-2.703	0.029	0.891	1.029	-0.100	0.420	0.352
0.6	1	0.8	0	-3.389	-0.489	1.069	-0.996	-0.741	-0.758	0.097	0.315
0.6	1	0.8	1	-2.435	-1.531	0.700	0.320	-1.440	0.476	-0.427	0.550
0.6	1	0.8	2	-0.913	-2.189	0.278	1.211	-1.704	1.377	-0.519	0.500
0.6	1	0.8	3	-0.171	-2.948	-0.026	1.924	-1.707	1.995	-0.758	0.452
0.6	1	0.8	4	1.517	-3.186	-0.071	2.629	-2.059	2.504	-0.734	0.957
0.6	1.5	0.8	0	-3.559	0.965	2.244	0.915	0.549	-0.800	-0.223	1.263
0.6	1.5	0.8	1	-3.247	-0.127	-0.633	-0.134	-0.523	1.400	-0.825	0.257
0.6	1.5	0.8	2	-1.713	-0.352	-1.345	-0.034	-2.160	0.604	-0.309	0.135
0.6	1.5	0.8	3	1.113	0.602	-0.626	0.672	-2.855	1.505	-0.097	0.257
0.6	1.5	0.8	4	0.366	-0.051	-2.578	0.476	-2.024	-0.305	-0.431	1.011
0.6	2	0.8	0	-5.316	0.737	1.264	0.511	2.815	0.767	-0.823	0.423
0.6	2	0.8	1	-4.302	0.648	0.064	0.452	0.322	-0.727	-0.313	0.195
0.6	2	0.8	2	-1.983	1.092	-0.008	1.624	-0.157	0.031	-0.549	0.193
0.6	2	0.8	3	-2.248	0.667	-1.731	0.792	-0.350	0.666	-0.356	0.430
0.6	2	0.8	4	-1.006	0.541	-2.685	0.049	-1.554	1.108	0.111	0.717
0.6	2.5	0.8	0	-6.867	0.800	1.170	2.181	3.782	-2.601	-0.989	-0.047
0.6	2.5	0.8	1	-5.790	0.413	-0.124	0.389	2.356	1.621	-0.548	-0.368
0.6	2.5	0.8	2	-4.530	0.414	-0.619	0.892	0.900	0.788	-0.357	-0.228
0.6	2.5	0.8	3	-3.539	0.386	-1.204	1.468	0.143	0.689	-0.149	0.039
0.6	2.5	0.8	4	-3.552	0.043	-2.360	1.450	-0.483	-0.161	0.032	-0.555
0.6	4	0.8	0	-5.933	0.971	0.641	0.163	2.455	1.988	0.800	-0.056
0.6	4	0.8	1	-2.710	1.628	0.493	1.671	-0.047	-0.925	0.892	1.213
0.6	4	0.8	2	-1.268	1.504	-0.142	1.734	-0.008	0.559	0.771	-0.198
0.6	4	0.8	3	-1.954	0.898	-1.738	1.763	0.012	-0.219	0.711	0.353
0.6	4	0.8	4	-1.669	0.250	-3.714	0.090	-0.268	1.720	1.145	-0.783
0.8	0.1	0.2	0	-2.153	1.128	0.523	-2.428	-0.764	-0.824	-0.681	0.107
0.8	0.1	0.2	1	1.285	1.722	0.750	-0.796	-0.654	-1.100	-0.922	-0.246
0.8	0.1	0.2	2	1.635	1.416	-0.329	-0.920	0.464	1.112	-1.351	-0.371
0.8	0.1	0.2	3	1.610	0.890	-2.093	-1.209	0.619	-0.560	-1.142	0.016
0.8	0.1	0.2	4	2.323	0.777	-2.730	-1.067	0.954	0.278	-1.157	0.878
0.8	0.5	0.2	0	-0.679	-0.724	2.182	-1.464	-0.228	0.080	0.303	-0.757
0.8	0.5	0.2	1	2.425	-1.112	2.481	-0.506	0.098	1.358	0.352	-0.813
0.8	0.5	0.2	2	3.005	-1.685	1.402	0.034	0.715	0.073	0.261	-0.584
0.8	0.5	0.2	3	0.985	-3.104	-0.816	-1.113	0.428	-0.589	0.499	0.380
0.8	0.5	0.2	4	4.020	-2.420	-0.305	0.400	1.237	0.514	0.351	1.738
0.8	1	0.2	0	-2.411	1.012	0.635	-1.591	0.064	0.202	-0.584	-0.135
0.8	1	0.2	1	0.130	1.053	0.617	-0.918	-0.473	0.486	-0.398	-0.555
0.8	1	0.2	2	2.448	1.000	0.615	-0.060	-0.550	0.618	0.082	-0.802
0.8	1	0.2	3	2.340	0.280	-0.610	-0.327	-0.444	-0.366	0.253	1.043
0.8	1	0.2	4	2.391	-0.368	-1.814	-0.063	-0.196	-2.144	0.290	0.457
0.8	1.5	0.2	0	-3.027	1.524	0.323	-1.433	-1.164	-1.226	-0.038	0.172

Table B.3: Continued

Mutation Rate	Virulence	Infection Rate	Crop Year	PC1	PC2	PC3	PC4	PC5	PC6	PC 7	PC 8
0.8	1.5	0.2	1	0.736	2.263	-0.175	-1.005	-1.023	0.399	0.104	1.071
0.8	1.5	0.2	2	0.313	2.191	-0.836	0.022	-0.099	0.301	-0.334	-0.531
0.8	1.5	0.2	3	2.350	2.609	-0.878	0.416	-0.311	2.065	-0.063	0.307
0.8	1.5	0.2	4	1.724	1.860	-3.707	-0.413	-0.038	-0.354	0.242	-0.566
0.8	2	0.2	0	-1.572	2.025	1.078	-1.531	0.113	2.589	0.052	-0.037
0.8	2	0.2	1	-0.245	2.031	-0.008	-0.792	-0.389	0.043	-0.014	0.795
0.8	2	0.2	2	1.934	2.565	-0.230	0.197	-0.027	0.592	-0.004	-0.852
0.8	2	0.2	3	2.751	2.527	-1.034	-0.059	0.138	2.159	0.169	0.043
0.8	2	0.2	4	1.760	1.819	-2.744	0.120	0.834	0.233	-0.278	0.856
0.8	2.5	0.2	0	-2.516	1.956	0.409	-1.737	-0.809	0.783	0.663	0.023
0.8	2.5	0.2	1	0.122	2.316	-0.021	-0.224	-0.004	0.161	0.046	-0.258
0.8	2.5	0.2	2	0.902	2.262	-0.817	-0.188	-0.408	-0.336	0.475	0.461
0.8	2.5	0.2	3	0.678	1.495	-3.186	-1.293	0.439	0.032	0.331	-0.320
0.8	2.5	0.2	4	3.120	2.465	-1.825	0.795	1.084	1.921	0.038	-0.491
0.8	4	0.2	0	-3.408	1.843	0.237	-0.615	0.341	-0.446	0.581	0.468
0.8	4	0.2	1	1.223	2.757	0.540	-0.229	-0.415	1.375	1.308	-0.267
0.8	4	0.2	2	-0.248	1.612	-2.262	-2.019	-0.332	0.876	1.514	-0.509
0.8	4	0.2	3	0.936	1.663	-2.743	-0.558	0.326	-0.675	1.264	0.173
0.8	4	0.2	4	2.975	2.234	-2.242	1.058	0.613	-0.966	1.276	0.407
0.8	0.1	0.8	0	-1.230	1.186	1.562	-1.414	-1.269	-1.316	-0.423	-0.020
0.8	0.1	0.8	1	1.122	1.531	0.606	-1.105	-0.674	-0.395	-0.710	0.022
0.8	0.1	0.8	2	3.085	1.844	0.620	0.084	0.243	0.844	-1.192	1.229
0.8	0.1	0.8	3	2.291	1.045	-1.699	-1.380	0.471	0.981	-0.948	1.635
0.8	0.1	0.8	4	4.107	1.387	-1.870	0.045	0.856	-0.241	-0.918	-0.037
0.8	0.5	0.8	0	-1.829	-1.453	1.886	-0.784	-0.464	-1.554	0.196	-0.024
0.8	0.5	0.8	1	-0.484	-2.389	1.435	-0.166	-0.060	-0.819	0.108	0.024
0.8	0.5	0.8	2	2.587	-2.098	1.595	0.862	0.546	0.377	-0.013	-0.668
0.8	0.5	0.8	3	1.949	-2.961	0.057	-0.006	0.259	0.574	0.348	-0.153
0.8	0.5	0.8	4	0.420	-4.001	-2.088	-0.572	0.753	-0.984	0.089	0.164
0.8	1	0.8	0	-4.487	0.113	0.781	-0.682	0.452	-0.714	-0.430	0.061
0.8	1	0.8	1	-1.818	-0.163	0.285	0.100	-1.047	1.245	-0.528	0.166
0.8	1	0.8	2	-0.058	-0.415	0.205	1.208	-1.667	0.875	-0.582	1.419
0.8	1	0.8	3	1.468	-0.860	-0.207	1.177	-2.284	1.046	-0.236	-0.990
0.8	1	0.8	4	4.252	-0.720	-0.230	2.452	-2.213	-0.280	0.078	0.100
0.8	1.5	0.8	0	-5.982	0.338	0.540	-0.249	2.478	0.805	-1.139	-0.410
0.8	1.5	0.8	1	-2.884	0.559	0.293	-0.243	-1.053	0.659	0.067	0.547
0.8	1.5	0.8	2	-0.829	1.100	-0.336	0.136	-2.195	0.645	-0.395	0.211
0.8	1.5	0.8	3	0.828	1.413	-0.781	1.020	-1.759	0.679	-0.409	0.155
0.8	1.5	0.8	4	2.489	1.697	-1.190	1.218	-1.192	1.923	-0.440	-0.391
0.8	2	0.8	0	-6.067	0.628	0.981	0.718	2.698	-0.950	-0.658	-0.106
0.8	2	0.8	1	-4.516	0.608	0.124	0.460	1.866	1.700	-0.894	0.120
0.8	2	0.8	2	-4.129	0.524	-0.784	0.743	0.419	0.028	-0.482	0.110
0.8	2	0.8	3	-3.305	0.520	-1.258	1.992	0.046	-1.111	-0.396	-0.092
0.8	2	0.8	4	-3.655	-0.123	-2.499	1.443	-0.568	-0.881	-0.244	-0.820
0.8	2.5	0.8	0	-5.683	0.810	0.816	0.291	2.803	0.978	-0.380	0.182
0.8	2.5	0.8	1	-4.310	0.793	0.531	1.403	1.288	-0.315	-0.337	0.624
0.8	2.5	0.8	2	-4.221	0.312	-0.794	0.842	0.048	-0.368	-0.286	-0.245
0.8	2.5	0.8	3	-4.115	-0.112	-2.007	0.652	-0.439	0.115	-0.098	-0.761
0.8	2.5	0.8	4	-4.264	-0.456	-3.152	0.790	-0.222	0.637	-0.238	-1.291
0.8	4	0.8	0	-5.103	1.384	1.120	1.356	2.394	0.077	0.409	0.778
0.8	4	0.8	1	-0.416	2.172	1.492	1.655	-0.410	1.815	1.062	1.197
0.8	4	0.8	2	-1.133	1.497	-0.842	0.509	-0.410	0.083	0.822	0.332

Table B.3: Continued

Mutation Rate	Virulence	Infection Rate	Crop Year	PC1	PC2	PC3	PC4	PC5	PC6	PC 7	PC 8
0.8	4	0.8	3	-1.540	0.952	-2.340	0.308	0.104	0.371	0.581	0.249
0.8	4	0.8	4	-1.834	0.610	-3.379	0.929	-0.404	-2.311	0.896	-0.130